SYMPOSIUM

BIOLOGICAL APPLICATIONS OF SYNCHROTRON RADIATION

W-PM-1S EXAFS STUDIES OF METALLOPROTEINS. R. G. Shulman, P. Eisenberger, B. M. Kincaid, G. S. Brown* and B. K. Teo, Bell Laboratories, Murray Hill, N.J. 07974

X-ray absorption spectra of metalloproteins have been made at the Stanford Synchrotron Radiation Laboratory. The Extended X-ray Absorption Fine Structure was measured and used to determine bond lengths. Methods of data analysis will be discussed briefly and in particular it will be shown how Fourier filtering combined with independent knowledge of the phase shifts allows determinations of distances to the first shell of neighbors. In carbonic anhydrase it will be shown that an iodide ion, acting as an inhibitor, is bonded directly to the zinc atom, at a distance of 2.65±0.06Å. In deoxyhemoglobin the Fe-N porphyrin distance was determined to be 2.055±0.01Å while in oxyhemoglobin it was 1.98±0.01Å. Corrections which remove from the data contributions from axial ligands of +0.01 and -0.04Å respectively are included. In deoxyhemoglobin these distances are consistent with the iron being up to 0.3Å above the nitrogen plane, with the best value being 0.2Å. These distances are identical with those measured simultaneously on the oxygenated and deoxygenated forms of "picket fence" porphyrins.

In rubredoxin, containing one iron bound to four cysteinyl sulfurs, the average Fe-S distance is determine to be 2.26±0.01Å in the oxidized state both in the powder and in solution. Upon reduction, in solution, it was 2.32±0.02Å. In the oxidized state detailed analysis showed that all four Fe-S bonds were the same length to within the errors, which were ±0.10Å.

In all three proteins these results represent refinements and modifications of the structures as previously determined by X-ray crystallography.

W-PM-2S X-RAY SPECTROSCOPIC STUDIES OF MANGANESE IN PHOTOSYNTHESIS AND OF MOLYBDENUM IN NITROGENASE.* N. Kafka, J.A. Kirby, M.P. Klein, A.S. Robertson, J.P. Smith and T.P. Walker, Laboratory of Chemical Biodynamics, Lawrence Berkeley Laboratory, University of CA., Berkeley, CA 94720.

Photosynthesis uses solar energy to split water to provide reduced substances and molecular oxygen. This process is poorly understood at the molecular level. In the water-splitting reaction it is known that metastable intermediates are produced following light absorption; manganese and chloride ion are implicated as essential catalytic cofactors. Concerted efforts to observe membrane-bound Mn by ESR spectroscopy have failed. Manganese is, in this instance, one of the refractory, "spectroscopically silent" atoms. We have inaugurated X-ray spectroscopic studies of manganese in chloroplast membranes to seek information on the oxidation state or states of Mn, its ligands, and any changes thereof which accompany the oscillatory production of O_2 following a series of brief saturating light flashes.

It has been known for many years that molybdenum is required for the growth of nitrogen fixing organisms. While molybdenum is invariably present in active preparations of purified nitrogenase, its function remains unclear because of its spectroscopic silence. Studies on nitrogenase model systems containing molybdenum provide circumstantial evidence to support the contention that it plays a central role in the reduction mechanism but no direct evidence has been presented which demonstrates the involvement of the metal in any nitrogenase reaction. We have examined the X-ray spectrum of molybdenum in nitrogenase isolated from Azotobacter vinelandii with the goals of determining if substrates, inhibitors, and cofactors interact directly with the metal, change its oxidation state(s), or both.

The X-ray experiments were performed at the Stanford Synchrotron Radiation Laboratory, a national facility sponsored by the National Science Foundation, under Proposals #43 and #142.

*This research was supported by the Division of Biological and Environmental Research of the U.S. Department of Energy.

W-PM-3S EDGE AND EXAFS STUDIES OF THE STRUCTURAL ORGANIZATION OF SOME METALLOPROTEINS AND CALCIUM BINDING IN BIOLOGICAL SYSTEMS, L. Powers, Bell Laboratories, Murray Hill, NJ 07974

X-ray absorption edge spectroscopy contains information about a) charge of the absorbing atom, b) degree of covalency of bonds, and c) coordination geometry. This technique has been used to investigate the various oxidation states of metal atoms involved in oxygen binding of the respiratory proteins cytochrome oxidase (two coppers and two irons) and hemocyanin (two coppers). The extended x-ray absorption fine structure technique (EXAFS) yields information about a) the average distance from the absorbing atom to each coordination shell, b) magnitude of neighbor atom distribution about the average distance, c) number of atoms in each coordination shell, and d) the Debye-Waller factor. Hemocyanin has been observed by this technique and model compounds for the proteins have been investigated. The models include polar and covalent compounds of Cu(I) and Cu(II); Fe(II) and Fe(III) complexes of tetraphenyl porphorin and protoporphorin IX dianion having 5th (and 6th) ligands polar and/or covalent; and Cu-Cu, Fe-Fe, and Fe-Cu complexes.

Calcium coordination has been studied with model compounds and a correlation between edge energy, average bond distance, and coordination number found. Ca^{++}-EDTA complex and $CaCl_2$ solution have been investigated and studies of phospholipid bilayers containing calcium have been made as functions of temperature and $CaCl_2$ solution content. Preliminary studies have also been conducted on both calcium activated and calcium modulated proteins.

W-PM-4S X-RAY ABSORPTION SPECTROSCOPY AS A STRUCTURAL PROBE OF METAL SITES IN PROTEINS† Keith O. Hodgson, Department of Chemistry, Stanford, University, Stanford, California 94305

X-ray absorption spectroscopy is a technique which can examine the electronic and structural environment of a particular element in any physical state. The availability of a high intensity, broad band synchrotron radiation source at Stanford has made data collection on dilute metallo protein samples feasible for the first time. Analysis of the data provides accurate distances to neighboring atoms and coordination numbers as well as qualitative identification of the type of ligands. This paper will discuss the applications of this technique to the study of the Mo environment in the nitrogenase enzyme system and of the Cu environment in the proteins hemocyanin azurin.

This research was supported by the National Science Foundation through Grant PCM 75-17105

M I N I S Y M P O S I U M

ATOMS AND MOLECULES TUNNELLING IN BIOLOGICAL SYSTEMS

W-PM-1M TUNNELING AND LOW-TEMPERATURE REACTIONS IN LIGAND BINDING TO BIOMOLECULES. Hans Frauenfelder, Department of Physics, University of Illinois at Urbana-Champaign, Urbana, IL 61801

Biomolecules provide a nearly ideal laboratory for investigations of low-temperature reactions. Reactions, such as dissociation and rebinding of small ligands to heme proteins, can be initiated by light pulses and followed by monitoring optical absorbance changes. Below about 200 K, the processes after photodissociation are intramolecular. Rebinding is nonexponential in time, thus providing evidence for distributed barriers. The probability densities for the distributions can be determined and turn out to be characteristic for the protein structures. The presence of distributions is explained by postulating that biomolecules can exist in many different conformational states, with slightly different structures and functional properties. Studies as function of pressure and temperature give information about conformational relaxation. Rebinding can be observed down to 2 K; below about 30 K, and in some cases below about 100 K, it must occur by quantum-mechanical molecular tunneling. The distributed nature of the tunneling barrier allows a study of tunneling as function of barrier height.

W-PM-2M ELECTRON TUNNELING WITH VIBRONIC COUPLING: THEORY, EXPERIMENTS, AND BIOLOGY. J.J. Hopfield, Princeton University, Princeton, N.J. 08540 and Bell Laboratories, Murray Hill, N.J. 07974

The theory of electron tunneling between two fixed sites requires vibronic coupling to provide energy conservation between initial and final states. The transfer rate is the product of a tunneling matrix element from electron wave function overlap and a vibronic factor, involving vibronic coupling parameters but independent of the tunneling matrix element. The theory is closely related to non-adiabatic outer sphere transfer of electrochemistry. Applied to charge separation in bacterial photosynthesis, the theory describes why some electron transfers have activation energies and others do not, how the quantum efficiency for charge separation is made high, and predicts approximate distance between the various sites. According to the theory, a weak transfer band, of molar extinction coefficient ~ 1, should exist for biological electron transfer complexes. Such bands have been observed in model and in biological systems, and their observed properties are a quantitative test of the electron transfer theory.

W-PM-3M PROTON TRANSLOCATION. THE PRIMARY PHOTOCHEMICAL EVENT IN VISION. M. L. Applebury*, K. S. Peters*, and P. M. Rentzepis, Princeton, New Jersey 08540 and Murray Hill, New Jersey 07974

The primary process of vision is initiated with the absorption of a photon by the molecular photoreceptor, rhodopsin, resulting in the formation of a new intermediate, prelumirhodopsin. Picosecond kinetic studies of this photochemical event indicate that the process involves a proton translocation. At room temperature prelumirhodopsin (λ max, 543 nm) is formed with 6×10^{-12} sec (6 psec), and the rise time for formation cannot be resolved. Studies of low temperature glasses of rhodopsin, however, allow the direct observation of formation of prelumirhodopsin at 20 K and below. Even at 4 K the formation is a rapid event, with a rise time of 36 psec. The temperature dependence of the rate of formation of prelumirhodopsin shows non-Arrhenius behavior; at very low temperatures the rate is nearly independent of temperature and has a finite value as the temperature approaches 0 K. Such behavior is characteristic of a quantum mechanical tunneling event such as the translocation of a proton. A plausible candidate for the tunneling process is the hydrogen of the protonated Schiff base formed between the protein opsin and the 11-*cis* retinal chromophore. This interpretation is supported by studies of the deuterium-exchanged rhodopsin in which the Schiff base proton is replaced by deuterium. The rate of formation of prelumirhodopsin in deuterium exchanged samples is also consistent with tunneling and shows a marked deuterium isotope effect $k_H/k_D \simeq 7$. Additional kinetic studies of the 9-*cis* retinal analog, isorhodopsin, and another retinal protein, bacteriorhodopsin, also support a model in which formation of prelumirhodopsin (or the appropriate first intermediate for the analogs) involves translocation of a proton associated with the Schiff base nitrogen of the retinal chromophore.

W-PM-4M ELECTRON TRANSFER PROCESSES INVOLVING BIOLOGICAL MOLECULES IN SOLUTION. James C. W. Chien* L. Charles Dickinson*, and Helen L. Gibson,* Department of Chemistry, University of Massachusetts, Amherst, Massachusetts 01003

The unique observations by Chance and coworkers of electron transfer (ET) in the light induced oxidation of cytochrome in the photosynthetic bacterium *chromatium* had stimulated much theoretic interests. Hopfield formulated a semi-classical ET theory isomorphous to the resonance energy transfer theory of Förster. Jortner provided a complete quantum mechanical description of a non-adiabatic multiphonon ET process. The two theories gave the same results at the high temperature limit. We have studied ET processes involving biological molecules in solution and found the results to be in agreement with theories. ET between Co-cyt *c* and Fe-cyt c^+ has been studied by stopped-flow kinetics. The second order rate constant (pH 7, 0.1 ionic strength, 0.2 M phosphate, 25°) is 8.3×10^3 (M sec)$^{-1}$ with no significant dependence on either ionic strength or pH. The activation parameters are: $\Delta H^{\ddagger}$=2.3 kcal. mole^{-1} and $\Delta S^{\ddagger}$=-33 eu. The self-exchange ET rate between Co-cyt *c* and Co-cyt c^+ was found to be less than 133 (M sec)$^{-1}$ from the relaxation time measurement of the pulsed pmr resonance of Met-80. The ET between Co-cyt *c* and Fe(EDTA)$^-$ has a second order rate constant of 68.3 (M sec)$^{-1}$ (25°, μ=0.1, pH 7 phosphate) and $\Delta H^{\ddagger}$=4.2 kcal. mole^{-1} and $\Delta S^{\ddagger}$=-36 eu. From the ionic strength dependence an effective "active-site charge" of +0.45 was estimated for Co-cyt *c*. The autoxidation of Co-cyt *c* was found to have a rate constant at 25° of 12.3 (M sec)$^{-1}$ and independent of ionic strength. The reduction of methemoglobin by Co-cyt *c* was studied using nine mediators of different redox potentials. With phenazine methosulfate, the rate constant is 2.9×10^4 (M sec)$^{-1}$ (25°, pH 7, 0.1M phosphate) and $\Delta H^{\ddagger}$=7 kcal. mole^{-1} and $\Delta S^{\ddagger}$=-18 eu. These results are compared with the corresponding ET processes involving the native proteins and found to be in excellent agreement with theories.

NEUROBIOLOGY III

W-PM-A1 THE EFFECT OF DEPOLARIZING AGENTS ON SYNAPTIC TRANSMISSION FAILURE DURING HYPOXIA. P. Lipton and T.S. Whittingham*. Univ. of Wisconsin Med School, Madison, WI

Guinea pig transverse hippocampal slices (.5mm) are incubated in bicarbonate Ringer solution aerated by O_2: CO_2 or N_2:CO_2 (hypoxia). Hypoxia leads to rapid ($\sim$3.0 min.) and reversible loss of the evoked (.2pps) postsynaptic field potentials in the dentate cell region. Increasing the extracellular potassium concentration above the normal 4.4mM results in an accelerated rate of synaptic block ($\sim$1.5 min. at [K+]=10.4mM). Decreased extracellular chloride concentration (substituting isethionate or gluconate) also partially depolarizes the neurons and leads to a more rapid transmission failure. Ouabain also increases the rate of hypoxic block in low concentrations (1x10^{-6}M). Higher concentrations (5x10^{-5} M) completely block the evoked potential at a rate similar to hypoxia. The results of the partial depolarizations support the theory that hypoxic block results from depolarization of the synaptic network. The ouabain studies demonstrate that inhibition of Na-K-ATPase can take place rapidly enough to cause this depolarization block. Supported by BNS 75-15290 (NSF).

W-PM-A2 DIFFERENTIAL EFFECTS OF PERHYDROHISTRIONICOTOXIN ON NEURALLY AND IONTOPHORETICALLY EVOKED ENDPLATE CURRENTS. E.X. Albuquerque,* and P.W. Gage.* (Intr. by L.J. Mullins). Pharm. & Exptl. Therap., Univ. Maryland, Sch. Med., Baltimore, MD 21201

Perhydrohistrionicotoxin (H_{12}HTX), at concentrations of 10^{-12} to 10^{-7} M, depressed the current generated by iontophoretic application of acetylcholine (ACh) to endplate regions of soleus and extensor digitorum longus muscles of rats. However, no changes in the amplitude or time course of spontaneous miniature endplate potentials or currents were seen with these concentrations of toxin Evoked endplate currents were also unaffected by the toxin. Similarly, the responses to ACh were depressed by these concentrations of H_{12}HTX in chronically denervated muscles. Depression of responses in both normal and chronically denervated muscles developed gradually, was greater at higher concentrations and was reversible. The different effects of the toxin on neurally evoked currents and currents produced by iontophoretic application of acetylcholine could be due to differences in ACh concentration in the vicinity of receptors or to the existence of two different populations of receptor complexes. (Supported by NIH Grant No. NS-12063)

W-PM-A3 EVIDENCE THAT CATECHOLAMINE INFLUX INTO CHROMAFFIN VESICLES IS COUPLED TO MEMBRANE POTENTIAL. R.W. Holz. Univ. of Mich. Med. Sch., Ann Arbor 48109.

The H^+ concentration gradient and membrane potential across bovine chromaffin vesicle membranes were estimated by determining concentration ratios of (^{14}C)-methylamine and (^{14}C)-thiocyanate. They were compared to catecholamine uptake in the absence of permeant anions at pH 7, 31°C. The H^+ concentration ratio (intravesicular: medium) was $\sim$17 in the presence and absence of 5mM ATP and 5mM Mg^{++}. ATP and Mg^{++} increased catecholamine influx 4-6 fold and altered the intravesicular membrane potential from a negative value to +50mV. The potential change increased the H^+ electrochemical gradient. 1 µM FCCP had no effect on the H^+ concentration gradient either in the presence or absence of ATP and Mg^{++}. However, with ATP and Mg^{++}, 1 µM FCCP inhibited catecholamine influx 70% and reduced membrane potential to 18mV. The reduced potential was expected if FCCP increased the H^+ conductance of the vesicle membrane with an outwardly directed H^+ conc. gradient. The effects of FCCP on catecholamine influx and on membrane potential were well correlated with effects on both occurring between 0.1-1.0 µM FCCP. Hence in the absence of permeant anions, catecholamine uptake into chromaffin vesicles is closely correlated with membrane potential.

W-PM-A4 DIFFERENTIAL EFFECTS OF SODIUM SUBSTITUTES ON ENDPLATE CONDUCTANCE. J. Fiekers* and E. G. Henderson, Univ. Conn. Health Center, Farmington, CT 06032

MEPCs and EPC_Is were measured in frog cutaneous pectoris muscle using a voltage clamp. NaCl was completely replaced by TRIS (TR), Glucosamine (GLU) and Sucrose (SUC). I-V relations (MEPCs and EPC_Is; -120mV to +40mV) were obtained for control and each Na-substitute. A nonlinear relation was obtained for TR and GLU indicating a voltage dependent block. In contrast SUC exhibited a linear relationship. Peak endplate current @-100mV was reduced 90% by all Na-substitutes, while only GLU depressed endplate current @+40mV. E_{rev}s were -36.6mV (TR) -49mV (GLU) and -67.3mV (SUC) for EPC_Is (not significantly different from values obtained from E_{rev}s of MEPC). Calculations based on either the Goldman (1943) or the Takeuchi (1960) equations did not yield a satisfactory description of the experimentally obtained currents in Na-substituted solutions. TR and SUC increased τ for MEPCs; GLU had no effect. It is suggested that each Na-substitute has a different effect on the endplate membrane, i.e., TR-voltage dependent block of endplate channels; GLU-cholinergic receptor antagonist; SUC-modification of surface potential. (Supported by NIH NS 12563.)

W-PM-A5 COMPARISON OF IONIC SELECTIVITY OF NA CHANNELS WITH DIFFERENT TTX DISSOCIATION CONSTANTS. L.M. Huang, W.A. Catterall* and G. Ehrenstein, Lab. of Biophysics, NINCDS, NIH, Bethesda, Maryland 20014 and Dept of Pharmacology, University of Washington, Seattle, Wash. 98195

We studied the permeability of alkali cations and organic molecules for Na^+ channels in two types of neuroblastoma cell lines ± C9 and N18. Batrachotoxin, a specific activator for Na^+ channel, induces Na^+ uptake with apparent dissociation constants $K_{0.5}$ = 1.2 µM for C9, 0.4 µM for N18 cells. The BTX-induced uptake can be inhibited by tetrodotoxin with $(K_I)_{0.5}$ = 1.8 X 10^{-6} M in C9 and $(K_I)_{0.5}$ = 10^{-8} M in N18. Thus, TTX binds to N18 about 200-fold more tightly than to C9. Permeabilities of the various test molecules were measured by the increase of tracer Na^+ uptake through the BTX-activated Na^+ channels. The Na^+ channels of these two cell lines have the same selectivity sequence for alkali cations: $Tl^+ \approx Na^+ > Rb > Cs$. Both Na^+ channels prefer charged guanidinium over uncharged urea although these two molecules are similar in size and shape. H^+ inhibits ^{22}Na uptake for both sodium channels (pK = 5.7). Thus, although C9 and N18 have very different TTX affinity, their selectivity properties are very similar.

W-PM-A6 OUTWARD-CURRENT COMPONENT ASSOCIATED WITH INTRACELLULAR Ca ACCUMULATION IN AEQUORIN-INJECTED, VOLTAGE-CLAMPED DORID NEURONS. R. Eckert and D. Tillotson. Dept. of Biology, UCLA, Los Angeles, CA 90024.

Activation of the Ca-dependent late outward current during 200-msec depolarizations was examined under voltage clamp in aequorin-injected giant neurons of the dorid mollusk Anisodoris nobilis, while the Ca-aequorin reaction was monitored photometrically. The square root of the aequorin signal was taken as approximately proportional to the increment in free Ca^{2+} near the membrane inner surface during Ca entry. The hump of the N-shaped late I-V plot was displaced up to +50 mV from the peak of the $[Ca]_i$ voltage plot. This is predicted from elementary electrophysiological considerations. The minimum of the N-shaped profile of the current-voltage plot coincided with the membrane voltage at which the aequorin signal was fully suppressed. The activation kinetics of the slow component of outward current were closely related to the kinetics of free Ca accumulation, both slowing greatly as Vm approached E_{Ca}. Thus, it appears to be the intracellular accumulation of Ca rather than the passage of Ca through the membrane that activates the Ca-sensitive K current. Supported by USPHS grant NS08364.

W-PM-A7 EFFECTS OF Ba^{2+} AND Cs^{+} ON VOLTAGE-AND CALCIUM-DEPENDENT POTASSIUM CURRENTS IN MOLLUSCAN NEURONS. A. Hermann* and A.L.F. Gorman, Dept. of Physiology, Boston U. Sch. of Med., Boston, MA 02118.

The effects of intra- and extracellular Ba^{2+} and Cs^{+} on the voltage- and calcium-dependent potassium outward current $I_{K(V)}$ and $I_{K(Ca)}$ were studied in voltage clamp experiments carried out in abdominal ganglion neurons of Aplysia. Membrane currents were examined by step depolarizations in zero Ca^{2+} solutions eliciting $I_{K(V)}$ and following electrophoretic injection of Ca^{2+} inducing $I_{K(Ca)}$. The injection of Cs^{+} substantially reduced $I_{K(V)}$ while $I_{K(Ca)}$ was not, or only slightly reduced, however, the K^{+} equilibrium potential was decreased. Ba-injection reduced $I_{K(V)}$ and unlike Cs-injection, blocked $I_{K(Ca)}$ in a dosage dependent manner. Replacement of Ba^{2+} for Ca^{2+} extracellularly increased the slow inward current in the low voltage range but did not produce the N-shape region of the I-V-curve in the high voltage range (+50 to +100 mV). Our results indicate that Ba^{2+} and Cs^{+} act intracellularly to block the voltage dependent K^{+} current, although Ba^{2+} appears to interact with an internal Ca-site to block $I_{K(Ca)}$.

W-PM-A8 VOLTAGE DEPENDENT Ca^{2+} ENTRY IN A MOLLUSCAN NEURON INVESTIGATED WITH ARSENAZO III. M.V. Thomas* and A.L.F. Gorman (Intr. by J. Head), Dept. of Physiology, Boston U. Sch. of Med., Boston, MA 02118.

Changes in free intracellular Ca^{2+}, [Ca]i, were measured with arsenazo III during step depolarizations of the Aplysia R15 neuron. Depolarizations of 5-10mV from a -50mV holding potential cause an increase in [Ca]i which persists throughout the pulse for pulse lengths of up to several minutes. Beyond about -35mV the absorbance change increases steeply with membrane depolarization and reaches a maximum at about +30mV. During a large step depolarization, both dye absorbance and the Ca-mediated K^{+} current increase linearly with time up to about 100msec, and the absorbance change during a pulse remains constant for successive pulses in a train. The absorbance change is not reduced by TTX, and although abolished by Ca-free saline, it is very insensitive to external Ca^{2+}, [Ca]o, for depolarizations up to about -10mV. Lowered [Ca]o causes a proportionately greater reduction of the absorbance change for larger depolarizations and causes a negative shift in the peak of the [Ca]i/voltage relation. Supported by NS11429.

W-PM-A9 Cs SUBSTITUTION FOR INTERNAL K REVEALS AN INACTIVATING Ca CURRENT IN APLYSIA NEURONS D. Tillotson and R. Horn, Dept. of Biology, UCLA, Los Angeles, CA 90024

Ca current in the absence of K current was examined in giant neurons R-15 and R-2 of Aplysia under voltage clamp. The impermeant species Cs was substituted for internal K with the aid of the antibiotic nystatin which renders the surface membrane highly permeable to monovalent cations. Following the removal of the nystatin the membrane resistance returned to normal, permitting the observation of a virtually uncontaminated inward Ca current. With paired 50-msec voltage clamp pulses Ca current inactivation dependent on voltage and time was observed without evidence of facilitated Ca entry. Voltage dependency was measured by varying the amplitude of two equal pulses separated by 200 msec. The maximum inactivation occurred between +20 and +40 mV. The time dependency of inactivation, tested by varying the interval between the two equal pulses, was found to be described by the sum of two exponential functions with time constants of approximately .5 and 4.5 sec. Supported by USPHS Grant NS 08364.

W-PM-A10 EFFECTS OF MG^{2+} AND OSMOTIC PRESSURE (π) ON BLACK WIDOW SPIDER VENOM (BWSV) ACTION. Stanley Misler* and W. P. Hurlbut* (Intr. by F. Brink, Jr.), Rockefeller University, NY.

BWSV increases mepp frequency (F) at the frog neuromuscular junction several hundredfold in the presence of extracellular Ca^{2+} or Mg^{2+} but has little or no effect on F in the presence of 1-2 mM EGTA and no Ca^{2+} or Mg^{2+}. After both applying BWSV for 20 min., and washing for 20 min. in the latter condition, adding 1-4 mM Mg^{2+} leads to a rise in F. The rate of rise of F is graded with Mg^{2+} and F returns to nearly zero within minutes of removing Mg^{2+}. These data suggest that BWSV might raise F by increasing the divalent cation permeability of the nerve terminal. Accordingly, F might decrease when BWSV is applied in hypertonic solutions containing EGTA, no Ca^{2+} or Mg^{2+} and 60-120 mM sucrose, much as F decreases when $[K^{+}]_o$ is elevated in similar solutions. However, when BWSV was applied in hypertonic 'zero' divalent cation solutions, F always increased. These combined data suggest that Mg^{2+} and π may be used to control BWSV action and that BWSV may raise F by some other mechanism(s) in addition to possibly increasing presynaptic divalent cation permeability.

CELL BIOLOGY II

W-PM-B1 ELECTROPHORETIC DISTINCTIONS OF PERIPHERAL HUMAN LYMPHOCYTES AND LEUKEMIC LYMPHOBLASTS. S. A. Smith and B. R. Ware, Department of Chemistry, Harvard University, Cambridge, MA 02138, and R. A. Yankee, Division of Blood Products Research, Sidney Farber Cancer Center and Harvard Medical School, Boston, MA 02115

Human T and B lymphocytes were found to be distinguishable on the basis of electrophoretic mobility, with the T cells having higher mobility, in agreement with previous reports. The effects of the enzyme neuraminidase on the electrophoretic mobilities of T and B lymphocytes were determined. T lymphocytes showed a greater decrease in electrophoretic mobility after neuraminidase treatment; the relative mobilities of T and B cells were reversed by neuraminidase treatment, and the electrophoretic distinguishability was enhanced. The electrophoretic mobility distributions of peripheral blood lymphoblasts from patients with acute lymphocytic leukemia were found to differ from those of normal cells in their response to neuraminidase treatment and to changes in solution ionic strength. These results imply that the surface structure of the leukemic cells differs from that of either T or B lymphocytes from normal donors.

W-PM-B2 THE PROLIFERATION KINETICS OF BURKITT'S LYMPHOMA CELLS IN VITRO. K. Woo, W. Funkhouser,* C. Sullivan,* and O. Alabaster,* Biological Markers Lab., FCRC, Frederick, MD 21701 and NCI, Bethesda, MD 20014.

The in vitro proliferation kinetics of North American Burkitt's lymphoma cells were characterized at three different growth phases: pre-exponential, exponential, and plateau. During the pre-exponential phase, the slow growth rate resulted from a long G_1 phase of the cell cycle and a high cell loss rate. The retardation of the growth rate observed as the culture entered the plateau phase was mainly due to an elongation of G_1 and G_2. A slight increase in cell loss rate was also seen. DNA histograms obtained by flow microfluorometry for unsynchronized and synchronized cell populations were analyzed in terms of the measured and calculated cell kinetic parameters utilizing the discrete-time kinetic model (Cell Tissue Kinet. 8:197, 1975). There was a good correlation between the in vitro proliferation kinetics at plateau phase and the in vivo kinetics of Burkitt's lymphoma, suggesting the potential clinical utility of information obtained by in vitro kinetic studies. (Research sponsored by NCI under Contract No. NO1-CO-25423 with Litton Bionetics, Inc.)

W-PM-B3 HIGH RESOLUTION 2-D ELECTROPHORESIS OF HUMAN HAIR FOLLICLES AND LYMPHOCYTES: APPLICATION TO GENETIC SCREENING. Leigh Anderson* and Norman G. Anderson Molecular Anatomy Program, Div. of Biol. & Med. Res., Argonne National Laboratory, Argonne, IL 60439

Using a high resolution two-dimensional electrophoresis system (ISO-DALT) more than 200 protein gene products are routinely observed in extracts of radioactively labeled single human hair follicles, while larger numbers are observed in lymphocyte microcultures. Approximately 1/3 of all amino acid substitutions result in charge shifts easily seen in this system. It is considered possible, using the ISO-DALT apparatus and computer-based systems for locating spots and comparing large numbers of patterns, to monitor the human mutation rate, estimate the average heterozygosity of cellular proteins, and also measure the somatic mutation rate. The follicle protein technique opens up the possibility of observing the effects of mutagens and carcinogens in animals; each follicle is a separate measurement, and many follicles may be obtained from each animal. Problems of standardization, reproducibility, and automation are discussed. (Work supported by U.S. DOE)

W-PM-B4 ON THE QUANTITATIVE EVALUATION OF THE RESPONSE OF QUIESCENT FIBROBLASTS TO GROWTH STIMULI. Mary N. Stamatiadou and Dimitri Stathakos,* Dept. of Biology, Nuclear Research Center "Demokritos", Aghia Paraskevi, Athens, Greece.

Within the framework of studying serum macromolecular growth factors, we have developed a system which permits quantitative evaluation of the response of quiescent 3T3 cells to different stimulatory treatments. In this system, the quantitative response to specific growth stimuli and the timing of induced DNA synthesis in stimulated quiescent cells are consistently independent of the length of duration of the state of quiescence, within a span of 1 to 6 days. Under our conditions, neither the quantitative response of quiescent cells to growth stimuli nor the basal level of DNA synthesis obtained at quiescence are affected by low molecular weight nutrients, including vitamin B_{12}, which is reported as a limiting factor in other systems (K. Mierzejewski and E. Rozengurt, Exp Cell Res 106:394, 1977).

W-PM-B5 CALCIUM AND PHOSPHOLIPID INTERACTIONS DURING ACTIVATION OF SUCCINIC DEHYDROGENASE AFTER THERMAL ACCLIMATION. James B. Hughes,* and Irving Gray, Department of Biology, Georgetown University, Washington, D.C. 20057.

Low temperature acclimation of rainbow trout results in increased SDH activity. While increased catalytic activity is associated with altered membrane phospholipids, calcium is required for the affect by phospholipids from cold acclimated organisms. Changes in the kinetic parameters suggest that low temperature acclimation causes the reversible removal of a modulator and that Ca^{2+} added to the 5°C enzyme reversed the effect. Spectrophotometric analyses of 5°C and 15°C enzyme preparations indicate calcium-dependent conformational changes involving chromophores whose absorption characteristics resemble the flavin and iron-sulfur components of the mammalian enzyme. Low temperature acclimation results in spectral changes similar to those produced by EDTA extraction of the 15°C enzyme. $^{45}Ca^{2+}$ binding demonstrates high and low affinity binding sites in the phospholipid of the complex, the proportion of each dependent upon acclimation temperature. Cardiolipin is implicated as being involved in calcium binding and enzyme activation.

W-PM-B6 MECHANISM OF PROTECTION AGAINST CADMIUM-MEDIATED CYTOTOXICITY IN CULTURED CHINESE HAMSTER CELLS. INDUCTION OF CADMIUM-BINDING METALLOTHIONEINS. C.E. Hildebrand, M. D. Enger, R. Tobey*, E. Campbell*, J. Hanners* & M. Jones* Los Alamos Scientific Laboratory, Los Alamos, NM 87545

We have approached the problem of protection against Cd toxicity using cultured cells to compare cytotoxic effects of Cd with intracellular Cd levels and subcellular distribution of Cd especially with regard to induction of Cd-binding metallothionein (MT) and sequestering of Cd in MT. Two cell types have been employed: (1) Chinese hamster (CHO) cells which are sensitive to 2 x 10^{-6} M $CdCl_2$ as judged by growth inhibition (no growth after 24 h) and by cell survival (~5% survival after 12 h) and (2) a Cd-resistant variant of CHO cells (CHO^{Cdr}) which shows no growth inhibition or loss of viability after 24 h exposure to 2 x 10^{-6} M Cd. Although both cell types accumulate the same amount of Cd, CHO^{Cdr} cells both induce MT more rapidly than CHO cells and sequester 4-fold more intracellular Cd into MT than CHO cells. These studies suggest that the ability of cells to induce synthesis of MT is closely related to protection against the cytotoxic effects of Cd. (This work was performed under the auspices of the Department of Energy.)

W-PM-B7 CELL ADHESION TO SUBSTRATES COVERED WITH ANTIBODY MOLECULES. I. Giaever, General Electric R&D Center, Schenectady, NY, 12301, and E. Ward,* Salk Institute, San Diego, CA, 92112

The nature of the interaction between cells and between cells and a substrate is an important and largely unsolved problem in biology. When most mammalian cells are propagated in tissue culture, the cells will not proliferate unless they are attached to a solid surface. Because tissue culture medium is commonly fortified with serum, this surface will be covered with a layer of serum protein. In this paper we look at the effect of precoating the surface with various pure protein molecules. We found that several cell types from heart, lung, and kidney of rats avoided surfaces covered with IgG molecules. On the other hand, other investigators[1] had found that at least one class of lymphocytes are attracted to such surfaces. The biological significance of these observations is not yet clarified.

[1] E. Alexander and P.J. Heubart, J. Exp. Med. 143, 329 (1976).

W-PM-B8 A DETERMINATION OF THE MOTILITY OF ARBACIA SPERM. Charles P. Bean, General Electric Corporate Research and Development, P. O. Box 8, Schenectady, NY 12301

A new method for determination of the number average of sperm velocity has been applied to suspensions of the sperm of the sea urchin, Arbacia punctulata. The assumptions of the method are: first, the sperm move in straight lines until colliding with a surface, and second, at least one surface adsorbs incident sperm in an irreversible fashion. A dilute suspension of sperm (N in a unit volume with an average velocity V) is put over an adsorbing surface to a layer thickness h. For times less than h/V, the surface density is given exactly as NVt/4. A sputtered film of gold is used as the adsorbing layer and periodic photographs made of the course of adsorption. Preliminary results at 25°C give an average velocity immediately following dilution of the "dry sperm" of approximately 280 μm per second. For the first hour or so, this average falls off exponentially with a time constant of 2,500 seconds. A simple integration gives a maximum range for sperm motion of 70 cm.

W-PM-B9 PROTECTION OF MAMMALIAN CELLS AGAINST COLD DAMAGE. J.R. Lepock,* G. Rule * and J. Kruuv,* Physics Dept., Univ. of Waterloo, Waterloo, Ont., Canada (Intr. by R. A. Snyder)

When survival at low temperatures, in terms of colony forming ability, is measured in unprotected Chinese hamster lung cells (V79), it varies inversely with temperature in the 10-25°C range. These survival-time curves on semi-log plots have a "shoulder" region followed by a linear region. An Arrhenius plot of the slopes of the linear region gives a straight line in this temperature range. The survival of cells at 5°C break the above pattern, i.e. there is a sharp break in the Arrhenius plot and survival is less than at 10°C. Pretreating the cells with 0.1 mM butylated hydroxytoluene (BHT) before exposure to 5°C afforded significant protection compared to controls and brought the survival back to the level predicted by the Arrhenius plot. BHT did not protect cells exposed to 20°C. The use of adamantane at 5°C also protected cells, but not as effectively as BHT. Using ESR and the lipid soluble spin probe 2N14, BHT was shown to reduce the viscosity of regions of the V79 cellular membranes.

W-PM-B10 INTRACELLULAR ICE NUCLEATION IN 8-CELL MOUSE EMBRYOS. W. F. Rall,[1] P. Mazur, and S. P. Leibo,* Univ. of Tenn.-Oak Ridge Grad. Sch. Biomed. Sci. and Biology Div., Oak Ridge Natl. Lab., Oak Ridge, Tenn. 37830

Cells cooled rapidly are killed by the formation of intracellular ice. One can physical chemically predict osmotic behavior and survival during cooling if a cell's nucleation behavior is known. Leibo et al. (Cryobiol., in press) have shown a correlation between intracellular freezing and death in mouse ova. Using death as the criterion, we determined the temperature dependence of intracellular nucleation in 8-cell mouse embryos equilibrated with 0 to 2.0 M dimethyl sulfoxide (Me_2SO) and cooled rapidly (~20°C/min). In saline survival dropped between -10 and -20°C. In 1.0, 1.5, and 2.0 M Me_2SO survival decreased over the temperature range -22 to -40°C, -37 to -42°C, and -42 to -44°C, respectively. These results suggest that the protective effect of increased Me_2SO concentration during rapid cooling is a result of colligative effects on heterogeneous and homogeneous intracellular ice nucleation. ([1]NRSA predoctoral fellow supported by NIH. Research supported by Dept. of Energy under contract with Union Carbide Corp.)

W-PM-B11 THE SELF-DIFFUSION OF WATER IN HYDRATED ARTEMIA CYSTS. P.K. Seitz* and C.F. Hazlewood. Rice University and Baylor College of Medicine. Houston, TX 77030.

Previous pulsed nuclear magnetic resonance (NMR) studies of water protons in cysts of the brine shrimp Artemia salina have shown that the T_1 and T_2 relaxation times are greatly reduced compared to pure water. A simple two fraction fast exchange model of cellular water structure (involving a small amount of tightly bound hydration water, the remainder acting essentially as free water) is insufficient to account for these data. Measurements of the self-diffusion coefficient (D) of water over the entire hydration range show a reduction in D of 10x even at the highest hydration (1.4 g/g). D is decreased by 2-3 orders of magnitude at lower hydrations. Using a current model for diffusion, calculations for the volume fraction (φ) of hydration water (at 1.4 g/g) necessary to fit the two fraction model indicate at least 70% of the total water would need to be immobile in order for the remaining molecules to retain the diffusional mobility of free water. A more gradual decrease in motional freedom (with distance from surfaces) is suggested. (Supported by Welch Q-390; ONR Contract N00014-76; and NIH grants RR-00188 and GM-20154.)

W-PM-B12 CATECHOLAMINES AND ERYTHROCYTE MEMBRANE POTENTIAL BY FLUORESCENCE. E. Lavie*, L. Friedhoff*, J. Ryan,* A. S. Schneider, and M. Sonenberg, Memorial Sloan-Kettering Cancer Center, New York, New York 10021

Upon adding erythrocytes (0.33%) to merocyanine 540 (7.2×10^{-7}M) in physiological buffer there was a two fold increase in quantum yield and a red shift of 14 nm in the emission. This is consistent with a decrease in the polarity of the medium as demonstrated by a series of solvents with merocyanine. Fluorescence has been calibrated to changes in membrane potential. At a merocyanine concentration of 2.9×10^{-6}M it was possible to demonstrate potential dependent responses by altering the chloride ratio but not with valinomycin. L-isoproterenol (10^{-6}M) caused a 20% decrease in merocyanine fluorescence in human erythrocyte suspensions and a 7% increase in fluorescence with the carbocyanine dye, CC_6. Ca^{++} (10^{-2}M) caused a 20% decrease in the quantum yield at 590 nm. It is suggested that the decrease in fluorescence reflects induced depolarization of human erythrocytes by catecholamine hormones. (Supported in part by grants CA-08748, CA-16889 and 18759 of the NIH).

PURPLE MEMBRANES II

W-PM-B13 MOBILITY AND PROXIMITY OF CELLULAR RECEPTORS MEASURED BY FLUORESCENCE ENERGY TRANSFER IN AN AUTOMATED CELL SORTER. Shirley S. Chan, D. J. Arndt-Jovin,* and T. M. Jovin,* Max Planck Institute for Biophysical Chemistry, D-3400 Goettingen-Nikolausberg, West Germany

The proximity and mobility of lectin receptor sites on Friend virus transformed mouse splenic cells have been studied by a Multiparameter Automated Computerized Cell Sorter. Tetrameric molecules of Concanavalin A that have been labeled with fluorescent chromophores(either fluorescein or rhodamine) are reacted with the cells individually or together. On the doubly-labeled cells we observe efficient fluorescence energy transfer from the flurescein donor to the rhodamine acceptor upon excitation of fluorescein with an argon laser at 488 nm. Further evidence for energy transfer is a substantial decrease in the emission anisotropy of rhodamine in the case of doubly-labeled as compared to the cells labeled only with rhodamine. These measurements are being applied to studies of macromolecular movements in the plasma membrane like patching, capping and internalization, in relation to functional states of the cell (antigenic modulation, blastogenesis, differentiation, or cytoskeletal disruption) and to other membrane properties (fluidity, lipid composition and phase transitions).

W-PM-C1 THE EFFECT OF ACID pH ON THE PROPERTIES OF BACTERIORHODOPSIN. P.C. Mowery, R. Lozier, Q. Chae*, Y.W. Tseng*, M. Taylor*, and W. Stoeckenius. Cardiovascular Research Institute and Dept. of Biochemistry and Biophysics, Univ. of Calif., San Francisco 94143

Bacteriorhodopsin (bR) from H. halobium was incorporated into 7½% polyacrylamide gels. At pH 7.0, CD spectra, visible spectra of light- and dark-adapted membranes, and the flash photolysis cycle were like those for bR suspensions. Titration of the gels showed the transition to a form absorbing at 605 nm (A605) at pH 2.7, and to a second form at 565 nm (A565) at pH 0.8. Dark-adapted gels showed an isosbestic point for each transition whereas light-adapted gels did not. Visible CD spectra of bR, A605 and A565 all showed the typical bilobed pattern. All showed photocycles under flash photolysis, with even A565 exhibiting a blue-shifted intermediate. Chromophore extraction of membrane suspensions showed all trans-retinal for A565 and a mixture of 13-cis- and trans isomers for A605. The significance of these results will be discussed.

W-PM-C2 LIGHT-INDUCED pH CHANGES INSIDE AND OUTSIDE GHOSTS OF HALOBACTERIUM HALOBIUM. R.H. Lozier, G. Sivorinovsky*, and W. Stoeckenius. Cardiovascular Research Institute and Dept. of Biochemistry and Biophysics, University of California, San Francisco 94143

Ghosts were prepared from H. halobium cells by dialysis vs. 1.8M KCl 50mM $MgCl_2$. Illumination of the ghosts causes a monotonic but multiphasic acidification of the suspending medium (determined with a glass electrode) which relaxes in the dark. The multiphasic behavior may be due to modulation of the proton pumping rate by bacteriorhodopsin as a pH gradient is generated across the membrane, and/or to modulation of the proton leak(s). The pH changes can also be followed spectrophotometrically using pH indicating dyes (e.g. p-nitrophenol); the observed absorbance changes of the dye in the suspending medium appear to dominate over possible absorbance changes of dye inside the ghosts, i.e., they are similar to the changes observed with the pH electrode. If supposedly non-permeating buffers are added (e.g., HEPES) the sign of the dye absorbance change is reversed; it is thus concluded that pH changes inside the ghosts can be measured in the presence of a permeant dye and an impermeant buffer. Time-resolved pH changes inside and outside the ghosts have been measured by flash photolysis.

W-PM-C3 pH AND TEMPERATURE EFFECTS ON THE STRUCTURE OF THE PURPLE MEMBRANE. D.D. Muccio and J.Y. Cassim Department of Biophysics, The Ohio State University, Columbus, Ohio, 43210.

Recently, the proton pumping action of purple membrane has been shown to diminish at the extreme pH limits while temperature variation has suggested a phase transition of the lipids. In view of these results we have examined the structural changes occuring for the pH range of 2-13 and a temperature range of 0°-60°C. using absorption and circular dichroic (CD) spectroscopy. In general the dark-adapted form becomes exceedingly more stable at extreme pH values and elevated temperatures. As the pH is further lowered (4.0-2.6) a new absorbing specie occurs at ca. 600 nm. The visible CD spectra show a simultaneous shift of the characteristic double band to the red with a new crossover occuring at ca. 600 nm with no change in band polarity. As the pH is raised (11.5 - 12.5) the absorption spectra blue shifts slightly to ca. 545 nm. The visible CD spectra show a rapid disappearance of the negative band relative to the positive band. Near and far UV spectra show continuous, but minor, changes. These results will be discussed in view of the exciton model recently proposed for this membrane.

W-PM-C4 EFFECTS OF SUCROSE AND GLYCEROL ON THE PURPLE MEMBRANE STRUCTURE OF HALOBACTERIUM HALOBIUM. T.L. Hsiao G.K. Papadopoulos, and J.Y. Cassim, Department of Biophysics, The Ohio State University, Columbus, Ohio 43210.

Recently publications have stressed the uncertainties in the visible circular dichroic spectrum of the purple membrane in aqueous suspensions due to optical artifacts induced by light scattering resulting from the particulate nature of the membrane. The solute-solvent refractive index matching method has been employed in an attempt to minimize such effects. Sucrose and glycerol up to 50% (w/w) and 60% (v/v) respectively have currently been used as additives. We have studied the effects of successive additions of these compounds to membrane suspensions on the membrane CD monitored over the entire accessible wavelength region. Our results indicate that although some minimization of the light scattering artifacts is achieved by these additions, significant structural alterations of the membrane are also evident. It is suggested that analysis of the spectra of membranes obtained in such suspensions should be considered with caution.

W-PM-C5 EFFECTS OF TRITON X-100 ON THE STRUCTURE OF THE PURPLE MEMBRANE FROM HALOBACTERIUM HALOBIUM. T.L. Hsiao, G.K. Papadopoulos, and J.Y. Cassim, Department of Biophysics, The Ohio State University, Columbus, Ohio, 43210.

Triton X-100, a mild non-ionic detergent, has been extensively used to solubilize cell membrane proteins. We have examined the effects on the purple membrane structure of increasing concentrations of the detergent (up to 7% (v/v)). At the highest detergent concentration, the absorption band is at 550 nm, showing a 20% decrease from the unperturbed state, but no bleaching. The double CD band centered at ca. 570 nm and the negative band at 317 nm decrease with increasing detergent concentration, eventually vanishing at 0.5% (v/v) detergent concentration. Although in the past, experiments with Triton X-100 have been interpreted in terms of an exciton interaction, a multiple transition model is equally possible from these results. Bleached purple membrane treated with the detergent cannot regenerate when all-trans retinal is added, even after complete dialysis of the detergent. We will discuss the implications of these results as they pertain to the structure of the purple membrane.

W-PM-C6 CALCULATIONS OF DISTORTIONS IN VISIBLE CIRCULAR DICHROISM OF THE PURPLE MEMBRANE. T.L. Hsiao, S.S. Wong, and J.Y. Cassim, Department of Biophysics, The Ohio State University, Columbus, Ohio, 43210.

We have made calculations regarding possible sources of distortions of visible CD spectrum of the purple membrane arising from light scattering and absorption flattening due to the particulate nature of the membrane. The computational procedures were as follows: Trial CD spectra were assumed. Complex refractive index of the particle was obtained from the Kronig-Kramers transformation of the measured absorption spectrum and from the linear dependency of the absorption coefficient on the index of attenuation. Complex refractive indices for circularly polarized light were obtained from solution measurements of absorbance, refractive index, CD, and ORD. Based upon a randomly oriented, isotropic, circular-disk particle model, a modified form of the Rayleigh-Debye scattering approximation was employed with the acceptance solid half-angle of 10° to obtain scattering factor. The trial spectrum was varied until the sum of the scattering factor and trial spectrum gave the best fit for the measured CD spectrum. The calculated spectrum obtained differed from the measured one by slight elevations of ellipticities of the double band centered at ca. 565 nm.

W-PM-C7 PROBES INTO SPECIALIZED MEMBRANE REGIONS OF HALOBACTERIUM HALOBIUM. G.K. Papadopoulos, J.E. Draheim, and J.Y. Cassim, Department of Biophysics, The Ohio State University, Columbus, Ohio, 43210.

Attempts to elucidate the events leading to the biosynthesis and assembly of purple membrane components in H. halobium have previously been reported. Two distinct membrane fractions have already been identified: P412, containing bacterio-opsin (λ_{max} = 412 nm) and a precursor membrane (called brown membrane), containing bacteriorhodopsin (λ_{max} = 568 nm) and a b-cytochrome (λ_{max} = 419 nm). We have extended these studies by investigating the structure of P412 by means of circular dichroism and detergent perturbation in the same manner as has previously been done for the study of the purple membrane structure. The relationship between the brown membrane and P412 is still unclear. However, an explanation of the possible role of P412 and its functional relationship to the purple membrane will be discussed.

W-PM-C8 PHOSPHOLIPID REQUIREMENT OF THE BACTERIORHODOPSIN PHOTOREACTION CYCLE. S.-B. Hwang, Department of Physiology, University of California, San Francisco CA 94143.

Purple membrane (PM) in 10% deoxycholate (DOC) isolated in a sucrose gradient contains 20% by weight of its original lipid. The X-ray diffraction pattern, circular dichroism spectra and negative stain electron microscopic images of DOC treated membranes are indistinguishable from those of intact PM. Also, the photoreaction cycle of bacteriorhodopsin is the same as that in intact membranes. However, at room temperature the kinetics of decay of M_{412} ($t_{1/2} \sim 100$ msec), N_{520} and O_{640} are slower in the DOC membranes. Upon addition of exogenous phospholipids (egg PC, egg PE, total lipid from H. halobium), this decay constant becomes faster as the PL/BR mole ratio increases, independently of the chemical nature of the phospholipid. In contrast, the M_{412} decay constant depends on the fluidity of the hydrocarbon region. When dipalmitoyl PC or dimyristoyl PC are added to these membranes, Arrhenius plots of the M_{412}decay constant reveal a break at the phase transition temperature of the respective phospholipid.

W-PM-C9 INTRAMOLECULAR PROTON TRANSFER DURING THE BACTERIORHODOPSIN PHOTOCHEMICAL CYCLE. R.A.Bogomolni, R. Renthal and J.K.Lanyi. Dept.Biochemistry and Biophysics, Univ. of Calif., San Francisco, 94143; The Univ of Texas at San Antonio,78285; and NASA-Ames Research Center, Moffett Field, Calif. 94035

Flash-induced absorbance changes of bacteriorhodopsin in the U.V.(actinic wavelength 560-580 nm, one millisec. after the flash) show an increase between 330 and 400 nm, corresponding to the tail of the M_{410} band. The difference spectrum shows maxima at 240 and 300 nm and a broad structured minimum (dips at 290,280 and 265 nm). We interpret this as a composite of tryptophan perturbation and the deprotonation of one tyrosine. Titration in the dark shows the deprotonation of about one tyrosine at pH 10.5, with characteristic peaks at 240 and 300 nm. The photocycle is lengthened ($t_{\frac{1}{2}}$= 0.5 sec) at pH 10.5, and the 240 and 300 nm maxima during flash disappear. The data suggest that a tyrosine is deprotonated in the normal photocycle, possibly acting as a proton donor in a chain of proton conducting groups. The tryptophan perturbation, which remains at high pH, may reflect direct interaction with retinal.

MUSCLE PHYSIOLOGY IV

W-PM-C10 TEMPERATURE DEPENDENT AGGREGATION OF BACTERIORHODOPSIN IN DIPALMITOYL- AND DIMYRISTOYLPHOSPHATIDYLCHOLINE VESICLES. M. P. Heyn, Dept. of Biophysical Chemistry, Biozentrum, CH-4056 Basel, Switzerland, R. J. Cherry* and U. Müller*, Lab. für Biochemie, ETH, CH-8092 Zürich, Switzerland, and R. Henderson*, MRC Lab. of Molecular Biology, Cambridge CB2 2QH, England.

Bacteriorhodopsin (BR) has been incorporated into large unilamellar vesicles of DPPC and DMPC. Its state of aggregation was investigated using X-ray diffraction, freeze fracture electron microscopy, circular dichroism (CD) and BR rotational diffusion measurements. At temperatures below the lipid phase transition, BR crystallizes into patches with the same hexagonal lattice observed in the purple membrane. Above the phase transition, the lattice disaggregates and the protein molecules are monomeric provided the lipid to protein ratio is sufficiently high. Small specific BR aggregates can be conveniently detected using the exciton coupling effects in the visible CD spectra.

W-PM-C11 LINEAR AND CIRCULAR DICHROISM OF ORIENTED PURPLE MEMBRANES. R. Bogomolni, S.-B. Hwang, Y.W. Tseng*and W. Stoeckenius. Cardiovascular Research Institute and Dept. of Biochemistry and Biophysics, Univ. of Calif., San Francisco 94143

Excited states of bacteriorhodopsin are split into exciton levels having transition moments perpendicular to the membrane plane (λ+state) and in-plane (λ-states). The linear and circular dichroism of oriented samples provide information on the geometry these excitonic transitions. Multilayers of purple membrane made from Langmuir films show dichroic ratios, decreasing monotonically across the absorption band towards shorter wavelength indicating that the λ+ transition lies at a longer wavelength than the λ-. The data posses an upper limit of $\leq$ 5nm for the splitting between exciton levels. The circular dichroism measured normal to the membrane plane shows a positive band peaking at around 563 nm. Because the light has no electric field component along the out-of-plane transition, this suggests that in-plane transitions have positive rotational strength. These results are inconsistent with published assignments and may significantly affect geometrical parameters estimated from CD data, e.g., larger interchromophore distances.

W-PM-D1 MEASUREMENT OF Na^+ ACTIVITY IN SHEEP PURKINJE FIBERS WITH Na^+-SELECTIVE GLASS MICROELECTRODES. C.O. Lee, J.H. Sokol* and K.S. Lee* N. Y., N.Y.

For the measurement of intracellular Na^+ activity, some properties of Na^+-selective glass microelectrodes with a sealed tip diameter less than 1μ were studied. The selectivity coefficient (k_{NaK}) and resistance (R) of the microelectrode were increased with aging in 3M NaCl, indicating that the microelectrode should be used as soon after filling as possible. The microelectrodes were insulated with a micropipette with a tip diameter less than 1μ by utilizing Thomas' design. The k_{NaK} and R of these microelectrodes increased as the exposed area of the Na^+-selective glass membrane decreased. Thus, intracellular measurements required an optimum exposed area for low k_{NaK} and R. We made the microelectrodes with an exposed tip length of about 70μ and a tip to tip length less than 10μ. The Na^+ activities in the fibers and Tyrode solution, measured directly, were 6 and 113 mM respectively. This result indicates an equilibrium potential of +74mV for the Na ion. (Supported by USPHS HL 21136 and HL 21014, and AHA Established Investigatorship).

W-PM-D2 QUANTIFICATION OF PLASMA MEMBRANE SPECIALIZATIONS IN VENTRICULAR MUSCLE CELLS. E. Page and M. F. Surdyk,* The University of Chicago, Chicago, Ill. 60637.

Plasma membrane area involved in diadic junctions with terminal cisterns (TC) of sarcoplasmic reticulum was estimated in electron micrographs of left ventricular myocardial cells of four 219-278 g female rats by an extension of the morphometric analysis of Stewart and Page (S&P), J. Ultrastruct. Res. in press. The areas so involved made up 7.7±0.8% of the external plasmalemmal envelope and 48±6% of the plasmalemma in the T-system (n=4 hearts), corresponding, respectively, to values (calculated from S&P) of .024 and .072 μm^2 plasmalemmal area/μm^3 myocardial cell volume. These values may be compared with S&P's values ($\mu m^2/\mu m^3$ cell volume) of .307±.005 (total external plasmalemma), .15±.01 (total T-system) and .0047±.0009 (nexus). If caveolar membrane area in rat heart is similar to that in rabbit heart (Levin and Page, J. Cell Biol. 75:317a:1977), an additional area of at least .10-.20 $\mu m^2/\mu m^3$ is contributed by caveolae. We suggest that in ventricle, as in skeletal muscle, release of stored Ca from TC is activated predominantly via the T-system. Supported by USPHS grants HL 10503 and HL 20592.

W-PM-D3 CELLULAR Cl CONCENTRATION OF AMPHIBIAN SKELETAL AND HEART MUSCLE IN VIVO. D.D. Macchia, E. Page, and P.I. Polimeni*, The University of Chicago, Chicago, Ill. 60637

Toads (Bufo marinus) and frogs (Rana pipiens) were injected i.p. with ^{36}Cl and $^{35}SO_4$. After in vivo equilibration of 20 to 180 min., animals were pithed, and their ventricular and semitendinosus muscles were excised. Measurements of total Cl (by titrimetry) and ^{36}Cl (by radioassay) showed that specific radio-activities of plasma and muscles approached equality within one hr after injection for toad skeletal and heart muscle and frog ventricles, indicating complete exchange of cellular Cl with ^{36}Cl. From the simultaneously measured muscle water contents and $^{35}SO_4$ spaces, intracellular Cl concentrations in vivo (in μmoles/g H_2O) for semitendinosus and ventricular muscles were calculated to be, respectively, 1.4 ± 0.3 and 2.3 ± 0.8 for Bufo and 1.7 ± 0.7 and 4.8 ± 2.4 for Rana. In view of these low values, active cellular Cl accumulation or sequestration of Cl in the sarcoplasmic reticulum seem improbable. Further, preliminary observations (Macchia, Baumgarten and Page) of in vivo membrane potential recordings of semitendinosus muscles in pithed toads are consistent with a passive distribution of Cl in these muscles. Supported by USPHS grants HL 10503 and 05551.

W-PM-D4 INTRACELLULAR Cl ACTIVITY OF SKELETAL AND HEART MUSCLE. C. M. Baumgarten* and H. A. Fozzard (Intr. by S. Glagov). U. of Chicago, Dept. Medicine, Chicago, IL. 60637

Open tip Cl ion-selective electrodes (ISE) were made of Corning 477315 liquid ion-exchanger. Frog (Rana pipiens) sartorius (FS) and quiescent rabbit papillary (H) muscles superfused with bicarbonate-free media were impaled 8 to 12 times with both ISE and 3M KCl-filled microelectrodes. Expected a^i_{Cl} was calculated from E_m and a^o_{Cl} assuming passive distribution, and E_{Cl} from a^o_{Cl} and observed a^i_{Cl}. Results (mean of means±SD) suggest that Cl is passively distributed in FS, and ISE sees 0.3-0.5 mM of extra Cl due to interfering anions. Pilot experiments (with Macchia and Page) on in vivo toad (Bufo marinus) semitendinosus gave similar results. In contrast, if the interference is the same in H and FS, then H a^i_{Cl} is far in excess of that required for passive distribution. Supported by USPHS HL 05673 and HL 20592.

	a^o_K (mM)	a^o_{Cl} (mM)	E_m (-mV) (obs)	a^i_{Cl} (mM) (calc)	a^i_{Cl} (mM) (obs)	E_{Cl} (-mV) (calc)
FS	1.9	90.3	93.9±2.4	2.2±0.2	2.5±0.2	90.8±1.5
FS	7.5	22.4	66.1±1.2	1.6±0.1	2.1±0.3	59.5±3.5
FS	1.9	22.4	93.5±3.1	0.6±0.1	1.0±0.2	80.2±3.8
H	3.9	119.6	76.1±3.1	6.1±0.9	14.2±1.7	54.0±3.0

W-PM-D5 INTRACELLULAR CHLORIDE ACTIVITY IN CARDIAC PURKINJE FIBERS. K.W. Spitzer*, J.L. Walker and W.G. Wier*, Dept. of Physiol., U. of Utah, Salt Lake City, UT 84108.

Chloride equilibrium potential (E_{Cl}) and intracellular chloride activity (a^i_{Cl}) were measured in canine Purkinje fibers (a^o_K=1.9 mM, a^o_{Cl}=100.4 mM) using Cl^- liquid ion exchanger microelectrodes. For stimulated preparations, membrane potential (E_m) and E_{Cl} were measured 5 sec after the maximum diastolic potential. The means ± SE for E_m, E_{Cl}, and a^i_{Cl} for 19 preparations stimulated (1.5 Hz) for 2-3 hrs were respectively: -100.3±0.7 mV, -42.7±0.6 mV and 20.4±0.5 mM. Continuous stimulation at 1.5 Hz for an additional 2-3 hrs resulted in a significant decline in E_m of 3.7±1.4 mV but not E_{Cl}. Preparations stimulated for 2 hrs at 1.5 Hz then at 0.3 Hz for 2-3 hrs also showed no change in E_{Cl} despite a fall in E_m of 9.2 ±0.3 mV. In addition, 2 hrs at 1.5 Hz then 2 hrs at rest (a^o_K=3.7 mM to suppress spontaneous firing) produced no change in E_{Cl} (-42.2 mV) even though E_m fell from -88.0±0.4 to -78.8±0.6 mV. Rate changes of this magnitude are predicted to change E_{Cl} if Cl^- distribution is passive (McAllister et al., J. Physiol. 251: 1, 1975; Hutter and Noble, J. Physiol. 157: 335, 1961). Supported by NIH grant HL 18053.

W-PM-D6 RELAXATION OF ISOLATED SMOOTH MUSCLE CELLS INDUCED BY INTRACELLULAR MICROINJECTION OF CYCLIC NUCLEOTIDES. F.S. Fay and S.R. Taylor, Mayo Foundation, Rochester, Minnesota 55901

Many studies have tested the possible role of cyclic nucleotides (cAMP) in the catecholamine-induced relaxation of smooth muscle. Relaxation was associated with increased cAMP in most studies. However, relaxation has also been observed without an increase, and an increase has in some cases been measured without relaxation. Hence, it remains uncertain if intracellular cAMP can in fact induce relaxation of smooth muscle. To test this directly we microinjected cAMP and other substances into single isolated smooth muscle cells. The cells were isolated by enzymatic digestion of the stomach muscularis of Bufo marinus (Am.J.Physiol. 232: C138,1977). Solutions were pressure injected into the cells through glass micropipettes (20-40 MΩ when filled with 3M KCl). The impalements, injections, and subsequent contractile responses to electrical stimulation were recorded by cinemicrography. The micrographs showed that the quantity of liquid usually injected was 2 to 8% of the cell volume. Insertion of a micropipette tended to initiate contraction, and the cells continued to contract and remained shortened when Ca^{2+}, Mg^{2+}, Na^+, or H_2O were injected. On the other hand, injection of cAMP (1mM) caused a prompt, rapid, extensive, and sustained relaxation. Injection of chelators (e.g., EDTA) also produced relaxation. This is the first direct evidence that increased intracellular cAMP can induce relaxation in smooth muscle. These findings strongly support the idea that relaxation observed in the presence of catecholamines is mediated by increased intracellular cAMP. (Supported by HL 14523 to FSF, and by NS 14268 and AHA 77983 to SRT.)

W-PM-D7 VARIATION OF PHOSPHATE METABOLITES IN NORMAL AND DUCHENNE HUMAN MUSCLE. C.T. Burt, M.J. Danon*, E.A. Millar*, F.L. Homa*, M.D. Vuolo*, M. Bárány and T. Glonek*, Univ. of Ill. Med. Ctr., Chicago, 60612 and Shriner's Hospital, Chicago, 60635

In the course of analyses of perchloric acid extracts by ^{31}P nmr we have tabulated differences between normal and diseased muscles. Values are given below in μmole/g muscle.

Muscle	Total P	PCr+P_i	ATP	GPC	(n)
Biceps	51.3	31.9	4.9	0.0	3
Gastrocnemius	53.3	31.8	4.9	1.7	4
Adult quadriceps	49.7	30.4	4.1	0.8	4
Child quadriceps	42.7	25.5	4.6	0.5	4
Duchenne quadriceps	22.9	12.3	1.7	0.1	14

Of all metabolites glycerol phosphoryl choline (GPC) shows the greatest range of variation. It is interesting that the muscles lowest in GPC are those most affected early while the gastrocnemius is relatively spared (Johnson et al., J. Neurol. Sci. 18, 111-129, 1973). We have also found a class of muscles which have elevated GPC levels particularly those with Werdnig-Hoffman syndrome. (Supported by Muscular Dystrophy Association and Chicago Heart Association).

W-PM-D8 SERINE ETHANOLAMINE PHOSPHODIESTER SYNTHASE AND DIESTERASE ACTIVITIES IN NORMAL AND DYSTROPHIC CHICKEN TISSUES. J.M. Chalovich*, M. Bárány, F.L. Homa*, and C.T. Burt, Dept. of Biological Chemistry, Univ. of Ill. Med. Ctr., Chicago, Ill. 60612.

We have recently shown that serine ethanolamine phosphodiester (SEP) is present in high levels (2.5 mM) in the pectoralis muscle of hereditary dystrophic chickens but is virtually absent from normal chicken muscle (Chalovich, et al., Arch. Biochem. Biophys. 182, 683, 1977). We have now assayed for the activities of SEP synthase and SEP phosphodiesterase in microsomes from the pectoralis muscle, kidney and intestinal mucosa of dystrophic and normal chickens. SEP phosphodiesterase activity was measured at pH 9.5 either as the rate of release of ^{14}C-ethanolamine phosphate from [^{14}C-ethanolamine]-SEP or by the release of P_i in the presence of alkaline phosphatase. SEP synthase activity was measured as the rate of [^3H-serine]-SEP production from CDP-ethanolamine and ^3H-serine at pH 7.5. The diesterase activity in dystrophic muscle was about 14 times that of normal muscle and the synthase activity was increased by more than 8 times. There was little difference in the enzymic activities of other tissues. (Supported by MDA, CHA & NS-12172 from NIH)

W-PM-D9 FUNCTIONAL HETEROGENEITY OF SARCOPLASMIC RETICULUM IN SKINNED FIBERS. M.M. Sorenson, J.P. Reuben, M. Orentlicher and G.M. Katz. H.H. Merritt Res. Ct. Dept. Neurology, Columbia University, New York, N.Y. 10032.

Light scattered at 90° by relaxed skinned fibers (rabbit psoas) is proportional to their protein content. When Ca^{++} (10^{-7}–10^{-6}M) and oxalate (0.5–25mM) were added scattering increased in proportion to the amount of ^{45}Ca accumulated. Thus scattering provides a quantitative measure of both rate of Ca accumulation and Ca capacity of SR under conditions in which Ca is not depleted from the medium. At saturating [oxalate], lowering [Ca^{++}] depresses rate of filling with little effect on maximal capacity. However, at fixed [Ca^{++}], lowering [oxalate] decreases capacity and rate of Ca accumulation in proportion to one another. From this proportionality, we infer that lowering [oxalate] reduces the fraction of SR that forms Ca oxalate precipitate, without affecting filling rates of remaining elements. We conclude that changing [oxalate] reveals a heterogeneity in the ability of the SR to accumulate net amounts of Ca. The SR is also heterogeneous in its interaction with caffeine and X-537A: like oxalate, these agents affect both rate and capacity proportionately. Supported by NIH and MDA.

W-PM-D10 THE EXTRACELLULAR SPACES OF FROG SKELETAL MUSCLE. Margaret C. Neville, University of Colorado Medical Center, Denver, Colorado, 80262.

Solute efflux from frog sartorius and semitendinosus muscles shows two components arising from compartments accessible to all constituents of the bathing medium. The fast component (A) appears to arise from the true extracellular space. The rate constants for the second component (B) were 6 to 10 times slower than those for A and were proportional to the diffusion coefficient of the solute in question. B arose from a compartment similar in size to the sarcoplasmic reticulum. It increases in size in hypertonic solutions. This compartment has now been shown to be accessible to inulin (M.W. 5000) and dextran (M.W. 17000). Sodium and sucrose efflux from single fibers from frog semitendinosus muscle was studied. Although a B component was present in 21 out of 24 fibers, it occupied a space only 1.8 ± 0.4 % of fiber volume. The size was not increased in hypertonic solution. These findings indicate that component B arises from an extrafibrillar space and imply that the fluid in the sarcoplasmic reticulum is similar in composition to intracellular fluid. (Supported by NIH grant AM 15807.)

W-PM-D11 SUBCELLULAR LOCALIZATION OF HRP EFFLUX COMPONENTS IN FROG SKELETAL MUSCLE. H. Rubin* and M.C. Neville, Dept. of Physiol. U. Colo. Med. Ctr., Denver, CO

Analysis of molecular efflux from frog sartorius muscle indicates three components, but the cytological origin of the intermediate component is unclear. In this study, we have correlated washout data with cytochemical localization of efflux components using horseradish peroxidase (HRP). HRP washout curves resolved into three components with half-times of 1, 7 and 63 min. The distribution space was 3.5% of muscle volume for the first two components and 10% for the third. These results were consistent with data from earlier washouts, with the slow HRP fraction being consistent with the intermediate molecular efflux component and the first two HRP fractions with the ECS. Electron cytochemistry showed that at t_0, HRP was localized in the perimysium, within capillaries and in the t-tubule system. After wash times of 12, 30 and 120 min., a uniform deposition of reaction product was observed only within capillaries. These data tend to favor localization of the fast HRP fraction in the ECS and the slow fraction in capillaries. The evidence suggests that the intermediate component of earlier studies may be associated with the vascular space.

W-PM-D12 LASER DIFFRACTION STUDIES OF SARCOMERES DURING RELAXATION. K.A.P. Edman, F.W. Flitney* and L. Glass*. Department of Pharmacology, University of Lund, Sweden.

Sarcomere behaviour during relaxation has been investigated further in single muscle fibres of R.temp. (Edman & Flitney, J.Physiol. 1978, in press, also earlier references). Sarcomere lengths (SL) were monitored by streak photography of diffraction spectra produced by illuminating the fibre with a laser at 1 mm consecutive intervals. SL changes during single (S) and double (D) twitches were compared to those in a fused tetanus (T). The times to onset (t_1) and peak length change (t_2) increased in order: S<D<T. t_1 occurred when tension fell to 73% (S and D) and 68% (T) of peak values (equivalent to 58% (S), 64% (D) and 68% (T) of peak tetanic force). SL changes during tetani were studied at different lengths (1.9-3.2 um) and temperatures (0-20°C). It is concluded that differences in the duration of activity along the fibre length determines sarcomere behaviour during relaxation. Local elastic forces in stretched regions of the fibre (i) limit shortening of sarcomeres having the longest duration of activity and (ii) restore sarcomeres to their initial length.

W-PM-D13 THE ULTRASTRUCTURE OF CHEMICALLY SKINNED HUMAN AND RABBIT SKELETAL MUSCLE. A.B. Eastwood*, D.S. Wood* and K.L. Bock* (Intr. by J.P. Reuben). H.H. Merritt Res. Ct. Dept. Neurology, Columbia U., New York, N.Y. 10032.

Exposure of mammalian skeletal muscle to "skinning" solution (S) containing (in mM): 170 KProp; 5 EGTA; 2 MgATP; 5 Imidazole at pH 7.0 and 5° C, causes irreversible loss of ion selective permeability of the sarcolemma, but contractile protein and sarcoplasmic reticulum (SR) function remain. Fibers were fixed for EM examination after exposure to S for varying times, by adding 0.4% formaldehyde and 1% glutaraldehyde to S, then osmicating and embedding. Gaps in the sarcolemma appear after 1 hr in S, and their size and number increased with time. T-tubules persisted, some SR elements vesiculated and mitochondria were swollen with severe disruption of outer and inner membranes. Storage for 1 month in S with 6 M glycerol at -20°C produced little further change in membrane ultrastructure. Ultrastructural changes observed suggest that (i) the basis for, and irreversibility of, the chemical skinning process is in part related to loss of sarcolemma, and (ii) the membrane systems differ in their sensitivity to low Ca^{++} solutions. The basis for these differences are being studied. Supported by NIH and MDA.

W-PM-D14 ANALYSIS OF FLUCTUATIONS IN INTER-BEAT INTERVAL (IBI) OF SMALL CLUSTERS OF SPONTANEOUSLY BEATING EMBRYONIC HEART CELLS. J.R.Clay and R.L.DeHaan, Dept. of Anatomy, Emory University, Atlanta, Ga. 30322.

We have recorded trains of interbeat intervals from small synchronously beating clusters containing 1 to 100 heart ventricular cells prepared from 7 day old chick embryos. The clusters normally beat spontaneously in 1.3mM K^+ at 38°C. This activity was monitored by a phototransistor positioned on the television image of a phase contrast microscope view of the preparation. The mean IBI was typically 400 to 550 ms. The larger clusters tended to beat more slowly. The fluctuations of beating were analyzed with IBI histograms calculated from 400-500 intervals. The coefficient of variation (CV) was 15-20% for clusters of 1-10 cells and 1-3% for groups of 50-100 cells. Data from 50 clusters suggest that $CV \sim N^{-\frac{1}{2}}$ (N=number of cells). Measurements of voltage noise and impedance from intracellular impalements of larger aggregates indicate that the RMS voltage noise amplitude is proportional to $R_i^{\frac{1}{2}}$ (R_i=input resistance) and that $R_i \sim 1/N$, suggesting that fluctuations in IBI of the small clusters is related to membrane voltage noise. (Supported by NIH HL16567, HL 05346).

W-PM-D15 CYCLOHEXIMIDE BLOCKS THE DEVELOPMENT OF SENSITIVITIES TO TTX AND K^+ IN EMBRYONIC HEART CELL AGGREGATES. R. D. Nathan, Dept. of Physiology, Texas Tech University School of Medicine, Lubbock, Texas 79409

Cycloheximide (CH), an inhibitor of protein synthesis, was added to the medium bathing aggregates of 3-day chick heart cells after 2 days in culture (3+2). After 2 additional days in CH, intracellular recordings were obtained from 3+4-day aggregates. These aggregates failed to differentiate fast Na^+ channels. Upstroke velocities were: (1) $\leq$ 20 V/s; (2) not influenced by TTX; (3) reduced 56-64% by D600. Untreated 3+4-day controls had upstroke velocities $\geq$ 90 V/s, reduced to $\leq$ 20 V/s in TTX but not affected by D600. The durations of action potentials in CH-treated aggregates were greater than those in untreated controls, and increased 10-68% in 12mM K^+. Spontaneous action potentials in treated aggregates continued at depolarized potentials of -53 to -28mV in 12-30mM K^+; however 3+4-day controls ceased beating in 12mM K^+ at potentials more positive than -60mV. These results suggest that products of protein synthesis are essential for *in vitro* development of electrical properties in embryonic cardiac muscle. Supported by NIH grant HL 20708.

NERVES AND AXONS IV

W-PM-E1 THE EFFECTS OF Ca^{++} ON BURSTING NEURONS: A MODELLING STUDY. Richard E. Plant, Dept. of Mathematics, University of California, Davis, CA 95616

Many observed effects of ionized calcium on bursting pacemaker neurons may be accounted for by assuming that calcium has multiple effects on the membrane conductance mechanisms. Two models are proposed which represent extreme cases of a set of possible models for these multiple effects. Both models are a priori designed to account for directly observed phenomena, and both are found to be able to simulate a posteriori certain observed phenomena including persistent inactivation, increasing spike width, and decreasing after-polarization. Experimental tests are proposed for the decision of validity between the set of models discussed and the null hypothesis, and for the decision of validity between the two models themselves. Extensions of the models are discussed. One of these extensions leads to a simulation of the behavior of the cell placed in a calcium-free bathing medium.

W-PM-E2 PROBLEMS IN DETERMINING IONIZED CALCIUM CONCENTRATION BY ARSENAZO III. S. Tsuyoshi Ohnishi. Hahnemann Medical College, Phila., Pa. 19102

As a metallochromic indicator for the assay of ionized Ca, arsenazo III (AZ) is 50 times more sensitive than murexide (MX). However, due to the high binding constant for Ca, a considerable amount of Ca (sometimes 80% of total Ca) is bound to AZ itself. Therfore, the absorbance changes of AZ do not directly show the concentration of ionized Ca.

A method has been developed whereby the ionized Ca concentration can be determined either by graphical analysis or by using the computer. It was found that the ratio of (ionized Ca)/(total Ca) changes depending upon the pH or the concentrations of AZ, Ca and other salts. For the assay of Ca in physiological media, it is preferable to have a high Ca/Mg sensitivity ratio. The ratios of MX, tetramethyl MX and AZ were found to be 1840 : 510 : 40. Although AZ is a useful indicator, these problems should be realized in using it.

W-PM-E3 COLORIMETRIC DETERMINATION OF CALCIUM AND pH CHANGES UNDER VOLTAGE CLAMP IN MOLLUSCAN NEURONS. J.A. Connor and Z. Ahmed*. Univ. of Illinois, Urbana, IL61801

The absorbance of injected indicator dyes was monitored simultaneously with transmembrane current in neural somata from the marine gastropod Archidoris monteryensis. Arsenazo III underwent a steady increase in absorbance during voltage clamp pulses. The slope of the absorbance signal increased with clamp voltage up to +40 mV. It decreased thereafter becoming vanishingly small or slightly reversing above +120 mV. The spectral dependence of the absorbance change matches the Ca-Arsenazo difference spectrum taken in the presence of Mg. Removing Ca from the external saline or chelating it internally with EGTA abolished the absorbance change. We conclude that the Arsenazo signal reflects an increase in internal [Ca] due to transmembrane influx. The post-pulse recovery of the Arsenazo signal only partially reflects the return of [Ca] to its rest level. There was a wavelength-dependent undershoot which was abolished by increasing the pH buffering capacity of the cell by injecting Imidizo (pH 7). Absorbance measurements using the pH indicator Bromocresol Purple showed a pH drop occurring with a similar time course to the Arsenazo signal undershoot.

W-PM-E4 THE EFFECT OF Ca_i^{++}, Na_i^+ AND ATP ON THE Ca INFLUX IN DIALYZED SQUID AXONS. R. DiPolo* (Intr. by G. Whittembury), IVIC, Caracas 101, Venezuela.

Ca influx was measured using a modification of the dialysis technique by controlling very carefully the dialyzed segment of the axon exposed to the external radioactive medium. In the presence of ATP and at low Ca_i^{++}= 0.066 μM, Na_i^+ activates the Ca influx along a sigmoid curve ($K_{1/2}$=65 mM). At high Ca_i^{++}=0.8 μM the activation curve changes markedly to a rectangular hyperbola ($K_{1/2}$= 32 mM). At zero Ca_i^{++} no Na_i-dependent Ca influx was observed. In the presence of internal sodium, Ca_i^{++} activates the Ca influx along a sigmoid curve. This activation is totally dependent on the presence of Na_i since there is no Ca_i-dependent Ca influx in the absence of Na_i. Removal of ATP completely inhibits the Na_i-dependent Ca influx. These results show first, that Ca_i^{++}, Na_i^+ and ATP are absolute requirements for the carrier mediated Ca influx. Second, that the stoichiometry of the Na_i-dependent Ca influx depends on Ca_i^{++}, and finally, that the absence of Ca_i-dependent Ca influx in the absence of Na_i^+ and/or ATP strongly argues against the existence of a Ca-Ca exchange mechanism.

(Supported by CONICIT, grant # 31.26.S1-0602)

W-PM-E5 SODIUM ELECTROCHEMICAL GRADIENT AND CALCIUM EFFLUX IN SQUID AXONS. J. Requena. Centro de Biofísica y Bioquímica, IVIC. Apartado 1827, Caracas 101-Venezuela.

The effect on Ca efflux of various Na_o and Na_i concentrations was explored in dialyzed giant axons from the tropical squid D.plei. In the absence of ATP_i, Ca efflux increased 3.4±0.2 fold when Na concentrations were reduced from 440/80 to 110/20 mM of Na_o/Na_i; that is, at constant electrochemical gradient for Na. In the presence of ATP_i, similar treatment did not have an appreciable effect. The inhibition of Ca efflux produced by Na_i, in the absence of ATP, was found to be of the uni-molecular non-competitive type (K_I=33±5 mM Na_i), while in the presence of ATP, it appears to be non-saturable with a K_I of ca. 180 mM Na_i. The effect of Na_o on Ca efflux was studied at low Na_i (8 mM). Under this condition, a K_A of 80 mM Na_o was obtained, independent of the ATP concentration. It is concluded that most probably the Ca efflux system uses the energy of the Na electrochemical gradient and that 4 or more Na_o are used in the exchange. The role of ATP appears to be that of a catalyst which prevents the binding of one Na ion to an internal site, which when occupied, inhibites the outward translocation of Ca.

(Supported by CONICIT project N° 3126-S1-0602).

W-PM-E6 ^{45}Ca EFFLUX FROM MYXICOLA GIANT AXONS. R.F. Abercrombie and R.A. Sjodin, University of Maryland School of Medicine, Baltimore, Maryland 21201

Calcium transport in the giant nerve cell of the marine annelid Myxicola infundibulum has been studied by injecting these cells with ^{45}Ca-EGTA buffers and following the efflux of ^{45}Ca into various artificial seawater solutions. Results indicate that Ca efflux is dependent on external Na and Ca. Na_o activation in the presence of Ca_o is one-half maximal when Na_o = ~150 mM. Ca_o activation is, however, more complicated. Experiments designed to determine Ca efflux as a function of Ca_o suggest that the Ca efflux is not only membrane limited but may reflect some intracellular process. External application of 2.5 mM caffeine increases the Ca efflux in these axons. These results are taken to support the hypothesis that Myxicola giant axons have an internal Ca buffering capacity which can alternately sequester or mobilize ionized Ca_i (even in the presence of EGTA) and that caffeine or elevated Ca_i leads to increased mobilization of Ca_i.

W-PM-E7 CONCENTRATION DEPENDENCE OF CALCIUM UPTAKE BY SQUID AXON MITOCHONDRIA MEASURED IN SITU. F. J. Brinley, Jr., T. Tiffert, and A. Scarpa, Univ. of Maryland Sch. of Med., Baltimore, Md. 21201 and Univ. of Pennsylvania Sch. of Med., Philadelphia, Pa. 19174.

The metallochromic indicators Arsenazo III and Antipyrylazo III, microinjected into isolated squid axons, were used to measure calcium uptake by structures presumed to be mitochondria on the basis of FCCP and/or cyanide sensitivity. Known amounts of calcium were loaded into fibers either by stimulation or by soaking in high calcium salines. The subsequent time course of intracellular ionized calcium was followed with the fiber in calcium and sodium free saline to minimize loss of total calcium. Metabolically dependent calcium uptake was minimal below 300 nM free Ca, but increased sigmoidally to a probable maximum of about 20-30 μmol Ca/kg axoplasm at 50 μM free Ca. Results indicate that at physiological concentrations of free calcium, homeostasis is not mediated by mitochondria but rather by membrane pumps or metabolically insensitive buffers. Supported by grants: HL 18708, NS-13402, BNS 76-19728, 7 F22 NS00021-03.

W-PM-E8 OXALATE PRODUCES PRECIPITATES IN ENDOPLASMIC RETICULUM OF Ca-LOADED SQUID AXONS. M. Henkart, AFRRI, Bethesda, Md. T.S. Reese, NIH, Bethesda and F.J.Brinley Dept. Physiol. U. Md. Schl. Med., Baltimore, Md.

Squid giant axons were loaded with Ca by stimulation in artificial sea water containing high Ca. Some loaded axons and some axons not loaded with Ca were injected with K-oxalate. All axons were rapidly frozen and transferred to osmium/acetone at liquid N_2 temperature. After freeze substitution axons were embedded in plastic, and thin sections were observed unstained in the electron microscope. In axons that were loaded with Ca and injected with oxalate, ppts were found within the ER and in mitochondria. In axons injected with oxalate without Ca loading the ER contained small amounts of ppt. In axons loaded with Ca but not injected with oxalate the ER and mitochondria appeared swollen, but neither contained ppts comparable to those in oxalate injected axons. Presumably these ppts are Ca-oxalate, and the results, then, strongly suggest that the ER is a compartment involved in control of cytoplasmic Ca in the squid giant axon.

Supported, in part, by grants from NIH NS 13420 and NSF BNS 76-19728.

W-PM-E9 CALCIUM AND FAST AXOPLASMIC TRANSPORT IN MAMMALIAN NERVE. S. Ochs, S. Y. Chan*, R. M. Worth*, and R. Jersild*. Indianapolis, Indiana 46202

The effect of Ca^{2+}-free media on axoplasmic transport in vitro was assessed in desheathed peroneal nerves. L7 dorsal root ganglia of cats were injected with ^3H-leucine and 2 hrs allowed for downflow of labeled polypeptides into tibial and peroneal nerve fibers. The sciatic nerve was then removed, the peroneal branch desheathed, the nerves placed in flasks and oxygenated at 38°C for further downflow in vitro. In a Ca^{2+}-free NaCl medium, a complete block of axoplasmic transport was seen in 2.6 hrs in the desheathed nerve. With 5 mM Ca^{2+} in isotonic NaCl or sucrose, the usual transport was maintained. With a [Ca^{2+}] of 1.5 to 3.0 mM, an addition of 4 mM K^+ was required to maintain the usual pattern of downflow. Substituting 5 mM Mg^{2+} for Ca^{2+} produced transport block after 3.5 hrs. Block also occurred at levels of Ca^{2+} above 25 mM. Loss of microtubules was seen at 95 mM. These results indicate that a regulation of Ca^{2+} in the fibers is required to maintain transport. Supported by NIH grant PHS R01 NS 8706-09, NSF grant BNS 75 03868-A03 and the Muscular Dystrophy Assoc. Inc.

W-PM-E10 PROTEIN RELEASE FROM THE INTERNAL SURFACE OF THE SQUID GIANT AXON DURING EXCITATION AND POTASSIUM DEPOLARIZATION. H. Pant, S. Terakawa*, J. Baumgold* and I. Tasaki, Bethesda, Maryland 20014.

The amount of protein released into the perfusate of internally perfused squid giant axons increased as a result of the following manipulations: 1) Repetitive electrical stimulation of the axon perfused with either normal KF containing perfusion solution or tetraethylammonium (TEA) containing perfusion solution, 2) depolarization of the axon with external application of a potassium rich solution and 3) perfusion with 4-aminopyridine solution which induces spontaneous electrical activity in the axon. Analyses by the method of SDS-polyacrylamide gel electrophoresis revealed that the proteins in the perfusate are different from those in the extruded axoplasm. These observations indicate that there exists a specific group of proteins closely associated with the axonal membrane and that these proteins play an important role in the membrane excitability.

PHOTOBIOLOGY AND OPTICAL SPECTROSCOPY

W-PM-F1 CHARACTERISTICS OF LIGHT EMISSION FROM SINGLE BIOLUMINESCENT CELLS. R. Krasnow*, E. Haas*, J. Dunlap*, and J.W. Hastings, The Biological Laboratories, and W. Vetterling, Physics Dept., Harvard University, Cambridge, MA 02138

Photon counting was used to measure the light output of luminescent cells. Two organisms with different characteristic light output were studied: marine bacteria and dinoflagellates. Bacterial emission is apparently continuous, $\sim 10^3$-10^4 q/sec/cell, this being highly variable because the luciferase system is inducible. Reported rhythmic variations (Biofizika 18, 285:1973) were reinvestigated by autocorrelation. In dinoflagellates emission is believed to involve subcellular structures and has two components, both of which exhibit circadian variations: an apparently continuous dim emission $\sim 10^3$ q/sec/cell at peak, and 0.1 sec flashes, $\sim 10^6$ q/flash/cell. These values are from measurements of populations. Studies with single cells suggest that the glow of a population may be composed of many small bursts (distinct from flashes because there are fewer quanta per burst). Flash rate and intensity were studied with different cell numbers to evaluate the possibility of cooperativity in flashing.

W-PM-F2 PROPERTIES OF GLYCOLUCIFERASE ISOLATED FROM *PHOTOBACTERIUM LEIOGNATHI*, strain s-1. P.McIlvaine,* W. C. Chen,* and N. Langerman, Utah State University, Department of Chemistry & Biochemistry, Logan, Utah 84322.

Glycoluciferase has been isolated from *Photobacterium leiognathi*, strain s-1. The enzyme exhibits bacterial luciferase activity with a specific activity of 1×10^{15} quanta/s/OD_{280} when tetradecanal is used. The enzyme cosediments with inner membrane marker proteins in a 30% - 60% sucrose gradient. The decay constant with tetradecanal is 1.3 s^{-1}. Also isolated from lysates of the same bacterium is a soluble form of the protein which apparently does NOT contain carbohydrate. The properties of this soluble luciferase are very similar to those of *Beneckea harveyi* luciferase; the specific activity and decay constant are 1×10^{14} quanta/s/OD_{280} and 0.33 s^{-1}, when decanal is used. A second relative maximum of the decay constant of 0.31 s^{-1} is obtained when tetradecanal is used. The distribution between glycoluciferase and soluble luciferase, *in vivo*, based on the activity of each in the initial lysates, from cells harvested in late log phase is about 70:30 in favor of the glycoprotein. Little, if any glycoluciferase is present prior to late log phase. (Supported in part by NIH grant GM 22049)

W-PM-F3 DOUBLE MUTANTS OF PHYCOMYCES WITH ABNORMAL PHOTOTROPISM. E.D. Lipson, D.T. Terasaka*, and P.S. Silverstein*, Department of Physics, Syracuse University, Syracuse, New York 13210

Seven genes (madA to madG) are known which affect the stimulus-response pathway for phototropism in Phycomyces. The present work is directed towards elucidating the dynamic interaction between the respective gene products. Double mutant strains are being constructed for all 21 pairwise combinations of the seven mad genes. The strains are isolated from the progeny of crosses between single mutants of opposite mating type. After physiological screening of the progeny, the double mutants are identified by complementation tests against the appropriate single mad mutants. The resulting strains are being examined first for their phototropic-geotropic equilibrium angle as a function of light intensity. Preliminary data on seven double mad strains indicate a limited reduction of phototropism relative to the parentals. So far none of the double mutants appear totally blind. These strains will be studied comparatively by system identification and analysis methods using white noise stimulus programs (Lipson, Biophysical J. 15: 989, 1975). Supported by NIH grant GM 24367.

W-PM-F4 ROLE OF LIPID REGION DAMAGE IN YEAST PHOTODYNAMIC INACTIVATION. G.E. Cohn J.M. Collins* and J.E. Clark*, Biophysics Laboratory, Physics Department, Illinois Institute of Technology, Chicago, IL 60616.

Eosin Y sensitizes the photodynamic inactivation of Saccharomyces cerevisiae by visible light primarily by generating singlet molecular oxygen in the extracellular medium. Spin label ESR spectroscopy of the hydrocarbon probe 12 NS_{me} has been employed to identify changes in lipid regions which follow inactivating irradiation. Spectra of 12 NS_{me} at 30°C before irradiation exhibited one 3-line signal characteristic of a more polar region, with a tumbling time $\tau_o \simeq 3.0$ ns. Following irradiation to 0.3% survival a large additional contribution appeared with a hyperfine splitting and g-factor of a nonpolar region, while the polar contribution became sharper. Experiments with the label 2N19 in Asolectin liposomes showed a postirradiation doubling of τ_o below the phase transition with minimal destruction. In view of kinetics and uptake data, these results indicate that damage to lipid regions, particularly the plasma membrane, plays a significant role in inactivation. (Supported by Research Corporation Cottrell Research Grant No. 7250 and by U.S. ERDA Contract E(11-1)-2217).

W-PM-F5 KINETICS OF PHOTODYNAMIC REACTIONS IN LARGE BIOLOGICAL TARGETS. L.I. Grossweiner, Illinois Institute of Technology, Chicago, Illinois 60616

Bimolecular reaction kinetics are not applicable if the diffusion range of the intermediates is comparable to the target dimensions. Ab initio solutions of Fick's 2nd law for isolated, spherical targets lead to effective bimolecular rate constants for the Type I process (e.g. triplet sensitizer): $k = 4\pi RDq(1+R/L)$ and Type II process (e.g. singlet oxygen or superoxide): $k' = 4\pi RD'q'[1+R/(L+L')]$; R is the target radius, D is the diffusion constant, L is the diffusion length and $1/q = 1+(4\pi RD/k^o)(1+R/L)$, where k^o is the equilibrium rate constant at the target surface. The L's depend on the irradiation conditions according to: $L^2 = D/a$ where a is the pseudo-first order scavenging rate constant. This formulation can be expressed in terms of quantum yields or "hits" with an appropriate damage efficiency foreach reactive intermediate. The results reduce to usual competition kinetics for small targets ($R \ll L$) but are significantly different for targets comparable to or larger than bacteriophage. (Supported by PHS Grant GM-20117 and ERDA Contract E(11-1)-2217).

W-PM-F6 LASER FLASH PHOTOLYSIS OF AQUEOUS TYROSINE. J.F. Baugher and L.I. Grossweiner, Illinois Institute of Technology, Chicago, Illinois 60616

Laser photolysis of aqueous TYR at 265 nm leads to the triplet state (^{3}Tyr) and the p-alanylphenoxyl radical (Tyr$^\cdot$) with quantum yield 0.14, formed by electron ejection (0.6) and bond splitting (0.4). In 4M Br^- the ^{3}Tyr yield increases by 1.6 accompanied by fluorescence quenching (0.2) but the photolysis yield remains the same. Assuming monophotonic photolysis from a precursor of the fluorescent state leads to: $\phi_T = \phi_S(F-1)/(FT-1)$ where ϕ_T is the intersystem crossing efficiency, ϕ_S is the quantum efficiency for populating the fluorescent state, F is the relative fluorescence quenching and T is the relative triplet enhancement by Br^-. The data lead to $\phi_T \gtrsim 0.49$, where the upper limit corresponds to negligible deactivation of the photolysis precursor. This value of ϕ_T agrees with low temperature phosphorescence measurements. Monophotonic photoionization of TYR is supported also by the dependence of initial product yields on laser intensity and measurements on the dipeptide TRP-TYR showing a high initial yield of the (Tyr$^\cdot$)-TRP radical. (Supported by ERDA Contract E(11-1)-2217.

W-PM-F7 LASER FLASH PHOTOLYSIS OF CARBOXYPEPTIDASE A. Joon Y. Lee and L.I. Grossweiner, Illinois Institute of Technology, Chicago, Illinois 60616

Transient spectra from 265 nm laser photolysis of CPA show that about 5 of the 7 TRP residues may be photoionized leading to Trp$^\cdot$ radicals. The ejected electrons are captured by the single cystyl bridge via an internal process and solvated in the medium as e^-_{aq}. The inactivation quantum yield of 0.010 ± 0.003 corresponds to the photolysis of one TRP residue in the primary act. The biochemical evidence that TRP is not essential in CPA can be explained by postulating TRP photolysis mediates the release of the essential zinc ion, specifically TRP 73 adjacent to the liganding GLU 72. In apo-CPA the number of photolabile TRP residues is reduced from 5 to 4, attributed to a shift of TRP 73 to a more hydrophobic environment in the inactive conformation. The pulsed laser techniques used in this work are convenient for measurements of enzyme inactivation quantum yields, requiring neither optically "thin" nor completely absorbing samples. (Supported by ERDA Contract E(11-1)-2217).

W-PM-F8 FLASH PHOTOLYSIS OF HUMAN SERUM ALBUMIN: CHARACTERIZATION OF THE INDOLE TRIPLET ABSORPTION SPECTRUM AND DECAY AT 293°K. B. Hicks*, M. White+*, C.A. Ghiron, R.R. Kuntz*, W.A. Volkert. Dept. of Biochem., Univ. of MO., Columbia, MO. 65201, Dept. of Chem.+, Central State Univ., Edmond, OK. 73034.

The method of flash photolysis was employed to identify the transient absorption spectrum and to characterize the decay kinetics of the indole triplet of Human Serum Albumin. This protein was studied because it contains a single indole side chain which is deeply buried in an expandable oily region and because the phosphorescence of this moiety could not be detected at 293°K. The transient was identified on these bases: (1) its triplet-triplet absorption spectrum ($\lambda_{max} \simeq 460$ nm) is very similar to those previously reported for indole and tryptophan; (2) it is quenched by small quantities of oxygen; and (3) it is photobleached by 370-700 nm light. In a nitrogen saturated solution at 293°K, the indole triplet decays exponentially for over one log with a lifetime of 0.5 ms. These observations suggest that because of its exponential decay and relatively long lifetime, the triplet will be a valuable intrinsic reporter group for the study of the structure and dynamics of proteins in solution.

W-PM-F9 UV LASER-INDUCED CATARACTS. D. Thomas* and K. Schepler, USAF School of Aerospace Medicine, Brooks AFB, Texas 78235.

Several authors[1,2] have shown that exposure to near ultraviolet laser radiation can cause the development of permanent cataracts in monkey and rabbit lenses. In experiments performed at this laboratory, rabbits have been exposed to near ultraviolet radiation from HeCd (325 nm) and N_2 (337 nm) lasers. Once cataracts had formed, laser Raman spectroscopy was used to detect molecular changes in lens tissue. The differences between Raman spectra of healthy and cataractous lenses will be presented and discussed.

1. D. MacKeen, S. Fine and B. Fine, Ophthal. Res., 5, 317-324 (1973).
2. R. Ebbers and D. Sears, Am. J. Optom. & Physiol. Optics, 52, 216-223 (1975).

The animals involved in this study were procured, maintained, and used in accordance with the Animal Welfare Act of 1970 and the Guide for the Care and Use of Laboratory Animals prepared by the Institute of Laboratory Animal Resources-National Research Council.

W-PM-F10 RUTHENIUM RED AS A RESONANCE RAMAN SCATTERING PROBE OF Ca^{++} BINDING. S. Rosenfeld and J. M. Friedman, Bell Laboratories, Murray Hill, New Jersey 07974

In an attempt to evaluate the use of ruthenium red as a resonance Raman scattering (RRS) probe of Ca^{++} binding sites in biological systems, we have systematically examined the interaction of ruthenium red with a series of Ca^{++} binding materials. In earlier work it was shown that the RRS spectrum of ruthenium red undergoes systematic changes when ruthenium red is added to known Ca^{++} chelating agents. We have obtained RRS titration curves for a series of divalent cation chelators (EDTA, EGTA, NTA and Chel CD). These studies indicate that ruthenium red can bind a maximum of three chelating agents, although in many instances it is divalent, possibly a result of steric factors. We have also examined the interaction of ruthenium red with several Ca^{++} binding proteins and phospholipid . Preliminary results raise the possibility of using ruthenium red to titrate divalent cation binding sites in Ca^{++} binding systems.

1) J. M. Friedman, D. L. Rousseau and G. Navon, submitted for publication.

W-PM-F11 KINETIC FLUORESCENCE POLARIZATION AND CIRCULAR DICHROISM STUDIES ON HEMERYTHRIN. D. E. Giblin*, L. J. Parkhurst, and D. J. Goss. Dept. of Chemistry, University of Nebraska, Lincoln, NE., 68588

A modular system for the transient monitoring of fluorescence polarization, emission anisotropy, and circular dichroism has been developed. The system is capable of a time resolution corresponding to a 100 μsec time constant. The optics are based on a Morvue PEM-1 photoelastic modulator and their modular nature allows them to be used in conjunction with stopped-flow, temperature jump, and flash photolysis. The electronics were designed with special attention given to bandwidth and filter characteristics in determining the actual time response to a transient signal. The system has been used with a specially designed fluorescence stopped-flow in the study of the changes in emission anisotropy of fluorescein-isothiocyanate (FITC) labelled hemerythrin (Goldfingia gouldii) upon pH jump and in the circular dichroism mode with the same stopped-flow to examine the CD changes which occur during ligand binding to the iron sites in met-hemerythrin from the same source.
Grant Support: NIH HL 15284-06, Research Corporation, Research Council, University of Nebraska

W-PM-F12 VIBRATIONAL CIRCULAR DICHROISM IN AMINO ACIDS AND PEPTIDES. M. Diem*, J. M. Kupfer*, P. J. Gotkin* and L. A. Nafie* (Introduced by Philip B. Dunham) Department of Chemistry, Syracuse University, Syracuse, New York 13210.

Vibrational circular dichroism (VCD), the differential absorption of left and right circularly polarized infrared radiation by vibrational transition, can be observed with good signal-to-noise ratio in the 2 to 5 μ region by using fast modulation and synthronous detection techniques. VCD combines the structural sensitivity of vibrational spectroscopy and electronic optical activity to yield a powerful new technique for the study of configuration and conformation of molecules in solution. We report results of the first application of this new technique to investigate amino acids and small peptides in aqueous solution. Among the most dramatic results is the sensitivity of VCD to distinguish between binary combination of two amino acids (e.g., Ala-Gly and Gly-Ala) which exhibit very similar vibrational spectra in the 2-5 μ range. The stereochemical sensitivity of VCD has been demonstrated using a variety of small oligopeptides and some polypeptides. Other factors influencing the observed spectral features will be discussed.

DNA INTERACTIONS

W-PM-F13 CIRCULAR DICHROISM IN THE VACUUM ULTRAVIOLET. J. N. Liang* and E. S. Stevens, Department of Chemistry, State University of New York, Binghamton, NY 13901

Circular dichroism (CD) measurements can now be made on several prototype instruments to 172-175 nm with aqueous solutions, 160-162 nm with fluoroalcohol solutions, and 135-150 nm with film samples.[1] Oligopeptides have been studied in order to distinguish parallel and antiparallel beta sheet formation; but the extended CD range also has application to the study of polysaccharides. Most recently we have followed the gelation of agarose using intensity changes in a newly observed CD band at 180 nm.[2] The temperature profile of this band shows sharp, discontinuous changes around the melting and setting points of the gel, which are interpreted in terms of cooperative intermolecular association through double helices. The hysteresis also observed reflects helix-helix aggregation.

[1] E. S. Pysh (Stevens), Ann. Rev. Biophys. Bioengin. 5, 63 (1976).

[2] In collaboration with E. R. Morris and D. A. Rees, Unilever Research Laboratory, Colworth House, England.

W-PM-F14 CONFORMATION AND SPIN STATE OF CYTOCHROME b-562 FROM E. COLI. P. A. Bullock* & Y. P. Myer, SUNYA, Albany

Circular dichroism and resonance Raman spectra of ferric and ferrous cytochrome b-562 from E. coli have been studied to discern the conformational and spin states of the protein. The intrinsic CD spectrum is that of a highly helical protein, 52% α helix in ferric and 49% in ferrous, with no indication of other organized structures. The aromatic CD spectra are distinct for the two oxido forms, typical of phenylalanine in the ferric form (peak at 260 nm) and of tyrosine in the ferrous (peaks at 274, 288 and 299 nm). The Soret spectra of the two forms are complex, reflecting an unusual heme environment, and distinct in complexity and magnitude, indicating an oxido-reduction conformational effect. The RR spectra exhibit multiple spin states in the ferric form, but only a low spin state in the ferrous. Gaussian analysis of the Soret CD spectrum showed the presence of contributions of at least three Cotton effects, and that the oxido-reduction alterations are due primarily to changes in one of the three. The ferric protein is thus a composite of two forms, low and high spin, and the ferrous, a composite of two conformationally distinct low-spin forms.

(Supported by NSF grant PCM 77-07441)

W-PM-G1 E. COLI ω CATALYZED LINKING OF SINGLE-STRANDED RINGS OF COMPLEMENTARY BASE SEQUENCE. K. Kirkegaard* and J.C. Wang, Department of Biochemistry and Molecular Biology, Harvard University, Cambridge, Mass. 02140.

E. coli ω protein (Eco DNA topoisomerase I) has been observed to catalyze the formation of double-stranded, covalently closed PM2 DNA rings. This represents a new reaction for the enzyme, which is known to catalyze the removal of negatively superhelical turns and the interconversion between single-stranded DNA rings with and without knots. Reaction of a mixture of single-stranded PM2 DNA rings of complementary base sequence to completion with ω yields species with a sedimentation coefficient characteristic of a covalently closed double-stranded DNA ring. Electron microscopy and agarose gel electrophoresis also identify the product as a covalently closed double-stranded ring. If the reaction is stopped short of completion, highly negatively supercoiled molecules are formed. This is in agreement with the expectation that as the ω catalyzed reaction proceeds, the linking number between the two complementary rings increases gradually. The ability of ω to topologically intertwine complementary single-stranded DNA rings provides further evidence that this enzyme can introduce transient breaks into DNA.

W-PM-G2 IDENTIFICATION OF THE SUBUNITS INVOLVED IN THE INTERACTION OF RNA POLYMERASE WITH T7 DNA. Z. Hillel and C.-W. Wu, Department of Biophysics, Albert Einstein College of Medicine, Bronx, New York 10461.

The role of the different subunits ($\alpha_2\beta\beta'\sigma$) of E. coli RNA polymerase in transcription is not fully understood. We have identified the subunits which are in close contact with the T7 phage DNA template using photochemical cross-linking. In non-specific T7 DNA-enzyme complexes which occur in all regions of the DNA, subunits σ, β, and β' were cross-linked to the DNA. In contrast, in the specific binary complexes which presumably occur at promoter sites, and in the initiation complex (holoenzyme + T7 DNA + three nucleoside triphosphates) only σ and β were cross-linked to DNA while β' was not. Our results (a) do not support the idea that the α subunits are involved in the enzyme-template interaction, (b) raise the possibility that σ subunit participates directly in promoter recognition even though isolated σ does not bind DNA, and (c) indicate different modes of interaction between RNA polymerase and DNA in non-specific and specific complexes. These findings are relevant to the mechanism by which RNA polymerase carries out selective transcription. Further studies of the enzyme-DNA interaction with emphasis on DNA strand specificity are in progress.

W-PM-G3 MOTION OF *E. COLI* RNA POLYMERASE BOUND TO DNA STUDIED BY TRIPLET ANISOTROPY. R. H. Austin, T.M.Jovin,* and G. Rhodes,* Max Planck Institute for Biophysical Chemistry, D-3400 Goettingen-Nikolausberg, West Germany.

E. coli ribonucleic acid polymerase (RNAP) stoichiometrically binds the inhibitory dye Rose Bengal (Ref. 1). The dye has a high triplet yield when excited at 500-540 nm, and quasi-linear symmetry so that a high absorbance anisotropy is created by photoselection with linearly polarized exciting light. We have used a nitrogen laser driven dye laser and a high speed data acquisition system (20 MHz sample rate) to study triplet lifetimes and rotational anisotropy decay times of RNAP both free in solution and bound to DNA. A physical model for the observed anisotropy decay times of RNAP bound to DNA will be presented.

Ref. 1. Wu, F. Y.-H., and Wu, C.-W., *Biochemistry* 12,4343 (1973).

W-PM-G4 HETEROGENOUS ENVIRONMENTS OF TRYPTOPHAN RESIDUES IN lac REPRESSOR, P. Bandyopadhyay*, F. Boschelli*, P. Lu and C.-W. Wu, Albert Einstein Col. of Med. Bronx, NY, 10461, and Univ. of Pennsylvania, Phila. Penn. 19104.

Heterogeneity in the environments of the two tryptophan residues (190 and 209) in lac repressor of E. coli was studied by fluorescence quenching in the presence of acrylamide and by excited-state lifetime measurements. Acrylamide caused a blue shift and quenching of fluorescence intensity of the repressor. A biphasic Stern-Volmer plot obtained indicates a heterogeneity in the accessibility of the two Trp residues to the quencher. Wild type lac repressor exhibited two excited-state lifetimes of 5 and 10 nsec, whereas 6 nsec was observed in presence of IPTG. Mutant lac repressors having only one Trp residue were also studied. The repressor containing only Trp-190 showed a single lifetime of 4.5 nsec, unaltered by IPTG. The repressor containing only Trp-209 exhibited two excited-state lifetimes of 3 and 9 nsec. It also responded to IPTG and acrylamide in a manner similar to the wild type repressor. These results suggest that Trp-209 is involved in the inducer binding and has two different environments, probably due to a mixture of different conformations or the asymmetric arrangement of subunits in the tetrameric repressor.

W-PM-G5 BINDING OF CATABOLITE ACTIVATING PROTEIN (CAP) TO DNA. S.A. Saxe* and A. Revzin, Biochemistry Department, Michigan State University, East Lansing, MI 48824

A cAMP-binding protein (CAP) is known to stimulate transcription at catabolite-sensitive operons in the presence of cAMP. The mechanism of action is obscure although it has been hypothesized that a cAMP-CAP complex may help to melt the DNA at CAP-sensitive promoters [Nakanishi, et al JBC 250, 8202 (1975)]. Several reports have shown that in the presence of cAMP, the protein will bind to DNA containing no specific CAP functional site. To elucidate molecular details of the CAP-DNA interaction, we have used physical methods to study binding to single- and double-stranded DNA, as a function of ionic strength, [Mg^{++}], and base sequence. We have found a cAMP-independent binding of CAP to "non-specific" DNAs at physiological pH. Centrifugation studies show that the cAMP-independent binding is cooperative; i.e., a fraction of DNA molecules binds all the CAP, leaving the rest of the DNA free of protein. The cAMP-dependent binding is non-cooperative, CAP being evenly distributed among all the DNA molecules. The binding site size is estimated to be 15 base pairs per molecule of CAP. Possible in vivo significance of the two types of non-specific binding will be discussed.

W-PM-G6 TRIPLETS OF ACRIDINE DYES BOUND TO DNA AS PROBES OF THE MOBILITY OF DNA-BOUND METAL IONS.
T. Prusik and N.E. Geacintov, New York University 10003

Metal ions such as Ag^{+}, Hg^{++} and Mn^{++} are known to bind to DNA in aqueous solution at room temperature. The dynamics of these metal-DNA complexes were studied using intercalated dye molecules as probes. It is demonstrated that metal ions bound to DNA in aqueous solutions at room temperature diffuse from base pair to base pair along the DNA helix. This study involves observing the triplet excited states of acridine orange and proflavine intercalated in DNA and monitoring the transient triplet decay in the presence of various amounts of DNA bound metal ions. The lifetimes of these triplets, in the absence of oxygen are typically in the range of 20-30 msec. These triplets are readily quenched by added metal ions and there is a uniform decrease in the lifetime of the triplets of the DNA bound dyes as metal ions are added. The decays of the triplets are exponential both in the absence and in the presence of small concentrations of metal ions, showing that all of the dye molecules are equally accessible to the mobile metal ion quenchers.

W-PM-G7 LUMINESCENCE OF INORGANIC PLATINUM-TYPE ANTICANCER COMPOUNDS. H. H. Patterson, J. A. LoMenzo, Jr.,* J. T. Tewksbury,* M. T. Hsu,* H. O. Hooper. University of Maine, Orono, Maine 04473

The luminescence spectra of cis- and trans-dichlorodiammineplatinum(II), and cis- and trans-dichlorobispyridineplatinum(II), have been measured over a temperature range of 2-300°K. The cis- isomers show a greater luminescence intensity than the trans- isomers. These results, coupled with the optical absorption and magnetic circular dichroism (MCD) measurements, help us to understand the nature of the electronic states in the cis- versus the trans- complexes. Also, molecular orbital and crystal field calculations have been carried out to characterize the difference in bonding between the two isomers. Finally, luminescence, absorption, and MCD experiments have been performed on the platinum blue complexes of $Pt(TMA)_2Cl_2$ (TMA = trimethylacetamide) to understand the nature of these compounds.

This research has been supported by the American Cancer Society.

W-PM-G8 INTERACTION OF CIS-$Pt(II)(NH_3)_2Cl_2$ WITH SV40 DNA. G. Cohen and W. Bauer, Dept. of Microbiology, State University of New York, Stony Brook, N.Y. 11794

The interaction of cis-dichlorodiammine Pt(II) with SV40 DNA has been analyzed by electrophoresis on agarose gels and by electron microscopy. The electrophoretic mobility of nicked circular DNA (II) increases monotonicly with increasing incubation time at constant drug:DNA. The mobility of superhelical DNA (I) is more complex: an initial increase is followed by decrease to a minimum coincident with DNA II. At longer times the mobility of DNA I again increases relative to II. The morphology of the corresponding Pt-DNA complexes has been examined by electron microscopy. In the case of DNA II, the molecular length is reduced by up to 20% upon spreading under nondenaturing conditions. DNA I is first unwound by drug binding. At longer times, supercoiled species of complex structure are again formed. The binding of the trans isomer of the drug, which lacks antitumor activity, requires considerably longer incubation times. Experiments are in progress to determine the extent of binding of cis-dichlorodiammine Pt(II) to SV40 DNA.

W-PM-G9 PHYSICAL STUDIES OF HG(II) AND AG(I) DNA COMPLEXES. D. Ding and F.S. Allen. Dept. of Chemistry, Univ. of New Mexico, Albuquerque, New Mexico 87131

The binding of HG(II) and Ag(I) to the bases of DNA and polynucleotides induces strong absorption and CD bands. From electric dichroism studies, the transition moment of the difference absorption band at 293 nm is in the plane of the bases and has a huge negative CD band at 285 nm; while the corresponding 293 nm difference absorption band of DNA-Ag(I) complex is relatively CD inactive. A second band at 270 nm in the difference absorption spectrum of the DNA-Ag(I) complex has a large associated CD band at 270 nm. This transition is out of the plane of the bases. The increase of the sedimentation coefficients of the rigid rod sonicated DNA by the heavy metal ions can be accounted for by the increase of molecular weight and the decrease of the partial specific volume. Either a charge transfer band between the bases and the heavy metal ions or a perturbation theory of the bases by the heavy metal ions would explain satisfactorily the experimental optical results of DNA-Hg(II) and DNA-Ag(I) complexes. (Supported by Grant CHE76 05684 from NSF for the purchase of JASCO J-4DC spectropolarimeter)

W-PM-G10 PYRENE-NUCLEOTIDES COMPLEXES. P. Lianos* and S. Georghiou, Physics Department, University of Tennessee, Knoxville, TN 37916

Pyrene has been found to form ground and excited electronic state complexes of 1:1 stoichiometry with GMP, CMP, TMP, and AMP. The values of their ground state association constants are 45 M^{-1}, 13 M^{-1}, 14 M^{-1}, and 52 M^{-1}, respectively. The fluorescence of pyrene is strongly quenched by GMP, CMP, and TMP but only slightly by AMP. Fluorescence quenching analysis has yielded the values 87 M^{-1}, 73 M^{-1}, and 154 M^{-1} for the excited state association constants with GMP, CMP, and TMP, respectively. The corresponding values for the excited state second-order rate constant for complex formation are: 3.3×10^9 $M^{-1}sec^{-1}$, 4.1×10^9 $M^{-1}sec^{-1}$, and 4.0×10^9 $M^{-1}sec^{-1}$. The probabilities of complex formation per collision between an excited pyrene molecule and a nucleotide are: 0.52, 0.64, and 0.63. The values for the excited state rate constant for dissociation of the complex are: 3.8×10^7 sec^{-1}, 5.6×10^7 sec^{-1}, and 2.6×10^7 sec^{-1}. The possibility that partial transfer of charge from pyrene to nucleotide may be playing a role in the complex formation process will be discussed. Supported by the American Cancer Society grant IN-89H.

W-PM-G11 SPECTROSCOPIC INVESTIGATION OF THE STRUCTURE OF THE COVALENT BENZO(a)PYRENE EPOXYDIOL-DNA COMPLEX. N.E. Geacintov and T. Prusik, Chemistry Department New York University, New York, N.Y. 10003.

Covalent complexes between 7,8-diol 9,10 epoxide benzo(a)pyrene (BPDE) and DNA were prepared *in vitro*. A.M. Jeffrey, I.B. Weinstein and their co-workers (Columbia University) have shown that this type of complex is formed when benzo(a)pyrene binds to DNA *in vivo* in bovine and human cells. Conventional and photon counting fluorescence techniques based on the bimolecular quenching of the pyrene-like fluorescence of BPDE are utilized to show that the BPDE moeity is bound externally to DNA and is probably located in one of the grooves of DNA. This is confirmed by electric linear dichroism measurements which indicate that the in-plane long axis of BPDE is oriented at an angle of $\lesssim 35^o$ with respect to the axis of the helix. (Supported by Grants CA20851 and CA-21111, National Cancer Institute, DHEW).

POSTER SESSIONS

CELL-SOLUTE AND CELL-VESICLE INTERACTIONS

W-POS-A1 MODULATION OF B-HYDROXYBUTYRATE DEHYDROGENASE (BDH) BY MEMBRANE-BOUND LECITHIN(PC). J.Vidal* Univ. of Buenos Aires, O.McIntyre* and Sidney Fleischer, Dept. of Molecular Biol., Vanderbilt Univ., Nashville,TN 37235

BDH activity in rat liver SMV exhibits a linear Arrhenius plot. It is inhibited when 60% of PC is exchanged by PC(14:0) or PC(16:0) using PC-exchange protein. The activity was regained by back-exchange with mitochondrial PC or PC(18:1). Substitution of 70% of SMV phospholipids by PC(14:0) through collision with PC(14:0) vesicles produced inactivation of BDH below 21° and a non-linear Arrhenius plot. Purified beef heart BDH was reinserted into control and PC(14:0)-substituted SMV; the rebound BDH showed Arrhenius plots similar to those of the endogenous rat liver enzyme. By contrast, the complex,purified BDH with PC(14:0) liposomes,showed a linear Arrhenius plot. We conclude: (1) the fatty acyl composition of membrane-bound PC strongly influences BDH activity, although it does not affect the energy of activation of purified BDH-PC complexes; and (2) the energy of activation of rebound BDH is a membrane parameter characteristic of the membrane and not of the source of enzyme. Supported by NIH AM 14632 and NSF US-Argentina Int. Prog.

W-POS-A2 Temperature Dependence of Calcium Induced Fusion of Acidic Phospholipid Vesicles. S.T. SUN, E.P. DAY, and J.T. HO, SUNY/Buffalo.--We have measured the temperature dependence of calcium induced fusion of acidic phospholipid vesicles to determine the relationship between vesicle fusion and the bilayer phase transition. Sonicated vesicles were incubated for several hours at constant temperature in the presence of a calcium concentration slightly below that required for precipitation of the resulting aggregates. The chelating agent EDTA was then added. The average size of the resulting large unilamellar vesicles was measured using dynamic light scattering. This final vesicle size served as a measure of calcium induced fusion during incubation. The graph of this extent of fusion against incubation temperature showed a sharp maximum. The results are interpreted in terms of the bilayer phase transition.

W-POS-A3 PHOSPHOLIPID ASYMMETRY IN PLASMA MEMBRANES OF MAMMALIAN CELLS AND ITS MODIFICATION BY LIPID VESICLES. A. Sandra* and R.E. Pagano. Carnegie Institution of Washington, 115 W. University Pkwy., Baltimore, Md. 21210.

The transbilayer distribution of the major phospholipids in mouse LM cell plasma membrane derivatives was studied. Cells were grown on radiolabeled phospholipid precursors and allowed to phagocytose latex spheres. Phosphatidylcholine (PC) and phosphatidylethanolamine (PE) asymmetry in isolated phagosomes was determined by use of the PC-specific exchange protein and trinitrobenzenesulfonic acid labeling. PE is enriched on the cytoplasmic face (70%vs30%), while sphingomyelin is enriched on the external face of the plasma membrane. PC is approximately equally distributed. The cytoplasmic face of the plasma membrane was also enriched in unsaturated fatty acids.

In order to modify this existing asymmetry, we have incubated small unilamellar vesicles (liposomes) with cells under conditions in which lipid transfer is the predominat mode of lipid uptake. Using isotopically asymmetric liposomes, the vesicle-cell exchange process was shown to occur between the outer vesicle monolayer and the cells.Studies are in progress to determine if the transferred lipids are introduced asymmetrically into the cell surface. Supported by GM22942

W-POS-A4 CONTROLLED FUSION OF PHOSPHATIDIC ACID-PHOSPHATIDYLCHOLINE MIXED LIPID VESICLES. M. Liao*, and J. Prestegard, Chem. D. Yale, New Haven, Ct. 06520

The transformation of phosphatidylcholine-phosphatidic acid vesicles to larger well defined unilamellar structures can be induced by addition of Ca^{2+} to sonicated vesicle preparations under conditions in which the Ca^{2+}:phosphatidic acid mole ratio remains below 1:1 and phosphatidic acid content remains less than 50%. During this process bilayer composition remains unchanged and internal contents are retained in the final structure. These properties are indicative of concerted 2 vesicle and multiple vesicle fusions. The effect of Ca^{2+}-phosphatidic acid mole ratios in determining ultimate vesicle size distributions is suggested to arise from a feed-back mechanism involving internal sequestering of Ca^{2+} during initial fusions. Nuclear Magnetic Resonance studies using ^{31}P and Cd^{2+} as a Ca^{2+} analogue are used to monitor transbilayer redistribution of phosphatidic acid and Cd^{2+}. The results support the suggested mechanism.

W-POS-A5 THE INTERACTIONS OF LARGE UNILAMELLAR PHOSPHOLIPID VESICLES WITH CULTURED CHINESE HAMSTERS CELLS. S.C. Ho,* and L. Huang, Department of Biochemistry, University of Tennessee, Knoxville, TN 37916.

Large unilamellar vesicles (LUV, diam. 0.2μ) composed of egg yolk lecithin were prepared by ether injection method. (BBA 443, 629, 1976). V79 cells in suspension were incubated with LUV (1mg lipid/ml) in balanced salt solution at 37°C for 1h. The rates of uptake of trapped content and lipid were different, suggesting that most vesicles were not taken up as intact structures. Small fraction of the lipid uptake was sensitive to energy inhibitors. Cells treated with LUV entrapped with 5-Br, 4-Cl,3-indoyl phosphate, substrate for lysosomal acid phosphatase, showed blue granules inside the cells. Electron microscopy revealed membraneous material in vacuoles resembling secondary lysosomes. These results indicated the endocytosis of LUV. Diffused fluorescence throughout the cells was observed after treatment of 6-carboxyfluorescein-entrapped LUV, suggesting that the release of the dye inside the cells after vesicle-cell fusion. It is concluded that LUV can be employed as vehicles to deliver substances into various subcellular compartments for therapeutic applications.

W-POS-A6 DIVALENT CATION INTERACTION WITH ACIDIC PHOSPHOLIPID VESICLES I. CATION BINDING AND ASSOCIATED CHANGES IN THERMOTROPIC TRANSITIONS. C. Newton, and D. Papahadjopoulos, SUNY at Buffalo and RPMI, Buffalo, New York 14263

It is well known that Ca^{2+} plays a vital role in natural membrane fusion phenomena while Mg^{2+} is ineffective in most systems. Observations of a parallel specificity in the induction of phase separation and fusion in pure acidic phospholipid vesicles have led to detailed investigation of the properties of the cation-lipid complexes. The binding of Ca^{2+} and Mg^{2+} to phosphatidylserine vesicles after equilibrium dialysis was studied using radioactive tracers and atomic absorption spectroscopy. Ca^{2+} was found to have a stronger affinity for phosphatidylserine than does Mg^{2+} and is able to effectively compete with Mg^{2+} when both cations are present. The effect of a pre-existing solid or fluid lipid phase on cation binding was determined. Differential scanning calorimetry indicated an upward shift of ~12° C. in the Tc following the addition of Mg^{2+} or Ca^{2+} at low concentrations; higher Ca^{2+} concentrations (>0.5mM) removed the transition peak from the range of 0 to 70° C. Apparent Ca^{2+} and Mg^{2+} cooperativity will be discussed.

W-POS-A7 DIVALENT CATION INTERACTION WITH ACIDIC PHOSPHOLIPID VESICLES II. KINETICS OF AGGREGATION AND INCREASED PERMEABILITY. A.R. Portis, Jr.,* and D. Papahadjopoulos, RPMI, Buffalo, New York 14263

Addition of Ca^{2+} but not Mg^{2+} to sonicated phosphatidylserine (PS) vesicles causes dramatic increases in permeability accompanied by fusion of the vesicles, formation of cochleate cylinders, release of heat, and removal of the thermotropic phase transition from the range 0°-70° C. We have used the fluorescent enhancement upon release of 100mM 6-Carboxyfluorescein (6-CF) from PS vesicles and light scattering as a sensitive assay for the kinetics of increased permeability and aggregation. Their dependence on concentration of vesicles and Ca^{2+} were determined. Aggregation was observed to precede the release of 6-CF in all cases. The presence of Mg^{2+} enhanced the effects observed with Ca^{2+} although Mg^{2+} alone had a negligible effect. The results are consistent with the hypothesis that fusion and the associated increase in permeability is due to Ca^{2+} binding between two opposed PS membranes (trans-complex) rather than to PS within the plane of one membrane (cis-complex). The Mg^{2+} complex could involve the later (cis) complex only. (CA-05467 and GM-18921)

W-POS-A8 DIVALENT CATION INTERACTIONS WITH ACIDIC PHOSPHOLIPID VESICLES. III X-RAY INVESTIGATIONS OF Ca^{2+} AND Mg^{2+} COMPLEXES. W.A. Pangborn[1], and D. Papahadjopoulos[2], Medical Foundation of Buffalo, Buffalo, NY 14203[1] and Roswell Park Mem. Inst., Buffalo, NY 14263[2]

X-Ray diffraction indicates striking differences between the phosphatidylserine (PS)/cation complexes of Ca^{2+} and Mg^{2+}. The PS/Ca complex is a 53Å lamellar structure. The hydrocarbon chains are packed in a crystalline lattice characterized by two sharp high angle reflections at 4.5Å and 4.1Å. On drying of the PS/Ca precipitate there is no change in spacing or relative intensities of the diffraction maxima, indicating the absence of free or loosely bound water. The PS/Mg complex is a 67Å lamellar structure with the characteristic 4.2Å spacing of hexagonally packed hydrocarbon chains, the most disordered of the solid chain packing arrangements. On drying, the PS/Mg lamellar structure shrinks to 60Å. Similar differences have been observed between the Ca^{2+} and Mg^{2+} complexes formed with dimyristoyl phosphatidyl glycerol. The implications of these structural differences induced by Ca^{2+} and Mg^{2+} with respect to a mechanism for Ca^{2+}-induced lipid vesicle fusion will be discussed. (Supported by GM21047, GM18921 & GM02348.)

W-POS-A9 EFFECTS OF LIMITED PRONASE TREATMENT ON THE ULTRASTRUCTURE AND PROTEIN COMPOSITION OF CHLOROPLAST MEMBRANES. IMPLICATIONS FOR INTERACTIONS OF THE LIGHT-HARVESTING COMPLEX. D.P. Carter* and L.A. Staehelin*, Dept. MCDB, University of Colorado, Boulder, CO 80309 Intr. by J.A. Gordon.

The enzymatic effects of 1 mg pronase/ml on isolated pea thylakoids have been studied by freeze-fracture electron microscopy and SDS-polyacrylamide gel electrophoresis. Pronase treatment of experimentally unstacked membranes produces an increase in EF-face particle density, in particles/μm^2, of 30%, and a shift in particle diameter from > 140A to <140A. Stacked membranes, in 5mM $MgCl_2$, are not affected. If unstacked, treated membranes are incubated in $MgCl_2$, restacking does not occur However, the diameter of EF-face particles increases markedly, and the particle density decreases to values observed for normal, unstacked membranes. Since pronase treatment also increases the migration of the chlorophyll-binding protein complex by gel electrophoresis, we believe that by inhibiting the stacking of membranes, pronase allows the observation of what may be the association of the light-harvesting complex with the photocenters. Supported by NIH Grant #5-F32-GM05613-02.

W-POS-A10 INTERACTION OF PHOSPHATIDYL GLYCEROL AND INTRINSIC PROTEINS IN MEMBRANES OF *ACHOLEPLASMA LAIDLAWII*. H.H. Wang, Division of Natural Sciences, University of California at Santa Cruz; E.M. Bevers*, J.A.F. Op den Kamp*, and L.L.M. van Deenen*, Laboratory of Biochemistry, State University of Utrecht, The Netherlands.

It has been established that 30% of the phosphatidyl glycerol in oleic acid enriched membranes of *Acholeplasma laidlawii* in the presence of porcine pancreatic phospholipase A_2 were protected against hydrolysis at temperatures below 10° C (Biochem. 16:1290-1295). Under similar experimental conditions, the amount of protected phosphatidylglycerol in membranes pretreated with 2,4,6-trinitrobenzenesulfonic acid or glutaraldehyde were greatly decreased. Bee venom phospholipase A2 and pretreatment with heat both led to decreased amounts of protected phosphatidylglycerol in the membrane. However, membrane pretreated with heat showed extensive aggregation of the intrinsic proteins as shown by freeze etch electron microscopy. These results and other experiments have led us to the conclusion that the protection against hydrolysis was due to an interaction of the phosphatidylglycerol with intrinsic membrane proteins.

W-POS-A11 INTERACTION OF AGGREGATING AGENTS WITH ERYTHROCYTE MEMBRANES. D.E. Brooks, J. Charalambous,* and J. Janzen, Department of Pathology, University of B.C., Vancouver, Canada, V6T 1W5.

Erythrocytes can be reversibly aggregated by soluble macromolecules, probably due to polymer bridge formation. To partly test this hypothesis we have measured the adsorption/desorption behavior of fibrinogen and six dextran fractions with human red cells. ^{3}H-dextran fractions of $\bar{M}_w$=26.5K-500K; conc'n=1%-12%w/w and human ^{125}I-fibrinogen conc'n=0.1-10 mg/ml in saline have been examined. Analysis of the apparent equilibrium adsorption and desorption upon multiple washing implies the existence of two types of binding sites for dextran, one of which (fast site) permits more rapid polymer desorption than the other (slow site). The slow site shows no molecular weight selectivity and its adsorption isotherms are linear through the aggregation-disaggregation transition (ADT). The fast site isotherms depend on $\bar{M}_w$. They are linear for the non-aggregating fractions but for higher molecular weights break upward at the ADT. Fibrinogen, which causes no ADT, also appears to bind to two types of sites, both of which exhibit linear isotherms. Supported by Canadian MRC and Heart Fndn.

W-POS-A12 CELL - TO - CELL SPREAD OF FLUORESCENT TRACER MOLECULES IN THE EARLY SQUID EMBRYO. B. Rose and I. Simpson.* Dept. Physiol. & Biophys. Univ. Miami, Miami FL.

The fluorescent tracer molecules fluorescein, $LRBSO_3H$. $FITC(gly)_6OH$, $LRB(gly)_6OH$, $LRB(glu)_3OH$, and $LRB(leu)_3-(glu)_2OH$ were found to spread from cell to cell in squid embryos, stages 7 to 11 (Loligo pealii, Woods Hole; LRB = lissamine rhodamine B, FITC = fluorescein isothiocyanate). The tracers were injected into cells singly or in pairs of differing label and mol. wt. Fluorescence-spread to neighbouring cells was observed with incident-light fluoromicroscopy and videorecorded by an image intensifier television system. Intercellular transit occurred in 4 to 18 min at stage 7 and 8, and in 10 sec to 2 min at the later stages, the larger molecules having the slowest transit times at all stages. Ca^{++} blocked transit of both tracers or of only the larger one when co-injected with the tracer pairs.

W-POS-A13 EFFECTS OF LECTINS ON $(Na^+ + K^+)$-ATPase. N. N. Tandon* and E. O. Titus, National Institutes of Health, Bethesda, Maryland 20014

After prior incubation of rabbit thymocytes for 24 hr in 10% fetal calf serum, exposure of these cells to concanavalin A for 1 hr caused a 50% increase in $(Na^+ + K^+)$-ATPase activity. When crude microsomes from rabbit kidney were incubated with concanavalin A, only inhibition was observed. Mn^{++} and Ca^{++} ions (0.5 mM) were required for full inhibitory action. A phytohemagglutin from kidney beans and lectins from wheat germ and lentil inhibited the purified rabbit kidney enzyme. Maturation of rabbit thymocytes by incubation with fetal calf serum increased the fluidity of the innermost lipids of the cell membrane as measured by fluorescence polarization with 1,6-diphenyl-1,3,5-hexatriene. Incubation with concanavalin A for 1 hr had no effect on membrane fluidity in either fresh or mature thymocytes.

W-POS-A14 HETEROGENEOUS PARTITIONING AND LOCALIZATION OF PYRENE IN PLASMA MEMBRANES. V. Glushko, C. Karp, and M. Thaler*, Temple University School of Medicine, Philadelphia, Pa., and USV Pharmaceutical Corp., Tuckahoe, N.Y.

Certain polyaromatic hydrocarbons (PAH) exhibit high carcinogenicity and there is considerable interest in elucidating the incorporation and distribution of PAH compounds in the cell. As a bulk phase process, pyrene and related PAH species partitioned into liver plasma membranes and erythrocyte ghosts with a coefficient approximating that found for octanol-water mixtures; however, at concentrations approaching picomole/mg/ml, the partitioning deviated from this relationship. In addition, membranes preloaded with pyrene produced a lower efflux than predicted by the coefficient determined from incorporation. Up to 0.1 nanomoles of pyrene was retained per mg membrane even at effective dilution ratios of 1,000,000 or more. By perturbation and degradation of the membranes, the microenvironment of the residual pyrene appears to depend on the maintenance of protein structure and much, 20-55%, of the pyrene may be associated with membrane proteins. (Supported in part by American Cancer Society Grant IN-88J).

PHOTOSYNTHESIS III

W-POS-B1 ON THE ROLE OF ELECTRIC FIELDS IN PHOTOINDUCED PRIMARY CHARGE SEPARATION. T. Yamamoto and A. C. Albrecht, Department of Chemistry, Cornell University, Ithaca, New York 14853

Recently the expected effects of high electric fields on the yield of photoinduced primary charge generation have been clearly demonstrated in two different organic systems. One consists of a thin organic photoconducting film, electrostatically charged (P. Borsenberger, submitted for publication). The other is a cell having a thin polycrystalline chlorophyll-a film sandwiched between two different metals. Here a high internal field follows from the contact potential between the metal and the chlorophyll (C. W. Tang and A. C. Albrecht, J. Chem. Phys. 62, 2139, 1975). In both cases it is seen how the efficiency of photoinduced charge generation improves drastically as fields towards 10^6V/cm are approached. In photosynthesis the presence of a permanent electric field of about 10^6V/cm has been implicated in the thylakoid membrane (H. T. Witt in Bioenergetics of Photosynthesis, Academic Press, New York, 1975). We explore a possible connection between this high field and efficient charge separation found in the photosynthetic system. Supported by NIH grant GM 10865.

W-POS-B2 MO CALCULATIONS OF CHLOROPHYLLS AND CHLORINS.† L.K.Hanson‡ M.S.Davis,* I.Fujita‡ and J.Fajer, Brookhaven National Laboratory, Upton, N. Y. 11973

Extended Huckel calculations have been performed for reduced, oxidized and neutral chlorophylls, bacteriochls, metallochlorins, and their free bases. The effect of the fifth and reduced rings, the ring substituents, the metal and its axial ligands on the spin and charge densities and the nature of the ground state have been examined. The calculated spin densities will be compared to SCF-PPP results as well as EPR and ENDOR data. Spin densities for a Chl a anion (I) and an A_2-type π cation (II) (without H_2O ligand) and charge densities for the neutral species with axial H_2O (III) are given below:

† This work was supported by the Division of Basic Energy Sciences, U. S. Department of Energy.

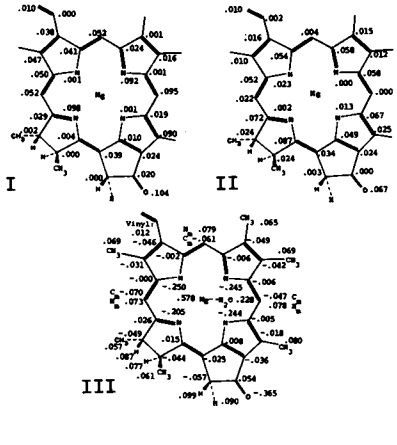

W-POS-B3 CHLOROPHYLLOPHANES. NEW MODELS OF SPECIAL PAIR CHLOROPHYLL.† M. R. Wasielewski, W. A. Svec,* and B. T. Cope,* Argonne National Laboratory, Argonne, IL 60439.

The first chlorophyllophane, i.e. a bis-chlorophyll cyclophane has been prepared in 8 steps from pheophytin a. The compound serves as a well-defined biomimetic model for studies of the photochemical and redox properties of photoreaction center chlorophyll as a function of special pair geometry. The two macrocycles are sandwiched directly atop one another with the ring I-ring III axis of one macrocycle approximately perpendicular to that of the second macrocycle. Visible absorption and fluorescence spectroscopy reveal that there is no electronic interaction between the macrocycles. Photooxidation of the chlorophyllophane results in the production of a cation radical which exhibits an exchange narrowed ESR signal similar to that of P700 in vivo. The chlorophyllophane is oxidized 70 mV more easily than Chl a. The results of this study support the proposal that special pair geometries exist which adequately account for both the redox and spin delocalization properties of chlorophyll special pairs in vivo, yet do not give rise to unusually red-shifted optical spectra.

†Work performed under BES of DOE.

W-POS-B4 STRUCTURAL ORGANIZATION OF THE REACTION CENTER AND ASSOCIATED c-CYTOCHROMES IN C. vinosum. D.M. Tiede, J.S. Leigh and P.L. Dutton, Dept. of Biochem. & Biophys., University of Pennsylvania, Phila., PA 19104

Magnetic interactions have been measured between the electron carriers of the reaction center and the associated c-cytochromes in C. vinosum. Interactions between the bacteriochlorophyll dimer, $(BChl)_2$, and the pair of low potential cyts.c_{553}, which are capable of reducing $(BChl)_2^+$ in a low temperature, tunnelling reaction, may result in a maximum of 2 gauss splitting of these EPR signals, suggesting a minimum separation of 21-24Å between unpaired spins, and a minimum distance of 12-14Å between the cyt.c_{553} heme edge and $(BChl)_2$. Interactions are not observed between $(BChl)_2$ and the pair of high potential cyts.c_{555}. The c-cyts. show no magnetic interaction with other components of the reaction center. Magnetic interactions indicate a cyt.c_{555} to c_{553} separation of 7-8A, while suggesting cyt.c_{555}-c_{555} and cyt.c_{553}-c_{553} separations of >10A. EPR studies with oriented chromatophores demonstrate that the cyt.c_{553} heme plane lies parallel, and the cyt.c_{555} heme plane lies perpendicular to the plane of the membrane surface. These results may suggest that parameters other than distance are important toward controlling electron transfer reactions.

W-POS-B5 INTERACTION OF THE PRIMARY QUINONE WITH IRON IN REACTION CENTERS OF PHOTOSYNTHETIC BACTERIA. D.M. Tiede, R.C. Prince* and P.L. Dutton, Dept. of Biochem. & Biophys., Univ. of Pennsylvania, Phila., PA 19104.

The EPR spectrum of the reduced iron-quinone complex, $Q^{\cdot}$-Fe, in C. vinosum chromatophores appears to be a single component with g values of 1.82 and 1.62, but in the isolated reaction centers (RC) there is an additional component near g 1.9. A similar variable presence of a g 1.9 component is encountered in RCs of Rps. sphaeroides and Rps. viridis, while in R. rubrum (chromatophores and RCs) $Q^{\cdot}$-Fe is entirely represented by a g 1.9 signal. All $Q^{\cdot}$-Fe signals can be eliminated by SDS or chaotropic agents, causing the low temperature photoinduced $Q^{\cdot}$ signal to appear at g 2.0045. Loss of the interaction with Fe causes the primary Q to become a 2 electron acceptor with an equilibrium n-value of 2. The shift of the $Q^{\cdot}$-Fe signal from g 1.82 to 1.9 may represent a changed, perhaps weaker, association between the Fe and Q, but $Q^{\cdot}$-Fe/QFe always seems to have a n-value of 1. These results suggest that the association with Fe provides a stabilization of the semiquinone $Q^{\cdot}$.

Supported by US PHS GM 12202.

W-POS-B6 POLARIZED ABSORPTION STUDIES OF REACTION CENTERS OF RHODOPSEUDOMONAS SPHAEROIDES IN DRIED GELATIN FILMS. C.N. Rafferty and R.K. Clayton. Div. of Biol. Sci., Cornell Univ., Ithaca, NY 14853

Reaction centers in a gelatin solution were dried to form films. Linear dichroism of reaction centers is shown by unstretched films when absorption is measured with the electric vector parallel and at 60° to the film plane. Upon stretching, reaction centers are oriented within the film plane and linear dichroism is shown when absorption is measured with the electric vector parallel and perpendicular to the stretching direction. In stretched films, the directions of the transition dipoles are distributed with uniaxial symmetry relative to the stretching direction. The degree of orientation is high in stretched films, equivalent to perfect orientation of at least 75% of the reaction centers and to random orientation of the remainder. Light minus dark difference spectra are polarized such that negative bands near 860 and 810 nm correspond to the disappearance of discrete bands of the bacteriochlorophyll dimer (Q_y transitions) upon oxidation. Exciton coupling is also suggested by the polarization of negative bands near 600 and 625 nm (Q_x transitions). Possible structures for the bacteriochlorophyll dimer will be discussed.

W-POS-B7 EFFECT OF QUINONE ANALOGS ON PHOTOTRAP ACTIVITY AND FLUORESCENCE PROPERTIES OF PHOTOSYNTHETIC BACTERIA. C. L. Bering and P. A. Loach, Northwestern University, Evanston, Il. 60201

Previously (Biophys. J. 17, 148a (1977)) we showed that the quinone antagonist DBMIB inhibited primary photochemistry in bacteria. The inhibition, seen by bacteriochlorophyll absorbance changes, was reversed by UQ as well as several other quinones. Among these were dimethylbenzoquinone, anthraquinone and menaquinone, which restored the ΔA to near 90% of the control value. DBMIB also inhibits fluorescence in these organisms and this inhibition can be reversed to approx. 90% of the control with UQ. A series of other quinones were tested for the ability to inhibit fluorescence. None were able to inhibit at as low a concentration as DBMIB although 1,2-naphthoquinone (1,2-NQ) and thymoquinone(TQ) showed fairly strong inhibition (I_{50} at 200 μM vs. 10 μM for DBMIB). When the effect of 1,2-NQ and TQ on fluorescence and ΔA properties were examined, they were found to be similar to those caused by o-phen; that is, the variable fluorescence decreased, the dark decay of the ΔA was accelerated and there was no reversal with UQ. The data indicate that 1,2-NQ and TQ may act at the same site as o-phen.

W-POS-B8 ENERGY TRANSFER STUDIES ON BILIPROTEINS. R. MacColl* and D. S. Berns. Div. of Labs. & Res., NYS Dept. of Health, Albany, New York 12201

Fluorescence techniques have been used to study the light gathering and energy transfer mechanisms for several cryptomonad biliproteins as compared to cyanophyta and rhodophyta biliproteins. Examination of the fluorescence emission spectra as a function of excitation wavelength demonstrates that emission emanates from a single ground state chromophore. Further spectroscopic data demonstrates that each cryptomonad biliprotein is composed of at least two distinct types of absorbing chromophore. Application of Forster dipole-dipole energy transfer theory is made to study the mechanism by which energy absorbed by biliproteins migrates to chlorophyll a. Evaluation of spectral overlap integrals between phycocyanin chlorophyll a and phycocyanin and chlorophyll c_2 suggests that phycocyanin might transfer energy directly to chlorophyll a without a chlorophyll c_2 intermediary. Radiation-less energy transfer among homogeneous biliproteins is shown to be feasible.

W-POS-B9 PRIMARY AND SECONDARY ELECTRON ACCEPTOR MOIETIES IN PHOTOSYSTEM 1. J.T. Warden and A. Rudnicki*, Biochemistry Program, Department of Chemistry, Rensselaer Polytechnic Institute, Troy, N.Y., 12181

Electron Spin Resonance at cryogenic temperatures has been utilized as a probe for photoreducible, membrane-bound electron acceptors in green-plant chloroplasts and algae. These studies have confirmed the presence of the four-iron, Fe-S centers[1] A (Em ∿ - 540 mV) and B (Em ∿ - 590 mV) and furthermore demonstrate the universal presence of a component X, displaying g-factor components of g_1 = 1.78, g_2 = 1.87 and g_3 = 2.07. The interaction and photoreducibility of these three acceptor components has been investigated in a variety of subchloroplast preparations and chemical treatments designed to remove the Fe-S centers. The results to be reported are consistent with the assignment of component X as the primary acceptor of PS 1.

[1]M.C.W. Evans et. al. Biochem. J. (1976) 158, 71-77.

W-POS-B10 LIGHT FLASH AND NMR EXPERIMENTS ON CHLOROPLAST SUSPENSIONS. THE ROLE OF MANGANESE IN OXYGEN EVOLUTION. S. Marks,* T. Wydrzynski, Govindjee, P. G. Schmidt and H. S. Gutowsky,* U. of Ill., Urbana, Illinois 61801

Work in this laboratory has identified the proton relaxation rates (T_1^{-1}, T_2^{-1}) of water in chloroplast suspensions with the amount of Mn(II) in the membranes, allowing analysis of the T_2^{-1} response pattern obtained by illumination of chloroplasts with short light flashes. The pattern has a periodicity of four and T_2^{-1} maximizes on the third light flash. This correlates with the O_2 yield response pattern observed by Kok, Forbush and McGloin (1970) and the T_2^{-1} data can be fitted to a model similar to Kok et al.'s O_2 model. The model infers: 1) cycling of the intermediate S involves oxidation of Mn(II), 2) existence of a special dark adapted S intermediate, 3) donation of an electron by water to the S intermediate prior to release of O_2 in the fourth and final step of the cycle and 4) altered cycling of the S intermediates with the addition of chemical modifiers. We acknowledge support of NSF grants PCM-76-1157 to Govindjee and MPS-73-0498 to H. S. Gutowsky.

W-POS-B11 ON THE REDOX PROPERTIES OF THE FLUORESCENCE QUENCHER OF CHLOROPLAST PHOTOSYSTEM II. Peter Horton and Edward Croze*, Div. Cell & Mol. Bio., SUNY at Buffalo.

Redox titration of the fluorescence yield of chloroplasts in weak light shows two components with $Em_{7.8}$ at -50 and -350 mV. In an attempt to elucidate the function of these two quenching components in terms of their relationship to the primary acceptor of PS II, the following observations were made. 1)Treatment of chloroplasts with either hear, NH_2OH and light, triton X-100 or trypsin resulted in a decfease in the proportion of fluorescence quenched by the high potential component. 2)The fluorescence induction curve in chloroplasts with fully oxidized quencher can be resolved into two first order components; with the redox potential poised such that the high potential quencher is fully reduced, a fast, monophasic rise curve is seen. 3)The excitation spectra of the fluorescence yield for the high and low potential quenchers show a small but significant difference in the ratio of chl a and b. 4)In heat-treated chloroplasts a new fluorescence emission band with a maximum at 705 nm at 77°k is detected. One interpretation of this data is that the two quenchers are indicative of the presence of two different PS II primary acceptors. Supported by NSF PCM7609669.

W-POS-B12 SURFACE POTENTIAL CHANGES OF ENERGIZED THYLAKOID MEMBRANES. A. T. Quintanilha and L. Packer, Membrane Bioenergetics Group, Lawrence Berkeley Laboratory, University of California, Berkeley, California 94720

Two photosystems (PSI and PSII) have been identified in higher plant chloroplast thylakoid membranes, each of which is coupled to phosphorylation. Energization of these membranes produces a large electrochemical gradient which is predominantly due to a pH change. If electrical forces are responsible for the control of energization at the membrane level then surface potential changes at each membrane interface may be important. We have used the partition between the membrane and the aqueous medium of the membrane impermeable positively-charged spin-labeled amphiphile 4-(dodecyl dimethyl ammonium)-1-oxyl-2,2,6,6-tetramethyl piperidine bromide (CAT12) to monitor surface potential changes. This method can be contrasted to electrophoresis which provides information only on the ζ-potential i.e. the potential at the surface of shear which is different from the surface potential. Light induced electron flow through either Photosystem II or Photosystems II + I decreases the surface potential of the outer half of the thylakoid membranes by about 14 mV. (Research supported by the Department of Energy.)

W-POS-B13 INTACT CHLOROPLAST BIOENERGETICS. R. Slovacek,* J. Mills and G. Hind, Brookhaven National Laboratory, Biology Department, Upton, New York 11973.

Measurements of chlorophyll fluorescence, adenosine 5'-triphosphate pool size and light scattering as well as the emission from the added probe 9-aminoacridine can be used to monitor energization of illuminated intact chloroplasts. Changes in these parameters, in response to the addition of antimycin, suggest that cyclic activity is in part responsible for energization. Cyclic electron flow seems to depend on optimal redox poising conditions. In the absence of endogenous electron acceptors, 3-(3,4 dichlorophenyl)-1,1-dimethylurea or O_2 is required. Alternatively, native acceptors such as HCO_3^- or oxaloacetate, which regenerate oxidized nicotinamide adenine dinucleotide phosphate, will serve to maintain optimal poising. (Research supported by U.S. D.O.E.)

PROTEINS AND POLYPEPTIDES II

W-POS-C1 RHODANESE HETEROGENEITY. K.Guido*,and P. Horowitz,U Texas Health Science Center,San Antonio,TX 78284

The enzyme rhodanese (EC 2.8 1 1) is apparently a single 33,000 M.W. species in SDS-PAGE, but can be resolved into 5 active subspecies(I-V in order of increasing electrophoretic mobility) using PAGE on 7.5% gels at pH 8.9. When DEAE derived A and B forms of rhodanese are individually electrophoresed, all 5 species are apparent in each, but the distribution of subspecies is different. Form I predominates in A, form II in B. Rhodanese treated with 30% by wt. chymotrypsin(20°,30min) shows a 10% loss of activity and SDS gel band intensity. Non-denaturing PAGE shows that bands I&II decrease, while III,IV,&V increase. These data indicate that crystalline rhodanese is more heterogeneous than previously suspected and that A & B forms of the enzyme differ in microheterogeneity. Further, since chymotrypsin can interconvert some species without changing their apparent MW, it is concluded that the differences among rhodanese species are not due to major differences in their polypeptide chains and may be restricted to one end of the polypeptide chain.

W-POS-C2 IDENTIFYING AN UNKNOWN PROTEIN. M.O. Dayhoff and B.C. Orcutt,* Nat. Biomed. Res. Found., Georgetown Univ. Med. Cntr., Washington, D.C. 20007.

In the process of determining the structures of all of the human proteins, there will soon be a time when many newly investigated proteins will be identical or very similar to a protein of known sequence derived from a different tissue or cell line. Identification of the new protein will clarify its structure and function and possibly even the control of its expression. In order to make a positive identification, it is sufficient to know the sequence of only a few residues. A comparison with all segments of the known sequences will produce an outstandingly high score for related or identical segments. It is not necessary that the positions filled by known amino acids be contiguous nor in fact that the positions be known to be filled by single amino acids. It suffices to know that certain positions are filled by a subset of amino acids and that the other positions are filled by the rest. Optimal experimental information will be discussed.

Supported by NIH grants GM 08710 and RR 05681.

W-POS-C3 AN IMPROVED SCORING MATRIX FOR IDENTIFYING EVOLUTIONARY RELATEDNESS AMONG PROTEINS. R.M. Schwartz and M.O. Dayhoff. Nat. Biomed. Res. Found., Georgetown Univ. Med. Cntr., Washington, D.C. 20007.

Statistical computer methods for protein sequence comparisons depend on accumulating scores from the comparison of each amino acid in one sequence with the corresponding amino acid in another sequence. When distantly related protein sequences are compared, a reasonably complex scoring matrix is required to exploit the information contained in both the amino acid identities and nonidentities. We have constructed such a scoring matrix on the basis of the observed exchanges and relative mutabilities of amino acids in closely related sequences from the broad cross-section of protein groups currently available. We have optimized this matrix as a function of evolutionary distance to identify relatedness between protein sequences 65-85% different. Comparisons with other scoring matrices, including earlier versions of this matrix based on less data, demonstrate that this matrix is superior in identifying relationships over the broad spectrum of known sequences.

Supported by NASA contract 3130 and NIH grant GM 08710.

W-POS-C4 EVOLUTIONARY RELATIONSHIPS AMONG PROTEASE INHIBITORS. L. K. Ketcham, W. C. Barker, and M. O. Dayhoff, National Biomedical Research Foundation, Georgetown University Medical Center, 3900 Reservoir Road, N.W., Washington, D.C. 20007

Protease inhibitors have been sequenced from vertebrates, invertebrates, plants, and a bacterium. Of the newly determined sequences, eight are obviously related to three previously characterized superfamilies. Evolutionary trees show that in these groups gene duplications producing several related inhibitors within the same organism have occurred. Certain similarities in size, amino acid composition, and sequence suggest that there may be additional distant relationships among the remaining protease inhibitors. We will discuss possible relationships detected by exhaustive intercomparisons of the amino acid sequences.

Supported by NIH Grant HD 09547.

W-POS-C5 EVOLUTION OF THE SERINE PROTEASE SUPERFAMILY INFERRED FROM SEQUENCES. C.L. Young, W.C. Barker, C.M. Tomaselli,* and M.O. Dayhoff, National Biomedical Research Foundation, Georgetown Univ., 3900 Reservoir Rd., Washington, D.C. 20007.

Sequences of serine proteases of many types, including trypsin, chymotrypsin, elastase, plasmin, thrombin, and Factor X are known from vertebrates, and related proteases are known from bacteria. In both eukaryotes and prokaryotes several types are produced by a single organism. An analysis of the evolutionary history has been made on the basis of sequence information. A time frame for the gene duplications and for the development of specificity and control functions is provided by species divergences. The early evolutionary history of the kringle regions of the precursors of thrombin and plasmin, which is different from that of the regions homologous with trypsin and chymotrypsin, will also be described. Epidermal growth factor is sufficiently similar to a region of Factor X to suggest that it is formed by proteolytic degradation of a related serine protease.

Supported by NIH grant GM 08710 and NASA contract 3130.

W-POS-C6 SIDE-CHAIN MOTION IN HELICAL POLYLYSINE. R. J. Wittebort, Attila Szabo and F. R. N. Gurd. Department of Chemistry Indiana University, Bloomington, Indiana 47401

The theory required to extract detailed motional information from NMR relaxation times of nuclei in an amino acid side-chain containing multiple internal rotations attached to a large macromolecule is developed. Two types of models for the motion of the side-chain are formulated: (1) the diffusional motion about bonds is assumed to be independent and excluded volume effects approximately handled by restricting the amplitude of certain internal rotations; (2) the side-chain is constrained to lie on a tetrahedral lattice and can jump among sterically allowed configurations by means of concerted motions involving partial rotations about several bonds which alter the positions of only a few atoms. The dynamics of jumping is described by a master equation. The ^{13}C relaxation times and nuclear overhauser enhancements of all the carbons in the side-chains of helical polylysine were measured at two spectrometer frequencies and the data analyzed within the framework of the above models.

This work is supported by Public Health Service Research Grants HL-21483 and HL-05556.

W-POS-C7 CARBON-13 NMR AND METAL BINDING PROPERTIES OF BLEOMYCIN. J.L. Benovic*, J.A. Ferretti and R.K. Gupta (Intr. by Philip Aisen), Institute for Cancer Research Philadelphia, PA 19111 and N.I.H., Bethesda, MD 20014

Bleomycin (M.W. ~ 1500), a glycopeptide antibiotic of low toxicity, is effective against a variety of human neoplasms and its complexes with radioactive metals are useful tumor scanning agents for diagnostic purposes. We have obtained undecoupled and proton-noise decoupled high resolution ^{13}C NMR spectra of bleomycin A_2, at 67.9 MHz and pH 8, which show 54 well resolved resonances assignable to individual carbon atoms in the molecule. The chemical shifts, the spin-multiplets observed in the absence of decoupling, the nuclear Overhauser effects, and T_1 measurements were used for spectral assignments. Complexation of bleomycin with Mn^{2+}, a paramagnetic probe, was studied via EPR spectroscopy which measures free Mn^{2+} directly. A Scatchard plot of the Mn^{2+} binding data revealed 0.8 ± 0.2 tight divalent cation sites (K_D^{Mn} ~ 100 μM) per molecule of bleomycin which may be significant in its in vivo action. (Generous gifts of bleomycin from Bristol Laboratories and NCI are gratefully acknowledged; supported in part by NIH grant AM19454 and RCDA AM00231).

W-POS-C8 ^1H NMR STUDIES OF L-HISTIDINE BINDING PROTEIN J OF S. TYPHIMURIUM. B. A. Manuck* and C. Ho, Dept. of Life Sciences, Univ. of Pittsburgh, Pittsburgh, PA. 15260

The first step in the transport of L-histidine, i.e., the binding of L-histidine to the J protein, has been studied by ^1H NMR. Both native and 2 mutant forms of this protein have been observed. One mutant is altered at the L-histidine binding site (TA301) and the second at the protein-protein interaction site (TA300). Comparison of the 250 MHz ^1H NMR spectra of mutants J with those of native J (TA1859) has shown that there are conformational differences among these proteins. The differences between TA300 and TA1859 or TA301 and TA1859 are not the same. Thus, the mutations have acted at different parts of the J molecule. A titration of each protein with the substrate shows conformational changes at the 2 sites of the J protein. These titrations have also yielded estimates of the rate constant k_{-1} for the binding of L-histidine to each of these proteins. We found that k_{-1} is the largest for J protein from TA301 and that TA300 and TA1859 have approximately the same k_{-1}. These data show that the mutation at the protein interaction sites in TA300 has not altered the L-histidine binding site in any significant way. (Supported by research grants from NIH and NSF.)

W-POS-C9 ^1H NMR STUDIES OF NEOCARZINOSTATIN (NCS). R.K. Gupta, J.L. Benovic* and J.M. Pesando. Institute for Cancer Research, Philadelphia, PA 19111 and Sidney Farber Cancer Institute, Boston, MA 02115

NCS is a protein antitumor agent of low toxicity currently undergoing clinical trials. NCS inhibits DNA synthesis in vivo, induces DNA strand scission and is rapidly inactivated by UV light. NMR spectra of NCS reveal 3 one proton resonances at δ = -0.8, -1.0 and -1.4 ppm assignable to an immobilized methyl group touching the face of an aromatic ring which disappear upon UV irradiation and at pH >11. Two titratable aromatic resonances (pKa ~ 11) at 6.3 and 6.5 ppm at pH 12 are assignable to the ring ^1H of the only Tyr. Some of the rings of the 5 Phe appear to be immobilized or located in magnetically different environments due to 3D-folding but become more equivalent upon UV irradiation and at pH >11. The spectra show a broad absorption at 9 ppm of ~20 unexchanged protons from amide groups of the β-sheet. This disappears upon heating and is reduced ~10% by UV light. These observations establish an irreversible change in 3D-folding of NCS as the mechanism of its inactivation by light. The spectra of NCS with DNA or mercaptoethanol argue against DNA binding or reduction of disulfide bonds in the action of this drug.

W-POS-C10 NMR STUDY OF COBROTOXIN. C.H. Fung, C.C. Chang*, and R.K. Gupta. Rutgers Medical School, Piscataway, N.J. 08854, Kaohsiung Medical College, Taiwan and Institute for Cancer Research, Philadelphia, Pa. 19111.

Cobrotoxin (MW 6950) which binds tightly to the acetyl choline receptor contains only 2 His, 2 Tyr, 1 Trp and no Phe that result in resolvable aromatic proton resonances ($\delta \nu_{\frac{1}{2}}$ ~ 3 Hz) in D_2O at 100 MHz. His32, Tyr25 and the Trp are essential for toxicity and may interact with the acetyl choline receptor. We assign the 4 titratable resonances (pK_a~5.3) at δ = 9.0, 8.8, 7.5 and 6.9 ppm at pH 3 and at 7.8, 7.7, 7.1 and 6.7 ppm at pH 8 to the C2 and C4 ring protons of the 2 His, respectively. The differences in δ values of the 2 His reflect chemically different microenvironments while their low pK_a's could arise from nearby + charges. A methyl resonance at δ ~ 0 ($\delta \nu_{\frac{1}{2}}$ = 8 Hz) gradually appears as the His rings are deprotonated and is tentatively assigned to the methyl group of Thr14 or 15 which, from X-ray studies of neurotoxins, may be H-bonded to His4. Further, we have tentatively identified the aromatic resonances of the invariant Trp and the 2 Tyr. Three broad (20 Hz), nontitrating peaks of labile protons (τ_{ex} > 1 week) at 10.1, 9.6 and 9.0 ppm may arise from amide groups of the β sheet in cobrotoxin (Supported by NIH grant AM19454 and RCDA AM00231).

W-POS-C11 HISTIDINE TITRATIONS BY PMR OF DIHYDROFOLATE REDUCTASE FROM TRIMETHOPRIM-RESISTANT ESCHERICHIA COLI STRAINS MB 3746 AND MB 3747. M. Poe, J.K. Wu*, C.R. Short, jr.* and K. Hoogsteen, Merck Institute, Rahway, New Jersey 07065.

The dependence upon pH of the 300 MHz proton magnetic resonance spectrum for binary methotrexate complexes of MB 3746 and MB 3747 dihydrofolate reductase was measured at 25° in D_2O. The two enzymes are closely related to one another and to the dihydrofolate reductase from E. coli MB 1428; they were isolated from trimethoprim-resistant, reductase-overproducing E. coli K12 mutants. The pmr spectra of the binary methotrexate complexes of the 3746 and 3747 reductases are similar. The pK' values of the five histidine residues are 8.15±0.20, 7.55, 6.90, 6.38 and 5.88 for the 3746 reductase:methotrexate complex and 8.23±0.20, 7.30, 6.72, 6.02 and 7.58 for the 3747 reductase:methotrexate complex. These pK' values are equal within experimental error to the pK' values of corresponding histidines in E. coli MB 1428 dihydrofolate reductase, except for histidine 5. The large difference in histidine 5 in 3747 reductase may be the source of this enzyme's different pH vs. activity profile.

HEMOGLOBIN III

W-POS-D1 HEME ENVIRORMENT INVESTIGATIONS BY CARBON-13 NMR. M. T. Kamlay,* H. Mizukami, and J. P. Oliver*
DRBB, Dept. Biology and Dept. Chemistry, Wayne State Univ., Detroit, Michigan 48202

The electronic state of the heme envirment was investigated by natural abundance carbon-13 NMR of HbNO and HbNO + inositol hexaphosphate. Paramagnetic shift and relaxation of those carbons that experience the NO free electron are observed. Chromatographically purified human hemoglobin A (5mM) in 0.05M phosphate buffer at pH 7.1 was used. HbNO was prepared by purging HbCO with NO gas. A Joel FX-60 FT-NMR was used. HbNO displays line broadening in the 45-67ppm (TMS) region which was previously considered to be solely aliphatic in origin. The line broadening observed can be assigned to the upfield shift of paramagnetically relaxed quaternary pyrrole carbons. Little line broadening was observed in the aromatic region (90-160ppm). Upon addition of IHP the peak (45-67ppm) partially reappears responding to the more favored "T" configuration of HbNO + IHP. Thses results demonstrate that the NO free electron delocalizes in a specific region of the porphyrin. Further investigations of high and low spin hemoglobin and hemin derivatives will also be reported.

W-POS-D2 ^{13}C NMR STUDIES OF POLYMERIZED SICKLE HEMOGLOBIN. J.W.H. Sutherland*, W.M. Egan*, D.A. Torchia & A.N. Schechter, NIH, Bethesda, Md. 20014.

Scalar and dipolar decoupled, natural abundance, ^{13}C pulsed Fourier-transform NMR techniques have been used to estimate the fraction of aggregated deoxyhemoglobin S in both cell free solutions and in intact erythrocytes. At 37°C, approximately 30% of the hemoglobin in a 28 g/dl solution is aggregated, whereas about two-thirds of the hemoglobin in whole deoxygenated sickle cells is aggregated. The rigid nature of the backbone of these aggregated molecules is indicated by (1) residual chemical shift anisotropic line broadenings of carbonyl carbons of 10^3 Hz and (2) relatively long ^{13}C spin lattice relaxation times of backbone carbons. The spectrum of the freely rotating deoxyhemoglobin S molecules is virtually unaffected by the presence of aggregated material, suggesting that this material behaves essentially as a two phase system of free hemoglobin plus polymer. In addition, cross-polarization spectra allow direct observation of the immobilized fraction of deoxyhemoglobin S without interference from the mobile fraction. These techniques offer a new approach to the direct study of the sickling phenomenon in intact cells.

W-POS-D3 ^{31}P NMR STUDIES OF THE BINDING OF ATP TO HUMAN HEMOGLOBIN. R.K. Gupta, J.L. Benovic* and Z.B. Rose*
(Intr. by T.F. Anderson), Institute for Cancer Research, Philadelphia, Pa. 19111

Reversible interactions of ATP and MgATP with oxy (HbO_2) and deoxy (Hb) hemoglobin were studied under physiological conditions by ^{31}P NMR. Although hemoglobin does not change the positions of the ^{31}P resonances of ATP or MgATP at pH 7.2, the NMR spectra provide evidence of interactions under aerobic and anaerobic conditions. The presence of Hb was found to displace the apparent equilibrium, $Mg^{2+} + ATP^{4-} \rightleftharpoons MgATP^{2-}$, as measured by ^{31}P chemical shifts, in favor of ATP showing competition between Hb and Mg^{2+} for binding ATP. HbO_2 produces similar but smaller changes in the apparent equilibrium. HbO_2 and Hb also broaden the ^{31}P resonances of ATP. A larger broadening is observed in Hb solutions compared to that in HbO_2 solutions and reflects the higher affinity of ATP and MgATP for Hb. While the affinities of ATP and MgATP for Hb differ ~10-fold, our data indicates only a 1.5-fold difference in their affinities for HbO_2. The NMR data corroborate the conclusion that binding constants of phosphorylated compounds do not change with Hb concentration. (Supported by NIH grants AM-19454, GM-19875 and USPHS RCDA AM-00231).

W-POS-D4 ENERGY LEVELS AND WIDTHS OF THE HIGH-SPIN FERRIC ION IN MYOGLOBIN AND HEMOGLOBIN CHAINS. D. A. Hampton*, A. S. Brill, and F. G. Fiamingo*, Dept. of Physics, U. of Virginia, Charlottesville 22901.

Frozen solution EPR spectra simulated with g-values and linewidths from single crystals differ from those obtained experimentally. There are differences in the rhombic/tetragonal ratio, E/D, and in the admixture of quartet states, η, between the same complex in crystals and in frozen solution, and among complexes. For solution spectra, it is also necessary to spread these factors; agreement is obtained with gaussian distributions, rms deviations $\sigma_{E/D}$ and σ_η. Thus it is possible to characterize heme sites by four parameters, two which determine the energy levels of the ferric ions and two which determine the widths of these levels. For example, aquo complexes of myoglobins and β-chains of hemoglobins have the same values of E/D and η, with $\sigma_{E/D}$ and σ_η 40% greater for myoglobin. Aquo α-chains are 50% more rhombic and have 20% more quartet in the ground state. Formation of the methanol complex sharpens the energy levels of myoglobin, reducing $\sigma_{E/D}$ by a factor of almost two without changing the central values of E/D or η. Formation of the methanol complex doubles the rhombic character of α- and β- chains.

W-POS-D5 SPIN STATE AND CONFORMATION IN Co^{2+}-HEMOGLOBIN. R.K. Gupta, T.S. Srivastava*, and T. Yonetani, Institute for Cancer Research, Philadelphia, PA 19111 and University of Pennsylvania, Philadelphia, PA 19174

Co^{2+}-oxyhemoglobin (CoHb) enhances the relaxation rate of water protons with a paramagnetic contribution to the molar relaxivity ($1/T_{1p}$) of ~500 s^{-1} at 24.3 MHz and 23°. The $1/T_{1p}$ decreases with increasing frequency (for $\omega_I^{-1} < \tau_S, \tau_R$) and temperature ($E_a \sim 3$ KCal) and is unchanged from pH 5 to 9 indicating the outer sphere origin of $1/T_{1p}$. The magnitude of $1/T_{1p}$, which is unaffected by IHP, indicates the accessibility of the spin on O_2 in CoHb for molecular contact with diffusing water molecules. Upon deoxygenation the $1/T_{1p}$ is decreased ~2-fold as the unpaired spin shifts to the Co^{2+} atom probably due to reduced accessibility of the spin on the metal to water. EPR spectra reveal that IHP, which increases auto-oxidation of CoHb, shifts the R-T equilibrium and reduces the oxygen-affinity of CoHb, does not alter the Co^{2+}-hyperfine and the ^{17}O-superfine interactions, the relaxation time and the g-tensor of the unpaired spin. These results indicate the absence of a coupling of the protein conformation to the spin state of Co^{2+} or oxygen. (Supported by NIH grants AM19454, HL14508, NSF Grant PCM77-00811 and NIH RCDA AM00231).

W-POS-D6 THE ASSOCIATED WATER IN SICKLE HEMOGLOBIN SOLUTION-SPIN PROBE STUDY. A.G.Beaudoin and H.Mizukami DRBB, Biology Dept., Wayne State University, Detroit, Michigan 48202.

Water associated with a protein matrix was probed by the non-binding ESR probe, Tempone. ESR spectra of Tempone consisted of either a narrow band triplet (mobile region), a broad band triplet (immobile region), or a composite five line spectrum (two phase region). Tumbling motion of Tempone within concentrated, evacuated sickle Hb solution is displayed as a phase diagram below. Along a 25°C isotherm, complete mobility is obtained at 18% H_2O (i.e. 0.22g H_2O/g Protein). Hb isotherms at 25°C have given the values 0.30 to 0.33g H_2O/g Protein (I.D.Kuntz and W. Kauzmann, Adv. Prot.Chem., vol. 28; 1974). The two phase region at 25°C extends from 13% to 18% H_2O and corresponds to an average increase across this region of 250 moles H_2O per mole Hb.

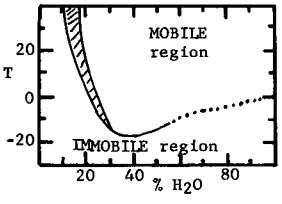

W-POS-D7 BINDING OF METAL IONS TO PHOSPHORYLATED RED CELL METABOLITES. R.K. Gupta and J.L. Benovic* (Intr. by T.H. Moss), Inst. for Cancer Research, Philadelphia, Pa.19111.

The binding of Mg^{2+} to intracellular components of the human red cell affects its function. A magnetic resonance study of the binding of Mg^{2+} and Mn^{2+} to major phosphorylated metabolites of the red cell, under physiological conditions, revealed two independent metal ion sites of equal affinity ($K_D \sim 3mM$) in the 2,3-DPG molecule, one on each phosphoryl group, contrary to assumptions in previous literature. At their intracellular levels, ATP and ADP, however, possess only one metal ion site in spite of the presence of multiple phosphoryl groups. These results are consistent with the chemistry of metal-chelation which requires the formation of 5- or 6-membered chelate-rings for stability. The affinity of Mg^{2+} for ATP (K_D = 38±4 μM) is ~2 to 7-fold higher than that used by others for the quantitation of intracellular distribution of Mg^{2+} in human erythrocytes and in the analysis of the effect of Mg^{2+} on the oxygen equilibria of hemoglobin (Hb). A reinterpretation of the effect of Mg^{2+} on the oxygen-equilibria of Hb-ATP system taking into account the binding of ATPMg to deoxyHb indicates that MgATP binding reduces the oxygen-affinity of Hb ~2-fold. (Supported by NIH grant AM19454 and RCDA AM00231).

W-POS-D8 EXTENSIVE TEST OF THEORETICAL CHARGE AND SPIN DISTRIBUTIONS IN A SERIES OF HIGH SPIN HEME AND METMYOGLOBIN COMPOUNDS THROUGH COMPARISON WITH RELATED EXPERIMENTAL DATA. M.K. Mallick, S.K. Mun, S. Mishra, J.C. Chang and T.P. Das, SUNY, Albany, N. Y. 12222

Using electronic wave-functions, obtained by the extended Hückel self-consistent charge procedure, for the high spin(S=5/2)compounds, hemin and its fluoro, bromo, iodo and hydroxy derivatives and metmyoglobin and fluoromyoglobin, we have analysed their magnetic hyperfine constants for iron, nitrogen and hydrogen nuclei and isomer shifts and splittings of X-ray photoemission spectra. The theoretical results and their comparison with experiment lead to the following conclusions. Satisfactory agreement is obtained in general in both absolute magnitudes and trends of all the properties indicating the satisfactory nature of the calculated charge and spin distributions. There is substantial covalent bonding between iron and its ligands and a consequent drainage of about 40% of the unpaired spin population from the iron. The spin populations on the iron and porphyrin nitrogens are rather stable but those on the other atoms, particularly the atoms of imidazole are rather sensitive to substitutions at the sixth ligand site. Grant support: NIH HL 15196.

W-POS-D9 EXTENSION OF DISCRETE CHARGE CALCULATIONS OF POTENTIOMETRIC TITRATIONS FOR MONOMERIC GLOBULAR PROTEINS TO THE HEMOGLOBIN TETRAMER AND ALLOSTERIC EFFECTORS. J. B. Matthew, G. I. H. Hanania*, and F. R. N. Gurd, Department of Chemistry, Indiana University, Bloomington, Indiana 47401

A modified Tanford-Kirkwood theory for intramolecular electrostatic interactions is applied to the hydrogen ion equilibria of several monomeric globular proteins and the hemoglobin tetramer. The theoretical titration curves at the appropriate ionic strengths compare closely with experimental potentiometric curves and the theoretical pK values for individual groups in each protein correspond to the available observed pK values. Treatment of the human hemoglobin tetramer allows the electrostatic effects of N-terminal carbamino formation and 2,3-diphosphoglycerate binding to be calculated. Predicted theoretical effects of quaternary state or allosteric effector interaction are discussed in terms of observed individual group pK values and the pH dependent binding of $^{13}CO_2$. Amino acid substitution in the coordinate list allows the prediction of electrostatic perturbation in hemoglobin mutants involving changed amino acid residues. (Supported by PHS Grants HL-05556 and TlGM-1046).

W-POS-D10 MECHANISM OF THE ALKALINE BOHR EFFECT AT VAL α1. S. O'Donnell, R. Mandaro, T. Schuster, Biological Sciences Group, University of Connecticut, Storrs, CT 06268, and A. Arnone,* Department of Biochemistry, University of Iowa, Iowa City, IO 52242

Crystallographic studies of human deoxyhemoglobin (Hb) carbamylated at the α-chain amino termini showed that the carbamyl group displaces an anion from a site between Val 1(α1) and Arg 141(α2)(Arnone, A., O'Donnell, S., and Schuster, T. 1976. Fed. Proc. 35, 1604.). This anion is thought to form a salt bridge between these two groups which is responsible for the high pK of Val α1 in Hb. To test this hypothesis we have performed direct titrations of the alkaline Bohr protons of both carbamylated and uncarbamylated hemoglobin at several salt concentrations. Here we present data which shows that this anion mediated salt bridge is involved in part of the alkaline Bohr effect. We also present equilibrium oxygen binding data for normal and α-chain carbamylated hemoglobin which is consistent with the presence of an oxygen linked anion mediated salt bridge in Hb. Supported by grants to S.O'D., NIH(HL05222), T.S., NIH (HL17494), NSF(BMS75-16093) and A.A., NIH(AM17563), NSF(GB43803)

W-POS-D11 FUNCTIONAL PROPERTIES OF THE MINOR COMPONENTS OF HUMAN ADULT HEMOGLOBIN. M.J. McDonald, M. Bleichman* and R.W. Noble, Peter Bent Brigham Hospital, Harvard Medical School, Boston, MA and S.U.N.Y. at Buffalo, N.Y.

A new chromatographic technique has been recently developed which allows purification of several negatively charged minor components, designated Hb A_{1a_1}, Hb A_{1a_2}, Hb A_{1b} and Hb A_{1c}. Oxygen equilibrium measurements at pH 7 and 20° in phosphate buffer reveal P50 values of 14, 9.8, 6.3, and 6.7 mm Hg respectively as compared with 7.8 mm Hg for Hb A_0. After being freed of phosphate the ligand affinity of Hb A_0 was noticeably increased (p50=4.3 mm Hg at pH 7, 20° in Bis Tris buffer) as was that of Hb A_{1b} and Hb A_{1c} whereas the affinities of Hb A_{1a_1} and Hb A_{1a_2} remain nearly the same (P50=14 and 8.1 mm Hg respectively). Carbon monoxide combination rates measured under similar conditions reflect the equilibrium results. These findings are consistent with the proposed structures of fructose 1,6-diphosphate Hb and glucose-6-phosphate Hb for Hb A_{1a_1} and Hb A_{1a_2} respectively. These sugar phosphates, presumably linked to the NH_2 terminal of the β chains, appear to mimic the effect of organic phosphate in lowering the affinity of and stabilizing the deoxy structure of these hemoglobins.

MEMBRANE STRUCTURE AND FUNCTION

W-POS-E1 A METHYL GROUP POSITION EFFECT ON THE INHIBITION OF SEVERAL PLASMA MEMBRANE FUNCTIONS BY MONO-SUBSTITUTED POLYCYCLIC AROMATIC HYDROCARBONS. M.E. Aberlin* and G.W. Litman, Sloan-Kettering Institute, New York, NY 10021

Examination of the interaction of noncovalently bound polycyclic aromatic hydrocarbons (PAHs) with the plasma membrane has led to the unexpected finding that both the presence and the position of a methyl group on the lipophilic PAH nucleus determines whether the compound functions as an inhibitor of erythrocyte membrane acetylcholinesterase (ACE) or of glucose exchange. 2-;6-;7-;11-; 12-; and 7,12-methylbenz(a)anthracenes (BAs) inhibit ACE in intact erythrocytes but not in ghosts. 3-; 5-;8-; and 9-methylBA and BA do not inhibit ACE. In the anthracene (A) series, 9-methylA inhibits while A and 2-methylA do not. Glucose exchange is inhibited by the same compounds as ACE. Arrhenius temperature-activity plots for ACE show a change in slope at ~18°C not seen in the presence of inhibitor. For glucose exchange the change in slope at ~23°C is not sensitive to the presence of inhibitor. These results suggest that noncovalently bound PAHs affect membrane lipid-protein interactions in a manner extremely dependent on the geometric shape of the inhibitory molecule. (Supported by NCI Grants CA-16889;-08748).

W-POS-E2 DIFFUSION, PATCHING AND CAPPING OF SYNTHETIC ANTIGENS ON CELLULAR AND MODEL MEMBRANES. D. E. Wolf*, W. W.Webb, Cornell Univ., Ithaca, N.Y., 14853, and P. Henkart, Immunology Branch, N.C.I., N.I.H., Bethesda, Md. 20014.

We have modeled cell membrane antigens with a series of fluorescent stearoylated dextrans, made antigenic by addition of controllable amounts of the hapten TNP. We have incorporated these molecules into planar BLM's and a variety of cell plasma membranes. Their behavior on cell membranes is similar to that of native membrane proteins. Using the technique of fluorescence photobleaching recovery we have found that, like proteins, these molecules have $D \sim 10^{-10}$ cm^2/sec with a significant immobile fraction ~30%. On BLM's D is ~10^{-8} to 10^{-9} cm^2/sec with no immobile fraction. On planar bilayers, and on the membranes of RBC's and certain tumor cells, the addition of cross-linking antibodies causes patching. On lymphocytes and fibroblasts both patching and capping are observed. Drug inhibition of capping is similar to that observed for native membrane proteins but drugs have little effect on diffusion or mobile fraction. We have determined the dependence of patching and capping on antigenic valence and mobility.

W-POS-E3 INHIBITION OF PHAGOCYTOSIS IN MOUSE PERITONEAL MACROPHAGES BY TERTIARY AMINE LOCAL ANESTHETICS. W. E. Fogler*, D. M. Gersten* (Intr. by H. B. Bosmann), Cancer Biology Program, NCI-Frederick Cancer Research Center, Frederick, Maryland 21701

Phagocytosis of opsonized sheep erythrocytes by cultured mouse peritoneal macrophages is inhibited by the tertiary amine anesthetics, tetracaine, dibucaine and procaine. The inhibition is reversible at low concentrations and is antagonized by Ca^{++}. The extent of the inhibition is proportional to the affinity of the anesthetics for lipid. Phagocytosis of particles is known to consist of a recognition step and an internalization step. Immune-mediated recognition of the sheep erythrocytes via the opsonizing mouse immunoglobulin by the macrophages is sensitive to the anesthetics. Non-immune recognition of unopsonized erythrocytes is not. However, post-recognition internalization of the sheep erythrocytes is also inhibited by the anesthetics. The basis for the inhibition of recognition appears to be steric, and related to anesthetic-induced clustering of receptors on the macrophage surface. The inhibition of ingestion is presumably due to disruption of the macrophage cyto-skeleton. (NCI Contract No. NO1-CO-75380).

W-POS-E4 FUNCTIONAL ALTERATIONS IN SARCOPLASMIC RETICULUM FROM DYSTROPHIC MUSCLE. M. A. Neymark*, S. J. Kopacz* and C. P. Lee, Department of Biochemistry, Wayne State University School of Medicine, Detroit, Michigan 48201

The phosphoenzyme level and the ATPase activity have been measured in sarcoplasmic reticulum preparations (SR) from two animal models of muscular dystrophy, myodystrophic (myd) and strain 129 (dys) mice. In SR from skeletal muscle of dys mice, the ATPase activities in the presence of 0.1 mM Ca^{++} or 1 mM EGTA are 6.51 ± 0.71 and 4.01 ± 0.59 μmoles P_i/mg.prot,/min, respectively. Both are significantly higher than the levels in controls (3.17 ± 0.33 and 0.69 ± 0.05, respectively). However,the Ca^{++}-dependent ATPase is normal. Similar results are seen with SR from myd mice; the ATPase activities in the presence of Ca^{++} or EGTA are 4.91 ± 0.27 and 1.52 ± 0.13 μmoles/mg.prot./min, respectively. The corresponding values for the controls are 3.39 ± 0.26 and 0.66 ± 0.05. The level of the Ca^{++}-dependent phosphoenzyme intermediate is decreased by 10-15% in SR from myd mice (3.03 nmoles/mg.prot.) as compared with controls (3.48 nmoles/mg.prot.) and is decreased approximately 40% in SR from dys mice (2.13 nmoles/mg.prot.) compared with controls (3.84 nmoles/mg.prot.). Supported by NIH and MDAA.

W-POS-E5 SPECIFIC LIGAND DEPENDENCE ON THE INTERACTION BETWEEN PYRUVATE OXIDASE AND DIPALMITOYL LECITHIN. Herbert L. Schrock*, Patricia Russell*, and Robert B. Gennis. Department of Chemistry, University of Illinois, Urbana, Illinois 61801.

Pyruvate oxidase is a peripheral membrane flavoenzyme from E. coli which catalyzes the oxidative decarboxylation of pyruvate to yield acetate plus CO_2. The enzymatic activity is enhanced about 25-fold when the assay is performed in the presence of phospholipids. Sucrose density centrifugation and gel filtration chromatography have shown that the substrate-reduced form of pyruvate oxidase interacts strongly with dipalmitoyl lecithin vesicles,but under identical conditions the oxidized form of the enzyme does not bind to lecithin vesicles. In the absence of the substrate, the lipid binding properties of pyruvate oxidase are greatly diminished. Cholate is being tested as a mediator in the reconstitution procedure. Controlled proteolysis has been used to specifically destroy the lipid binding properties of pyruvate oxidase. SDS-acrylamide gels indicate the subunit molecular weight of the modified enzyme is reduced from 60,000 to 56,000. N-terminal analysis tentatively indicates that the site of cleavage, and, presumably, the lipid binding site is located at the C-terminus.

W-POS-E6 PURIFICATION OF ALKALINE PHOSPHATASE AND CA^{++}-ATPASE FROM BASAL LATERAL MEMBRANES OF RAT DUODENUM. S. Hanna,* A. Mircheff,* and E. Wright, UCLA, Los Angeles, CA 90024

Alkaline phosphatase has been purified at least 5,000 fold from the basal lateral membranes of rat intestinal epithelia. The purification steps involved are (1) density gradient centrifugation to isolate basal lateral membranes, (2) butanol extraction of the basal laterals, (3) acetone fractionation of the butanol fraction, and (4) preparative electrophoresis of the acetone fraction. The purified enzyme is a dimer with a molecular weight of approximately 150,000 daltons, and the monomers are held together by disulfide bonds. Dissociation of the dimer with mercaptoethanol produces two subunits with slightly different molecular weights, and neither subunit contains enzyme activity. The purified enzyme also exhibits calcium ATPase activity, implying that alkaline phosphatase and calcium ATPase activities may be different manifestations of the same enzyme. (Supported by USPHS grants NS 09666 and AM 19567).

W-POS-E7 DISTRIBUTION OF INTRAMEMBRANOUS PARTICLES IN ERYTHROCYTE MEMBRANES R. Pearson,* T. P. Stewart* and S. W. Hui, Roswell Park Memorial Institute, Buffalo, N. Y. 14263

A variety of statistical methods are used to provide a quantitative description of the planar distribution of intramembranous particles (IMP) seen in freeze fracture electron micrographs of human erythrocyte membranes. Membrane ghosts are treated in various ways so as to alter the distribution of IMP's. The distribution parameters to be analysed include: radial distribution, angular relationships between neighbors, occupancy number of designated areas and the scale of organization. The Fourier transforms of various distribution functions are computed and compared to the expected diffraction patterns. The purpose of the analysis is to discern any organization of IMP and to detect any uneven IMP partition in phase-separated lipid domains, as against a totally random distribution. These results are then related to the chemical treatments of the erythrocyte membranes.

W-POS-E8 STRUCTURE OF UROTHELIUM LUMINAL MEMBRANES BY IMAGE PROCESSING AND X-RAY DIFFRACTION. L. Cordova* and J. Vergara* (Intr. by Harry C. Beall). Dept. of Anatomy, Duke University, Durham, North Carolina 27710.

The outer surface of membranes of mammalian urothelium present a hexagonal structure with a typical unit side of 16nm made up of subunits about 5nm in diameter packed on a p6 lattice. A method of isolation of these specialized cell surfaces with minimal perturbation of the membrane matrix components has been devised based on their comparatively low density (1.14 g/ml). The yield of the separation procedure permits correlated studies of the structure by thin sectioning, x-ray diffraction and image processing of micrographs from negatively stained specimens. Thin sections show the asymmetric nature of the profile characterized by a peak-to-peak distance of 7.7nm and a total bilayer width of 15.3nm. X-ray diffraction of membrane pellets at normal incidence gives reflections indexing on a hexagonal lattice at 13.9, 8.2, 7.1, 5.4 and 3.5nm. At tangential incidence a strong reflection is found at 80Å, interpreted as the bilayer peak-to-peak spacing. Image processing supports the view that each hexagon comprises six elongated subunits. Supported by NIH Grant #3 P01 NS10299.

W-POS-E9 EFFECTS OF MEMBRANE STRUCTURAL ALTERATIONS ON MONOOXYGENASE ACTIVITY. J.F. Becker, T. Meehan, and J.C. Bartholomew, Laboratory of Chemical Biodynamics, Lawrence Berkeley Laboratory, Univ. of Calif., Berkeley, CA 94720

The enzyme aryl hydrocarbon hydroxylase (AHH) metabolizes benzo(a)pyrene (BaP) to its ultimate carcinogenic form. The Arrhenius plot exhibited by AHH in rat liver microsomes is biphasic and at a substrate concentration of 4 μM the pahse transition occurs at 29°C. As the substrate concentration is increased the break temperature remains approx. constant but the activation energy (E_A) above the transition increases and E_A below it decreases until the transition is no longer observable. On the other hand, increasing the average saturation of membrane fatty acids significantly affects the break temperature of the enzyme (4±1°C). Dissolving large amounts of BaP in the microsomal membrane destroys the observed phase transition while the fatty acid composition alters its value. Thus, the structure of the membrane in the vicinity of the enzyme profoundly affects its activity and properties. (Supported by NIH-DHEW contract UOI-CP-50203 and Grant 1F32 CA05573-01 and DBER of US ERDA.)

W-POS-E10 FREEZE-FRACTURE LOCALIZATION OF IMMUNOGLOBULINS ON THE SURFACE OF MACROPHAGES. H. Bank, D. Emerson,* P. Sannes,* S. Spicer* Charleston, South Carolina 29403

Using a high resolution freeze-fracture technique, we have visualized an antigen-antibody complex on the surface of alveolar macrophages. Macrophages were reacted with a soluble horseradish peroxidase - anti-horseradish peroxidase IgG at 4°C and subsequently warmed to 37°C. The membrane bound antibody receptor complexes were visualized as discrete surface particles without cytochemical amplification and ranged in size from 5-15nm in diameter, these complexes occupied <2% of the cell surface. The complexes were initially randomly distributed on the surface of the plasma membrane. Within 5 min. of warming to 37°C many of these complexes were found in concave depressions of the cell surface, followed by endocytosis. Even after aggregation of the complex, the distribution of intramembranous particles was not affected, indicating that the receptor molecules for immunoglobulins are not identifiable by the freeze-fracture procedure. In epon embedded preparations exposed to diaminobenzidine - hydrogen peroxide, a similar process of translocation of reactive sites followed by aggregation and endocytosis was observed.

PHYSICAL PROPERTIES OF MEMBRANES

AND MODEL MEMBRANES

W-POS-F1 HIGH RESOLUTION ^{31}P AND ^{13}C NMR SPECTRA OF UNSONICATED MODEL MEMBRANES. R. Haberkorn*, J. Herzfeld and R. G. Griffin*. Francis Bitter National Magnet Laboratory, MIT, Cambridge, MA 02138 and Biophysical Laboratory, Harvard Medical School, Boston, MA 02115.

The broad linewidths ordinarily seen in NMR spectra of membranes arise primarily from anisotropies in the chemical shift and dipolar interactions which are incompletely averaged due to restricted molecular motion. Thus, it has been common in NMR studies to increase the molecular motion by sonicating and heating the membranes. In order to avoid these procedures, we have used magic angle spinning, combined with high power dipolar decoupling, to obtain high resolution spectra of multilamellar lipid bilayers in a 6.8 T field, at ~21°C. For dipalmitoyl lecithin (DPL), we narrow a 7.2 kHz wide ^{31}P powder spectrum to a centerband flanked by two pairs of sidebands, each 95 Hz wide. For dimyristoyl lecithin (DML) and DPL, we obtain ^{13}C linewidths of ~20 Hz and resolve all of the lines observed when these lipids are dissolved in organic solvents. The two ^{13}C spectra are similar, except that whereas only two distinct glycerol lines are seen in the DML spectrum, all three are resolved in the DPL spectrum. (Support: NSF C-670; NIH GM-23316 & GM-23289.)

W-POS-F2 TUNABLE SMALL ANGLE X-RAY DIFFRACTION STUDIES OF L-α-DIPALMITOYL PHOSPHATIDYLCHOLINE (DPPC) MULTILAYERS USING SYNCHROTRON RADIATION, J. Stamatoff, L. Powers, P. Eisenberger*, Bell Laboratories, Murray Hill, NJ 07974; H. H. Wickman, R. K. Lytz, Dept. of Chemistry, Oregon State University, Oregon.

The tunable X-ray beam at the Stanford Synchrotron Radiation Laboratory provided X-rays of variable wavelengths for diffraction studies of DPPC. Highly oriented samples of DPPC, prepared by the methods of Powers and Clark[1], were incorporated with Zn^{++} cations. Fourteen orders of lamellar diffraction were recorded using a rise-time position sensitive X-ray detector for several wavelengths about the zinc K-edge. The results of this experiment and the use of changes in the relative intensities to provide phase angle information will be discussed.

[1]Powers, L., and N. A. Clark, PNAS (USA) 72, 840.

W-POS-F3 EFFECTS OF CA-ATPASE ON PHOSPHOLIPID BILAYER FLUIDITY: BOUNDARY LIPID. B.M. Moore*, B.R. Lentz and G. Meissner* (intr. by J. White), Department of Biochemistry, Univ. of North Carolina, Chapel Hill, N.C. 27514.

Membrane vesicles containing Ca-ATPase were isolated from rabbit skeletal muscle and then successively delipidated by treatment with cholate. Lipid analysis showed nonselective loss of phospholipid. After removal of 99.9% of the cholate, a hydrophobic membrane probe, 1,6-diphenyl-1,3,5-hexatriene, was incorporated into the membranes and the anisotropy of its fluorescence was measured in the temperature range 5-40° for each delipidated membrane. We have attempted to fit the anisotropy measurements to a model that assumes that the probe partitions between a solvation annulus of "rigid" lipid surrounding the Ca-ATPase and a bulk lipid domain. This probe has been shown to partition equally between phospholipid bilayers of different fluidities. The model was found to represent the data well at low temperatures but not at high temperatures. Our tentative conclusion is that there exists an annulus of "rigid" lipid around the Ca-ATPase at low temperatures but not at physiological temperatures. Supported by NSF grant #PCM76-10701 (BRL) and USPHS grant #AM18687 (GM).

W-POS-F4 X-RAY SCATTERING FROM LIPID BILAYERS AND RED CELL MEMBRANES, J. Stamatoff, T. Bilash, and Y. Ching, Bell Laboratories, Murray Hill, NJ 07974

X-ray scattering studies on suspensions of L-α-dipalmitoyl phosphatidylcholine (DPPC) single bilayers and hemoglobin free red cell membranes were performed using a new high flux, high brightness X-ray system. X-rays from a bright rotating anode source (70KW/mm^2) were point focused to a (0.5mm)^2 spot using a large doubly curved crystal (75mm x 25mm). The scattered X-rays were detected using a stable position sensitive X-ray detector with a nichrome wire anode filled with Ar-CH_4 at 100 lbs/in^2. This apparatus makes possible the accurate recording of patterns from both lipid bilayers and membranes in suspension (avoiding the use of high g centrifugation).

We have used heavy atom stains to determine the thickness of single lipid bilayers in suspension. In addition, heavy atom stains (including one which is specific for membrane protein) have been applied to red cell membranes to determine their thickness. Analysis of the results also permits a determination of the distribution of the stain.

W-POS-F5 LATERAL DIFFUSION OF A MYELIN MEMBRANE PROTEIN INCORPORATED INTO PHOSPHOLIPID MULTIBILAYERS. Z. Derzko,* & K. Jacobson, Biophysics Dept. SUNY/Buffalo & Expt. Pathology, Roswell Park Memorial Institute, Buffalo NY 14263.

The method of fluorescence recovery after photobleaching (FRAP) has been used to measure the temperature dependence of the lateral diffusion coefficient (D) of a fluorescein labelled, hydrophobic, myelin protein, lipophilin (N2), incorporated into phospholipid multibilayers of various compositions. For lipophilin incorporated dimyristoylphosphatidylcholine multibilayers, the apparent D is: (1.3 ± 0.7) X 10^{-9}cm^2/sec below T_m with about 45% recovery, indicating a substantial amount of immobilized protein. Above T_m, D increases by a factor of five with nearly complete recovery. For egg phosphatidylcholine multibilayers at 41°C, D for lipophilin was about (15.8 ± 7.7) X 10^{-9}cm^2/sec. Incorporating equimolar cholesterol into the multibilayers decreased the protein diffusion coefficient. Unlabelled lipophilin reduced the mobility of the fluorescent lipid analog, NBD-phosphatidylethanolamine. This work was supported by NIH Grant CA 16743. K.J. is an Established Investigator of the American Heart Association.

W-POS-F6 SPIN LABEL STUDY OF STRUCTURAL EFFECTS AND REACTIVITY OF LIPID HYDROPEROXIDES IN MEMBRANE MATRICES. S. Schreier, Instituto de Química, Universidade de São Paulo, C.P.20780 São Paulo, Brazil.

Hydroperoxy derivatives had the same effects as cholesterol on membranes of dipalmitoyl or egg phosphatidyl choline, as monitored by the electron paramagnetic resonance (EPR) spectra of spin probes. However, attempts to form membranes of phosphatidyl ethanolamine and hydroperoxides yielded spectra that indicated a very low degree of ordering. This was probably due to the interaction and/or further reactions between the phospholipid amino group and the hydroperoxy moiety. Addition of ferrous ions to membranes containing hydroperoxides induced formation of radicals which reacted with the N-O group, as seen by loss of the EPR signal. The rate of signal decay depended on lipid composition. The results indicate that both the structural and chemical behavior of hydroperoxides depend on membrane composition.

Supported by the project Bioq/FAPESP.

W-POS-F7 DEUTERIUM NMR OF LIPID BILAYERS: HEAD GROUP CONFORMATION,EFFECT OF IONS AND CHOLESTEROL, RELAXATION RATE STUDIES. M. F. Brown and J. Seelig*, Biocenter, Univ. of Basel, Switzerland.

1) The deuterium and phosphorus NMR spectra of DPPC and DPPE labeled with ^2H in the polar region suggest that the head groups are oriented parallel to the bilayer surface. 2) Addition of cholesterol leaves the PC and PE dipoles oriented parallel to the membrane surface. 3) Addition of trivalent ions (shift reagents) induces drastic changes in the NMR spectra of head group labeled DPPC. The effects of Ca^{++} are currently being investigated. 4) Quadrupolar relaxation time measurements of DPPC bilayers deuterated in the hydrocarbon region have been made and a theory developed to account for the effects of order and motion on the relaxation rates. Knowledge of the deuterium quadrupole splittings and the T_1 and T_2 relaxation times allows interpretation of the data in terms of a simple diffusional model with an anisotropic restoring potential. The profile of motion in the hydrocarbon region of both unsonicated multibilayers and sonicated vesicles will be discussed.

W-POS-F8 HYDRATION NUMBER OF SODIUM AT A NEGATIVELY CHARGED INTERFACE. M.J.McCreery* and H.J.C.Yeh*, AFRRI and NIAMDD, NIH, Bethesda, Md. (Intr. by D.O.Carpenter).

The various cation selectivities observed in biological and nonliving systems have been attributed to the differential attractive forces exerted on cations between water and the negatively charged surface (Eisenman,1961). The hydration number for cations adjacent to the interface should reflect these forces. We have inferred the hydration number of Na^+ at the negatively charged interface of a model system, the Aerosol-OT (AOT)/H_2O/octane reversed micelle. The pool of water dissolved within these spherical aggregates may be continuously altered from a diameter of 75 Å to 10 Å by varying $[H_2O]/[AOT]$. Utilizing the temperature sensitivity of the chemical shift of the proton magnetic resonance of H_2O, our studies have yielded apparent hydration numbers from 1.0 to 0.3 correlating well with the charge density calculated for the negative interface. These data may be compared to the hydration number of 4.5 for this ion obtained in concentrated salt solutions using the same technique (Creekmore and Reilley, 1969). The results suggest strong ion pairing between Na^+ and the negative interface leaving the nearly unhydrated sphere in this region.

W-POS-F9 MOLECULAR DYNAMICS SIMULATION OF PHOSPHOLIPID MONOLAYERS. Terence R. Thompson* and David A. Goldstein (Intr. by W. Bernhard) Dept. of Radiation Biology & Biophysics, The University of Rochester, Rochester, New York 14642.

A dynamic model of a phospholipid monolayer has been constructed which moves phospholipid-like centers of force according to an integrated law of motion in finite-difference form. Forces on each phospholipid analog are derived from the gradient of the local potential which is in the sum of Coulombic and short-range terms. The Coulombic term is obtained by solving a finite-difference form of Poisson's equation in three dimentions. The short-range term results from finite-radius, pairwise summation of one of several phenomenological intermolecular potentials. Boundary potentials are treated in such a way that the model is effectively infinite in extent in the plane of the monolayer. The two-dimentional virial theorem is used to find the surface pressure (Π) of the monolayer as a function of molecular area (A). Π versus A curves are plotted for different values of model parameters including structure and orientation of head groups and hydrocarbon tails.

W-POS-F10 ANALYSIS OF THE LAMELLAR NEUTRON DIFFRACTION FROM FUNCTIONAL SARCOPLASMIC RETICULUM. L. Herbette, A. Scarpa, B. Schoenborn, and J.K. Blasie. Univ. of Pa., Phila., PA 19104; Brookhaven Nat'l Lab, Upton, NY 11973

Lamellar neutron diffraction from oriented multilayers of functional sarcoplasmic reticulum (SR) vesicles was obtained as a function of the H_2O/D_2O ratio for several states of hydration. A generalized Patterson function analysis, previously developed for treating lamellar diffraction from lattice-disordered multilayers, was used to phase the appropriately corrected lamellar neutron diffraction from multilayers equilibrated at three different hydration states in 100% D_2O. The phase determination was consistent for the different lamellar periodicities. These phased lamellar intensity data were then used to calculate the neutron scattering profiles for the multilayer unit cell as a function of the H_2O/D_2O ratio at a specified hydration state. Differences between scaled pairs of such profiles allowed the determination of the neutron scattering profile of the water layers in the multilayer unit cell, consistent with the electron density profiles obtained from X-ray diffraction.

W-POS-F11 X-RAY AND NEUTRON DIFFRACTION STUDIES OF RECONSTITUTED SARCOPLASMIC RETICULUM. L. Herbette, C.T. Wang*, A. Scarpa, S. Fleischer, B. Schoenborn, and J.K. Blasie. Univ. of Pa., Phila., PA 19104; Vanderbilt Univ., Nashville, TN 37235; Brookhaven Nat'l Lab, Upton, NY.

ATP-induced Ca^{++} uptake and ATPase activity of reconstituted membraneous vesicles of sarcoplasmic reticulum (RSR) were measured at eight lipid/protein (L/P) ratios over a range of 35-115 mole phosphorus/mole protein. Hydrated oriented multilayers of RSR vesicles were shown to give rise to lamellar X-ray and neutron diffraction. Electron density profiles were determined by analysis of the lamellar X-ray diffraction data at a resolution of 10 Å for the same L/P ratios. Analysis of the lamellar neutron diffraction data obtained under H_2O/D_2O exchange in RSR multilayers determined the neutron scattering profile of the membrane and water layers of the unit cell consistent with the electron density profiles previously determined over the same L/P range. These studies have indicated the location of the Ca^{++} ATPase in the membrane profile as a function of the L/P ratio, the location of water in the various unit cell profiles and a basis for the correlation of modifications of membrane profile structure with modifications in Ca^{++} uptake activity as a function of L/P ratio.

W-POS-F12 CHANGES OF MEMBRANE PROPERTIES IN *THERMOPLASMA ACIDOPHILUM* UPON LOW TEMPERATURE ADAPTATION. Li L. Yang and A. Haug*, Department of Biophysics and MSU/ERDA Plant Research Laboratory, Michigan State University, East Lansing, Michigan 48824

Thermoplasma acidophilum, a mycoplasma-like organism, grows optimally at 56°C and pH 2. The low temperature extreme of growth is 37°C. In the following we report about experiments concerning the role of temperature on physico-biochemical membrane characteristics. Membrane lipids which comprise 25% of the membrane dry weight consist mainly of 2,3-glycerol diethers with highly branched C_{40} side chains as determined by gas chromatography-mass spectrometry. Lipid analysis reveals that 37°C grown *T. acidophilum* shows 36% more unsaturation of the side chains. Phospholipid and serine content decrease by about 10% each, carbohydrate content increases by 5%. EPR studies demonstrate an increase in membrane lipid fluidity of 37°C grown cells with an upper transition temperature shifted down by 10°C. Membrane-bound ATPase activities also indicate similar changes upon adaptation. There is a close correlation between membrane fluidity and physiological functioning of the membrane-bound enzyme.

NERVES AND AXONS V

W-POS-F13 EFFECT OF PROTEIN CLUSTERING ON LIPID MOTION IN THE E. COLI MEMBRANE. M. P. N. Gent and C. Ho, Dept. of Life Sciences, Univ. of Pittsburgh, Pittsburgh, PA. 15260

Myristic acids labeled with a difluoromethylene group are incorporated into the membrane phospholipids of an unsaturated fatty acid auxotroph, K1060B5, of E. coli. The ^{19}F NMR line shape can be fit with an absorption curve derived from the basic theory of magnetic resonance relaxation. Using computer aided line fitting the following parameters are measured: the separate intensities due to the fluid and the frozen lipids; the order parameter for the fluid lipid; and the narrowing of the center of the resonance, a parameter that is especially sensitive to protein-lipid interactions. This technique reveals that the temperature dependence of the motional behavior of the phospholipids is different in the E. coli cytoplasmic membrane than in lipid extracts thereof or synthetic lipid membranes. This behavior is explained by the temperature dependent protein clustering in E. coli. In addition, there is a premelting phenomenon due to the heterogeneous distribution of lipid and protein in the E. coli membrane below the transition temperature. (Supported by research grants from NIH and NSF, and a NRSA of NIH.)

W-POS-F14 DESIGN OF ELECTROCHROMIC PROBES OF MEMBRANE POTENTIAL. L.M. Loew, G.W. Bonneville,* S. Scully,* J. Surow,* A. Hassner,* and V. Alexanian, Chemistry Dept., SUNY at Binghamton, Binghamton, NY 13901

An electrochromic response may be found for an extrinsic probe satisfying two conditions: 1) it must undergo a large electron redistribution upon excitation; 2) it must be properly and rigidly oriented with respect to a changing local or transmembrane electric field. We have developed a molecular orbital theory approach which can be used to calculate how well a new probe structure meets these criteria. The approach also rationalizes the failure of many of the most successful existing probes to adopt a direct electrochromic mechanism. We have synthesized a new probe, 4-(p-dipentylaminostyryl)-1-methylpyridinium iodide which, our calculation predicts, has an amphipathic ground state and experiences a migration of its charge down the long molecular axis upon excitation. Absorbance and fluorescence experiments in various solvents and in the presence of lipid bilayers support a rigid orientation of the long axis perpendicular to the membrane surface. In addition, the probe shifts its spectrum in response to a valinomycin induced K^+ diffusion potential.

W-POS-G1 CAPACITANCE CHANGES OF SQUID AXON MEMBRANE DURING ACTION POTENTIALS. S. Takashima and R. Yantorno, Department of Bioengineering D2, University of Pennsylvania, Philadelphia, Pa. 19104.

Previously we investigated the voltage dependence of capacitance of squid axon membrane using externally applied hyper- and depolarizing pulses. We found a capacitance increase from 0.9 to 1.25 uF/cm^2 between -160 and +40 mV membrane potentials. In the present work, capacitance is measured during the action potential. With normal action potential, the increase in capacitance is only from 0.9 to 1.0 uF/cm^2, in agreement with Cole and Curtis' measurements. However, there is strong indication that this result is due to the compensation of a possible capacitance increase by an inductive component. The inductive reactance can be eliminated by blocking K-currents by use of internal TEA (15mM). During these prolonged action potentials, we found that the capacitance of the axon membrane increased to 1.3 uF/cm^2 with a small change in membrane conductance. Thus we concluded that the capacitance of axon membrane is variable during the action potential. This research is partially supported by ONR N-00014-76-C-642.

W-POS-G2 VERATRIDINE AND SODIUM CHANNELS IN SQUID AXONS. V. Scruggs & D. Landowne, Univ. of Miami, Miami, Fl 33152.

The currents associated with 3-6ms depolarizing voltage pulses have been studied in voltage-clamped squid giant axons. When the axons were internally perfused with a solution containing 50μM veratridine the peak INa was somewhat decreased and a small inward Itail appeared which declined exponentially with a time constant of about 600ms at -60mV and 9°C. During 20/sec, 8 pulse trains there was a decrease of the peak INa and an increase of the Itail toward steady-state values. It was found that the Itail was larger when the test pulse duration or amplitude was increased or if the pulse was preceded by a hyperpolarizing prepulse which removed steady-state inactivation of the peak INa. The Itail but not the peak INa was reduced about 50% when Li was substituted for external Na. Both the peak INa and Itail were blocked by tetrodotoxin, by replacing external Na with Tris or choline, and by 1mM $ZnCl_2$. These findings suggest that veratridine interacts with the normal Na channel, modifies its kinetics, and possibly its selectivity.

W-POS-G3 ACTION MODE OF TERTIARY AMINE LOCAL ANESTHETICS ON SQUID AXON MEMBRANE EXCITABILITY. S. Ohki, C. Gravis, SUNYAB, Buffalo, N.Y. 14226, and H. Pant, National Institute of Mental Health, Bethesda, MD 20014

Measurements included the time to exert narcotic action after application of given concentrations of local anesthetics to the extracellular solutions at various pH. A theoretical relationship describing the mode of action was obtained in terms of the internal and external pH's, the external concentration of local anesthetics, their permeabilities to the membrane and the time to exert narcotic action. The analysis of the experimental data by the theory developed concluded that the predominant mode of action of tertiary amine local anesthetics is, first to penetrate into the axon interior in a neutral form, and then to react in a cationic form from the intracellular phase. The direct measurements of permeability of the local anesthetics by use of a radioisotope tracer method gave a good agreement with those obtained by the above electrophysiological method.

W-POS-G4 POTASSIUM-ION MOBILITY AND PARTITION COEFFICIENT OF SQUID-AXON MEMBRANE. H. Richard Leuchtag, Department of Physics, Indiana University (present address: Physics Today, 335 E. 45 Street, New York, N. Y. 10017)

For the model consisting of potassium ions in electrodiffusion across a planar membrane, an exact solution exists.[1] As previously described, the boundary conditions specifying the external ion concentrations, when applied to this solution, lead to a transcendental equation, which was solved by a numerical method.[1] Data for squid axons, by K.S. Cole and J.W. Moore[2] and by E. Rojas and G. Ehrenstein (in seawater and isotonic K^+),[3] were fitted to the resulting current-voltage curves. The data fit yields three parameters, which are functions of the temperature, boundary concentrations, membrane thickness, dielectric constant ϵ, partition coefficient β, and mobility u. With an assumed ϵ of 7.6, the values found (averaged for the four curves) were $\beta \approx 0.008$ and $u \approx 4 \times 10^{-7}$ cm sec^{-1} $dyne^{-1}$.

1. H.R. Leuchtag, J.C. Swihart, Biophys. J. 17, 27 (1977); Fed. Proc. 33, 1339 (1974); Bull.APS 20, 41(1975).
2. K.S. Cole, J.W. Moore, J.Gen.Physiol. 44, 123(1960).
3. E. Rojas, G. Ehrenstein, J. Cell. Comp. Physiol. 66 (Suppl. 2), 71 (1965).

W-POS-G5 ION AND DRUG INTERACTIONS AT THE SAXITOXIN BINDING SITE. C.M. Hansen Bay* and G.R. Strichartz, Dept.of Physiol.& Biophysics, SUNY, Stony Brook, Stony Brook, N.Y. 11794

The saturable binding of tritium labelled saxitoxin(*STX) to nerves of lobster walking legs at 3-5°C is characterized by one class of receptors with K_D=8-12 nM, ranging in population from 90 to 210 fmoles/mg wet. *STX binding is competitively inhibited by TTX(K_I=3.5-5.5nM) and by a crude extract of octopus venom, maculotoxin: K_I=0.5-1.5μg/ml. Aconitine, a drug which modifies gating and relative permeability of g_{Na} in nerves, produced a small but consistent inhibition: 11.4±2.3% at 10^{-4}M. Scorpion venoms from L.quinquestriatus and C.sculpturatus had no effect. The pK_a of the site is 4.5-4.8. Monovalent organic cations competitively block STX binding in the order: HOguanidine>H_2Nguan≅ hydrazine>guanidine≅H_3Chydrazine≅NH_4^+≅H_3Cguan.> formamidine>acetamidine>$H_3CNH_3^+$. This is different from the order in which they block Na^+ currents in frog nodes (Hille, J.Gen.Physiol. 66, 535,1975). Supported by USPHS NS-12828

W-POS-G6 A NEW TECHNIQUE FOR SIMULTANEOUS INTERNAL DIALYSIS AND VOLTAGE-CLAMP IN MYXICOLA: ASYMMETRY CURRENTS. C. L. Schauf and J. O. Bullock. Rush College of the Health Sciences, Chicago, Illinois 60612.

Myxicola axons may be voltage-clamped and the internal composition rapidly controlled by insertion of axial electrodes inside a 180 μ cellulose acetate dialysis tubing. In contrast to perfused axons, dialyzed axons have normal leak conductances and remain viable for several hours. Sodium channel selectivity is somewhat higher than in perfused axons. Asymmetry currents are easily recorded and for pulse durations sufficiently short Q_{on}= Q_{off} with a maximum charge displacement of 10 nC/cm^2 (0.21nC/mmho) and half the charge displaced by a step to -32mv. Maximum slope of the Q(V) curve is 15mv/e-fold change in charge displaced. The time constant τ_{on} has a maximum of 325 μsec at -23mv. The time course of g_{Na} in the range -40 to 40mv could not be adequately described by $(Q/Q_\infty)^x$ for any single value of x. For small potentials g_{Na} lags integral charge movement by more than predicted for x=3, while for large positive potentials g_{Na} is proportional to Q/Q_∞ after an initial lag.

W-POS-G7 PROCEDURES CAUSING INACTIVATION OF ASYMMETRY CURRENTS IN MYXICOLA AXONS: RELATIONSHIP TO SODIUM INACTIVATION. J. O. Bullock and C. L. Schauf. Department of Physiology, Rush College of the Health Sciences, Chicago, Illinois 60612.

In Myxicola axons dialyzed with mixtures of CsF and Cs glutamate the measured asymmetry currents can be inactivated by several distinct procedures. In axons repetitively voltage-clamped at frequencies of 0.1 to 50Hz I_{Na} is markedly decreased with increasing frequency due to a process of slow sodium inactivation. The relative decrease in asymmetry current is identical to the decrease in I_{Na} measured in the same axons under these conditions. However, during a long-lasting depolarization the magnitude of the Q_{off}/Q_{on} ratio decreases to a value of 0.2-0.3 with a time course substantially slower than the time course of sodium inactivation. As the magnitude of this ratio decreases a distinct slow component appears in the off response. No such component is detectible in the on response. Finally, depolarizing prepulses reduce the magnitude of the asymmetry current evident during a subsequent pair of test pulses, and recovery from this decrease is more closely correlated with recovery from sodium inactivation.

W-POS-G8 RADIAL DIFFUSION OF SOLUTES IN "INTERNALLY DIALYZED" GIANT FIBER. F.P.J. Diecke*, W. Perl*, M.A. Stout* and D.W. Diecke* (Intr. by B.A. Schottelius), CMDNJ-New Jersey Med. School, Newark, N.J. 07103.

The steady state radial diffusion and the concentration profile of small permeable solutes, ATP and EGTA-buffered Ca^{++} have been modeled using the equations for diffusion in the composite hollow cylinder of n regions with diffusion coefficients $D_1..D_n$. Transmembrane fluxes and the diffusion coefficients for various porous capillaries were measured or obtained from the literature. The computations indicate that membrane boundary concentrations of Na^+ and K^+ are identical to their concentrations in the dialysis fluid at resting transmembrane fluxes. However, in the fully poisoned giant axon or muscle fiber dialyzed with ATP, considerable ATP gradients between the core of the capillary and the membrane may exist. Moreover, under these conditions low ATP/ADP ratios may be generated at the inner membrane surface which may lead to significant distortions of transport kinetics. Lastly, the model predicts that Ca^{++} transmembrane flux at constant $(Ca^{++})_i$ may be significantly affected by low EGTA-buffer concentrations. (Supported by grant NS-05188 from NINCDS).

W-POS-G9 CALCIUM BINDING AND ITS RELATION TO CALCIUM CURRENT NOISE IN SNAIL NEURONS. N. Akaike, K. S. Lee,* H. M. Fishman, L. E. Moore and A. M. Brown, University of Texas Medical Branch, Galveston, Texas 77550

A calcium current, I_{Ca}, is present in Helix neurons and in addition to 10^{-8}A changes, smaller 10^{-12}A fluctuations occur in response to step changes in membrane potential. This current noise was detected using a low noise suction pipette method for voltage clamp and internal perfusion. K^+ and Na^+ currents were suppressed by Cs^+ and Tris substitution. I_{Ca} was blocked by Ni^{2+}. Amplitude histograms (AH) and power spectra (PS) were computed from the fluctuations. Spectral densities were 2-3 orders above thermal levels. Difference spectra (before and after Ni^{2+} treatment) were fitted by a single Lorentzian function. The variances computed from AH or PS were similar and gave unit conductances for Ca^{2+}, γ_{Ca} of 0.6 to 0.06 pS. These γ's are lower than those reported for Na^+ and K^+ systems in axons and transmitter-activated systems in molluscan neurons. I_{Ca} saturated with small increases in $[Ca^{2+}]_o$ and various divalent cations blocked I_{Ca}. Saturation and blockage were fitted by an adsorption model and the adsorbing site may cause the low γ_{Ca}.

W-POS-G10 THE ROLE OF ATP ON THE RATE OF Ca EXTRUSION FROM SQUID AXONS. H. Rojas*, R. Blanco*, R. DiPolo*, and C. Caputo. IVIC, Caracas 101, Venezuela.

We have studied the ability of squid axons to control an imposed rise in the Ca_i^{++} under different experimental conditions. For this we have observed changes in the Ca_i^{++} by measuring absorbance of the Ca binding dye arsenazo III using differential absorption spectroscopy. Changing the external medium from full Na_o,$3Ca_o$ to full Na_o,$60Ca_o$ increases the Ca_i^{++}. Subsequent removal of Na_o and Ca_o maintains the Ca_i^{++} at a high stable value for periods greater than 45 min. Readdition of full $Na_o 3Ca_o$ decreases the Ca_i^{++} to the initial value. Axons fully poisoned with FCCP+cyanide+iodoacetate fail to extrude the Ca_i^{++} load. Injection of ATP allows them to extrude again the imposed load. Axons injected with apyrase, to reduce their ATP content, behave as fully poisoned axons. These results indicate first, that the rate of Ca extrusion depends on ATP, and second, that an imposed in the Ca_i^{++} can only be extruded if Na is present in the external medium. This argues against the role of an uncoupled Ca pump in the regulation of the ionized calcium concentration.

(CONICIT, grant No. 31.26.S1-0602).

W-POS-G11 IONIC EXCHANGE IN SYNAPTOSOMES AND RELEASE OF SEROTONIN. A. P. Carvalho, Depart. of Zoology, Univ. Coimbra, Portugal

Synaptosomes from sheep brain are impermeable to Ca^{2+}, Mg^{2+}, K^+, Li^+, Na^+, Cl^-, $SO_4^{=}$, $PO_4^{\equiv}$ and oxalate, and are permeable to acetate, propionate, erythritol and glicerol. Valynomycin plus FCCP, or X-537 A, cause net production of protons in KCl medium, but do not cause swelling of the synaptosomes; In potassium acetate or propionate, no net production of protons is observed, but swelling occurs. The relative permeability of the various cations and anions was measured, and the results suggest that acetate and propionate enter the synaptosomes after protonation as a consequence of H^+ efflux. The Ca^{2+} ionophore A 23187 increases the influx of Ca^{2+} into synaptosomes loaded with serotonin and induces its release, but A 23187 also releases serotonin in the absence of Ca^{2+}, which suggests a direct effect of A 23187 on serotonin release. (Supported by I.N.I.C., Portuguese Ministry of Education and Scientific Research)

W-POS-G12 SOLUBILIZATION AND CONCANAVALIN A-SEPHAROSE AFFINITY CHROMATOGRAPHY OF AXON PLASMA MEMBRANE FRAGMENTS. D. C. Hilt* and J. K. Marquis, Dept. of Biochem. & Pharmacol., Tufts Univ. Sch. of Med., Boston, MA 02111.

Detergents including Tween 20, Tween 80, Triton X-100 and Lubrol WX; digitonin and lysolecithin; and the processes of sonication and high salt (1M NaCl) extraction were used in attempts to solubilize axon membrane proteins from a membrane-enriched fraction of lobster walking leg nerve bundles. The solubilized fractions were applied to Concanavalin A-sepharose columns (1ml) and eluted with a-methyl mannoside to isolate the glycoprotein components. 25 $\pm$ 6% of the total protein was eluted in the glycoprotein fraction and quantitative recovery of total protein was observed. A 10-fold enrichment of AChE activity was achieved. The solubilized fractions and chromatographed fractions were characterized for specific binding of ^{3}H-quinuclidinyl benzilate and ^{125}I-α-bungarotoxin, muscarinic and nicotinic antagonists, respectively, previously seen to exhibit high affinity, saturable binding to axon membrane fragments. This work was supported by The Medical Fdtn. and the Charlton Fund (JKM); The PMAF (DCH) and by a grant to H.G.Mautner from the NINDS (NS09608).

W-POS-G13 A MODEL OF A MOLECULAR STRUCTURE FOR PART OF THE SODIUM CHANNEL. J.R. Smythies, M.D., Birmingham, Alabama 35294

The complex molecules of batrachotoxin (BTX), aconitine and veratridine all act at the same locus on the sodium channel so as to delay sodium inactivation. This communication presents CPK models of a simple protein structure that composes a channel capable of transmitting Na+ with an internal electrogenic gate. The system consists of two 4-tiered β-pleated sheets, each composed of -gln-x-gln-, facing each other. Each gln binds to the gln opposite by two h-bonds. When the gate is open each gln binds in addition to the vertical gln neighbour(s) by 1-2 more h-bonds. To shut the gate each gln rotates through 90^0 at the α-β C-C bond and reforms the h-bond pattern with the horizontal gln neighbour. The mechanism works like a venetian blind. This system is complementary in different ways to the molecules of BTX, aconitine and veratridine which would prevent the "gate" from closing. It is also complementary to the molecules of aplysiatoxin and haplophytine which toxins are predicted by this hypothesis to act like BTX. The model also indicates a possible tertiary structure for scorpion neurotoxin.

RNA LIGANDS

W-POS-H1 INHIBITION OF AMV REVERSE TRANSCRIPTASE BY SPIN-LABELED NUCLEIC ACIDS. P.E. Warwick,* A. Hakem* and A.M. Bobst, Chemistry 172, University of Cincinnati, Cincinnati, Ohio 45221

Some nucleic acids such as $(U)_n$ and $(dUfl)_n$ have been shown to act as inhibitors of AMV reverse transcriptase. This has led to a project in which spin-labeled nucleic acids are used to study the interaction between the enzyme and its nucleic acid inhibitors. Previously, it was shown that spin-labeled nucleic acids can be used in competition experiments to determine the relative affinity of proteins for nucleic acids (BBRC 67, 562 (1975)). At the outset of the present study we examined whether the spin moiety (1 spin per 75-100 bases) affects the inhibitory activity of the nucleic acids. With oligo dG:poly rC as primer:template the enzymatic activity was measured in terms of [^{3}H]dGMP/min/ml incorporation. The amount of labeled versus unlabeled inhibitors required for 50% inhibition (compared to controls without inhibitors) was determined with a primer:template concentration 8 x K_m. The results suggest that the spin label has no significant effect on the inhibitory activity of the nucleic acids. Supported in part by NIH grant CA 15717.

W-POS-H2 PHYSICAL CHARACTERIZATION OF A 5S DNA-PROTEIN COMPLEX FROM HALOBACTERIUM CUTIRIBRUM. **G.E. Willick*, Nat. Res. Coun., Ottawa, and A.T. Matheson*, Univ. of Victoria, Victoria, Canada.** (Intr. by J.R. Colvin)

A 5S RNA-protein complex, isolated from Halobacterium cutiribrum, an extreme halophile with a high internal salt concentration, was only stable in high salt. It contained two proteins, designated HL-13(MW=18,700) and HL-19(MW=18,000). The complex bound less ethidium bromide(EB) than the 5S RNA. Only one protein, HL-13, chased bound EB, suggesting a functional correspondence to E. coli 5S RNA binding protein L-18(Feunteun et al, JMB, 93, 535(1975)). Agarose gel chromatography and sedimentation equilibrium studies indicated it dissociated below 1.5M KCl, 10mM Mg^{2+}. Sedimentation equilibrium data on the native complex yielded an estimation of the 5S RNA-protein association constants. Under optimum ionic strength conditions(3.4M KCl, 100mM Mg^{2+}) the overall association constant was 10^{14} M^{-2}. C.D. measurements suggested that the RNA structure was enhanced in the presence of the proteins and that the secondary structure of both proteins underwent a salt induced conformational change centered at 2M KCl. The results suggested that the RNA stabilized the protein structure in the complex.

W-POS-H3 ELECTRON MICROSCOPIC DETERMINATION OF THE BINDING SITES OF RIBOSOMAL PROTEINS S15 AND S20 ON 16S RNA. M.D. Cole*, and M. Beer, Department of Biophysics, Johns Hopkins Univ., Baltimore, MD 21218 and W.A. Strycharz and M. Nomura, Institute for Enzyme Research, University of Wisconsin, Madison, Wisc. 53706

Specific complexes between ribosomal protein S15 or S20 and 16S RNA were fixed with formaldehyde and spread for microscopy by a protein free technique. Protein binding preserves an easily recognized configuration in the RNA that allows determination of the binding site. S15 binds in the middle of 16S RNA to a hairpin which is often bent at its middle. This probably arises from three unpaired bases on one side. The S20-16S RNA complex is a blob containing about 100 nucleotides located at least 350 bases from one end of the 16S RNA. This would place it outside of the binding region determined from nuclease protection experiments. Binding sites for three proteins that we have determined are displaced about 80 nucleotides toward the 3' end from those found by nuclease. One interpretation is that the published sequence of 16S RNA lacks a segment of 60-80 nucleotides, probably between L and H".

W-POS-H4 DISTANCE BETWEEN THE ANTICODONS OF TWO tRNA'S BOUND TO THE RIBOSOME. R.H. Fairclough* and C.R. Cantor, Columbia University, New York, N.Y.10027.

Yeast $tRNA^{Phe}_{Pf}$, in which proflavine (Pf) is chemically substituted for the naturally occurring Y base next to the 3' base of the anticodon, exhibits changes in fluorescence upon interaction with poly(U)-programmed ribosomes. Using these changes to quantitate the binding, we have found the binding consistent with a two site sequential binding model with association constants of 1.0×10^9 M^{-1} and $3.4\times10^7 M^{-1}$ under conditions of high Mg^{++} (25mM) and low temperature (7°C). The emission spectrum arising from ribosomes binding two $tRNA^{Phe}_{Pf}$'s presents evidence for two way Förster energy transfer which places the two Pf's less than 20Å apart. The distance obtained using one way Förster transfer between the Y base and Pf is 18±4Å. The emission anisotropy of $tRNA^{Phe}_{Pf}$ bound to the first site, to the second site, and to both sites is 0.31,0.24, and 0.21 respectively. The decreased anisotropy when both sites are filled is interpreted as resulting from transfer depolarization. This decrease is related to the angle between the two Pf's which can be calculated to be 147± 10° or 33±10°. Part of this work is a collaboration with W. Wintermeyer and H.G. Zachau of the University of Munich. (Supported by NIH GM 14825).

W-POS-H5 KINETIC STUDIES ON THE INTERACTION OF GDP WITH ELONGATION FACTORS Tu AND Ts. V. Chau*, G. Romero*, R. Biltonen* (Intr. by H. Kutchai), Department of Biochemistry, University of Virginia, Charlottesville, VA 22903

The dissociation rate constant of GDP from the complex Tu·GDP obtained from the isotope exchange reaction:

$$Tu\cdot(^3H)GDP + GDP_{excess} \rightleftharpoons Tu\cdot GDP + [GDP_{excess} + (^3H)GDP]$$

was found to be 1.7×10^{-3} sec^{-1} at 21°C. Temperature dependence studies yield an activation enthalpy of 15 kcal/mole. In the presence of a catalytic amount of Ts, the dissociation rate is greatly accelerated. Detailed kinetic studies of the reaction made, using a rapid mixing and filtration apparatus, indicated that Ts acts as a catalyst, and that the exchange reaction can be described by the following mechanism

$$Tu\cdot[^3H]GDP + Ts \underset{k_{-1}}{\overset{k_1}{\rightleftharpoons}} Tu\cdot[^3H]GDP\cdot Ts \underset{k_2}{\overset{k_{-2}}{\rightleftharpoons}} Tu\cdot Ts + [^3H]GDP$$

$$Tu\cdot Ts + GDP \underset{k_{-2}}{\overset{k_2}{\rightleftharpoons}} Tu\cdot GDP\cdot Ts \underset{k_1}{\overset{k_{-1}}{\rightleftharpoons}} Tu\cdot GDP + Ts$$

Analysis of the kinetic results give k_{-2} = 50 sec^{-1} and $(k_{-1} + k_{-2})/k_1 = 1.6 \times 10^{-6}$ M^{-1}.

W-POS-H6 PURIFICATION OF MYOSIN mRNP-TRANSLATIONAL CONTROL RNA AND ITS INHIBITORY ACTION ON DIFFERENT MESSENGERS. S. Heywood and D. Kennedy* Genetics and Cell Biology, University of Connecticut, Storrs, Conn. 06268.

Oligo-U containing myosin mRNP-tcRNA has been previously isolated by dialysis of the 80-100S mRNP fraction from embryonic chick muscle (Bester et al, PNAS, 72, 1523, 1975). This has been necessary due to the inability to separate nucleic acids by molecular weight on agarose beads (Zeichner and Stern, Biochemistry, 16, 1378, 1977). The use of cross-linked Sepharose 4-B allows for the separation of nucleic acids by molecular weight presumably due to removal of charged groups by the covalent cross-linking. Utilizing this type of column we have increased the yield of recoverable tcRNA, demonstrated that it is found only associated with the myosin mRNP particles (not with the ribosomes fraction of the 80-100S material), and verified its homogeneous size as a 2-3S RNA. In studying its inhibitory activity in protein synthesis using several purified messengers, the importance of pre-hybridizing the tcRNA to the individual messengers prior to addition to cell free systems is demonstrated by the comparison of its differential effect on the translation of these messengers.

DNA AND NUCLEOTIDES

W-POS-H7 INDUCTION AND DECAY OF MOUSE INTERFERON MESSENGER RNA, N.B.K. Raj,* B. F. Fernie* and P. M. Pitha, Johns Hopkins Oncology Center, Baltimore, MD 21205

Translation of mRNA injected into *Xenopus laevis* oöcytes has been used as a highly sensitive and quantitative assay for interferon mRNA. Injection into oöcytes of poly(A)-containing RNA isolated from poly I·C and DEAE dextran induced C-243 cells resulted in the production of biologically active interferon with antigenic characteristics of mouse interferon. Functionally active interferon mRNA is detectable between 5-8 hrs after induction with a maximum accumulation at 7 hrs. Comparison of cellular interferon synthesis with relative accumulation of interferon mRNA after induction showed a general correlation. α-Amanitin at concentrations similar to those required to inhibit cellular DNA-dependent RNA polymerase form II inhibited completely the interferon production. Addition of α-amanitin at 3, 5 or 7 hrs after induction stimulated the subsequent interferon production by 2-4 fold, while actinomycin D treatment decreased the interferon production. This suggests that the interferon gene(s) is transcribed over an entire period of induction with a maximum accumulation of interferon mRNA in cytoplasm at 7 hrs.

W-POS-I1 COMPUTER GRAPHICS ILLUSTRATION OF DOUBLE-STRANDED NUCLEIC ACIDS. L.S. Kan, J.R. Kast*, D.Y. Ts'o*, and P.O.P. Ts'o. Div. of Biophysics, Sch. of Hyg. and Publ. Hlth., Johns Hopkins Univ., Balt., MD 21205.

A computer program (named GINA) in Fortran has been written for the calculation of NMR and other properties of nucleic acids. One-half of GINA (SEQ) prints out the Cartesian and cylindrical coordinates of all atoms of a double-stranded helix of nucleic acid in the A,A', or B conformation having any specified base sequence up to 30 nucleotides. The program can be readily modified for longer helices or for other conformations. In addition, the distance between any 2 atoms or the distance from the base ring center to any atom in the helix can be calculated by SEQ. The other half of GINA (MOLTEK) is an interactive graphics program which uses structure information files generated by SEQ. MOLTEK can illustrate a molecular structure on a graphics terminal. The structure on the screen can be enlarged, rotated, selected, and translated. This information has been used to calculate the ring current effects on the ^{1}H chemical shift of 2 short helices, r(AAGCUU)$_2$ and d(AAAGCTTT)$_2$. Data obtained using this approach agree well with that from Kendrew-model construction (Biochem. 14, 4847) and from the table by Arter and Schmidt (Nucleic Acids Res. 3, 1437). (Supported by NSF PCM-74-23423 and NIH GM-16066)

W-POS-I2 CIRCULAR DICHROISM OF DNA. C. A. Sprecher* and W. C. Johnson, Jr., Department of Biochemistry and Biophysics, Oregon State University, Corvallis, Oregon 97331

Circular dichroism spectra have been measured for A-form, B-form, C-form and denatured conformations of DNA to 165 nm. The bands recorded in the vacuum UV region (below 200 nm) for various DNA's are sensitive to the source of the nucleic acid. Comparison of these spectra with circular dichroism spectra of the monomers recorded to 165 nm demonstrates that the vacuum UV is the region of choice for studying base-base interactions.

W-POS-13 THE ROLE OF SOLVENT IN THE STABILIZATION OF HELICAL STRUCTURE. K.J. Breslauer, C. Bodnar,* and J. McCarthy,* Department of Chemistry, Douglass College, Rutgers University, New Brunswick, New Jersey 08903.

Experimental investigations of helix to coil transitions in ribo-oligonucleotides traditionally have been carried out in aqueous, neutral buffer solutions. To gain insight into the role that solvent plays in the determination of nucleic acid structure, we have investigated conformational stability as a function of solvent conditions. UV melting curves have been used to determine the stability of low pH ribo-oligo A double helices in a series of mixed aqueous/organic solvent systems. We found that the extent of helix destabilization depended in a reasonably predictable fashion on both the quantity and the nature of the added organic solvent. The observed trends are interpreted in terms of the influence of hydrophobic forces on the stability of nucleic acid structures. Analysis of the optical melting curves revealed that the van't Hoff enthalpy change remained relatively constant despite shifts in the melting temperature of nearly 30°C. This indicates that the observed solvent induced destabilization of the helix is almost entirely an entropic phenomenon.

W-POS-14 THE SUPRAORGANIZATION OF EUCARYOTIC DNA SEQUENCES. D. L. Vizard and A. T. Ansevin, M. D. Anderson Hospital and Tumor Institute, Houston, Texas 77030

The supraorganization of complex eucaryotic DNA sequences can be studied using thermal denaturation techniques involving partial denaturation, renaturation,and re-denaturation in the absence of reassociation. Satellite populations within a genome, which are readily distinguishable as repeated sequences, comprise unique molecular classes, whereas the bulk of the DNA (for most species) appears to form a distribution of molecules that are continuously dispersed with respect to base composition. Within this continuously dispersed population of molecules, the proximity of DNA sequences of widely varying base composition can be assessed, and relatively large deviations from randomly organized sequences can be detected. For instance, within a"typical" molecule composing the primate genome, (A·T)-rich sequences appear to be in close proximity to the most (G·C)-rich sequences. Furthermore, some classes of interspersed repeated sequences become evident upon the renaturation of partially denatured duplex molecules.
(Supported by NIH Grant GM 20367)

W-POS-15 A MODEL FOR THE SINGLE STRANDED COIL FORM OF POLYDEOXYNUCLEOTIDES FROM MINIMUM ENERGY CONFORMATIONS OF A DIMERIC SUBUNIT. B. Hingerty*, and S. Broyde, MRC Lab. of molecular Biology, Cambridge, England and Biology Dept., New York University, N.Y.,N.Y. 10003

The minimum energy conformations of dApdA were examined for their suitability as building blocks of the single stranded coil form of polynucleotides. Calculations of the characteristic ratio $C_\infty = \langle r_o \rangle^2 / n\ell^2$ were made for a polymer generated from all the low energy conformers, as well as for selected combinations. A polymer composed of a conformer with ω', ω = t,g^+, ψ=t, C-(2')-endo type pucker, in combination with the 'B' form, has a C_∞ equal to that observed in coils of apurinic acid[1] when the fraction of 'B' form conformers is ∿40 and ∿91%. The t,g^+ conformer is the second lowest energy form in the C-(2')-endo puckering domain, following the 'B' form.

1. Achter, E. and Felsenfeld, G. (1971) Biopolymers 10, 1625-1634.

W-POS-16 MECHANISM FOR FORMALDEHYDE INDUCED POLYNUCLEOTIDE UNWINDING. T. Ree Chay, Department of Life Sciences, University of Pittsburgh, Pittsburgh, PA. 15260

If the pH in a solution is high enough, there exists a critical point such that the unwinding of polynucleotide induced by formaldehyde occurs by means of two separate chemical reactions, either by the HCHO-imino reaction alone or by the HCHO-amino reaction alone. The critical point dependends on the ionic strength, temperature, and the formaldehyde concentration, satisfying $s=1+K_U\lambda$, where s is a measure of hydrogen bond strength, K_U is the binding concstant for the HCHO-imino reaction, and λ is the formaldehyde concentration. We have incorporated this chemical process into the master equation and formulated a mathematical model for the polynucleotide unwinding process. When this model is applied to synthetic and real polynucleotides, we find a very good agreement between the theory and experiment.

This research is supported by the National Institutes of Health Career Development Award (5 K04 GM 70015-05), National Institutes of Health Grant GM 20569-03, and National Science Foundation Grant PCM 76-81543.

W-POS-17 DNA CONFORMATIONAL KINETICS. S.C. Szu and R.L. Jernigan, Lab. of Theor. Biol., DCBD, NCI, NIH, Bethesda, MD 20014

The comprehensive series of experiments by Record and Zimm indicate major differences between denaturation and renaturation kinetics in viral DNA. The time varying denaturation rates appear to depend strictly on the current conformational state; whereas, the constant renaturation rate depends only on the initial and final conditions. A model for the time dependence of DNA conformational states is formulated in the form of first order differential equations. Only two states, helix and coil, are considered; relaxation rates are calculated for finite perturbations. Qualitative agreement with experiments is found in denaturation and for the series of renaturation experiments with the same initial condition. However, partial agreement with series of renaturation experiments having the same final condition is obtained only by including an initial bimolecular step with properly matched pairs of strands. We have found no single model that agrees with all groups of experiments. Comparison of all experiments with calculated rates yields $5\times10^4 min^{-1}$ as the step rate for melting an average base pair.

W-POS-18 HYDROGEN AND FLUORINE NMR STUDIES ON THE CONFORMATION AND INTERACTION OF FLUORINATED NUCLEIC ACIDS. J. L. Alderfer and G. Hazel,* Department of Biophysics, Roswell Park Memorial Institute, Buffalo, New York 14263

Chemical shifts and coupling constants (^1H and ^{19}F) are reported for nucleosides and nucleotides of the mutagenic 5-fluoro-uracil and -cytosine in D_2O and DMSO-d_6 solutions. Conformational populations obtained from coupling constants are (0.1M/D_2O,27°): (1) fUrd(pH5), C2'-endo(0.45), C3'-endo(0.55); ϕ(C4'-C5'), g^+(0.69), g^-(0.21), t(0.10); (2) fUrd(pH8), C2'-endo(0.45), C3'-endo(0.55); ϕ(C4'-C5'), g^+(0.69), g^-(0.22), t(0.09); and (3) fCyd(pH8), C2'-endo(0.36), C3'-endo(0.64); ϕ(C4'-C5'), g^+(0.74), g^-(0.19), t(0.07). In DMSO-d_6(27°), the $-NH_2$ resonance of Cyd appears as a single resonance, while for fCyd two well resolved peaks ($\Delta\delta$ = 0.133 ppm) are found, which merge at higher temperatures. The ^{19}F chemical shifts are very sensitive to interactions and the ionization state of the base and phosphate(5') moieties. In DMSO-d_6(27°) fCyd(10mM) plus Guo(50 and 250 mM) produces downfield shifts of the ^{19}F resonance of 0.14 and 0.67 ppm, respectively, relative to fCyd alone. A pH change from 6.4 to 7.0 (in D_2O) shifts the F5 downfield 0.25 ppm for 5'-fUMP and 0.14 ppm for 5'fCMP.

LIPID BILAYERS IV

W-POS-J1 TRANSPORT AND PARTITIONING OF METHYLMERCURY CHLORIDE IN PHOSPHOLIPID VESICLES AS STUDIED BY FLUORESCENCE QUENCHING. Steven J. Rakow‡ Joseph R. Lakowicz, and John M. Wood‡ Freshwater Biological Institute, University of Minnesota, P.O. Box 100, Navarre, MN 55392.

Fluorescence spectroscopy can provide information about the transport and partitioning of a small molecule across a membrane. The ability of methylmercury chloride (MMC), a potent neurotoxin, to quench a variety of fluorescent probes allows this approach to be used to study the interaction of MMC with membranes.

Results indicate that the permeability of DPL vesicles to MMC varies from 6 to 40% of an equivalent thickness of water or solvent, with the bilayer surface providing a greater energy barrier than the alkyl side chain region. Partitioning of MMC into lipid bilayers under these conditions is very low ($P < 10$).

In conclusion, lipid bilayers provide little resistance to MMC transport, and partitioning into the hydrocarbon region is limited. It appears likely that the quenching method will permit the correlation of membrane transport rates with mercurial toxicity.

W-POS-J2 CONFORMATIONAL NON-EQUIVALENCE OF CHAINS 1 AND 2 OF DIPALMITOYL PHOSPHATIDYLCHOLINE. B. Gaber, P. Yager,* and W.L. Peticolas, University of Oregon, Eugene, Oregon, 97403

RAMAN SPECTROSCOPY is able to monitor the conformational state of either chains of a phosphatidylcholine molecule in which one of the chains is isotopically differentiated. We have synthesized the lecithins, 1-palmitoyl, 2-palmitoyl-d_{31} phosphatidylcholine and 1-palmitoyl-d_{31}, 2-palmitoyl phosphatidylcholine. Aqueous dispersions of both phospholipids display both premelting and melting transitions approximately midway between the temperatures of the transitions of DPPC and chain-perdeuterated DPPC. The two compounds show significant differences. We attribute these Raman spectral differences to differing conformations of the fatty acyl chains attached at the 1' and 2' position on the phospholipid. Difference spectra indicate that below the pre-transitions, the conformation of the 2' chain is, on average, slightly less all-*trans* than is the chain at the 1' position, and that some differences in conformation between the two chains persist even above T_m. Supported by grants from NSF, and an NRS Award (CA5488-0) from the NCI.

W-POS-J3 RATE OF THE PRE-TRANSITION IN DIPALMITOYL PHOSPHATIDYLCHOLINE. B. R. Lentz and R. L. Biltonen*, Department of Biochemistry, Univ. of North Carolina, Chapel Hill, N. C. 27514 and Department of Pharmacology, Univ. of Virginia, Charlottesville, Va. 22901.

Discrepancies between calorimetric and fluorescence depolarization monitoring of the pre-transition are shown to result from the slow rate of this transition. The depolarization of fluorescence of the hydrophobic, membrane-associated dye 1,6-diphenyl-1,3,5-hexatriene has been used to determine the temperature of the pre-transition for a series of heating and cooling scan rates. These temperatures, when plotted versus scan rate, extrapolated linearly to the phase transition temperature at zero scan rate, t_c=29.7±0.8. The slopes obtained from these plots yielded the characteristic times for the transition, 8±2 min and 21±6 min, for heating and cooling, respectively. Analysis of temperature jump experiments, assuming first order kinetics, gave corresponding times of 5±2 min and 4.9±0.1 min. Further small discrepancies between our fluorescence and calorimetric results were noted and are discussed in terms of the location of the fluorescent probe in the membrane.
This work was supported by NSF grant #PCM76-16761 to BRL and grant #PCM75-23245 to RLB.

W-POS-J4 PARTITIONING AND DIFFUSION OF CHLORINATED HYDROCARBON INSECTICIDES IN MEMBRANES AS STUDIED BY FLUORESCENCE QUENCHING OF CARBOZOLE LABELED PHOSPHOLIPIDS. G. Omann*, J.R. Lakowicz, D. Hogen*, Freshwater Biological Institute, Navarre, MN 55392

Chlorinated hydrocarbons such as DDT, DDE, lindane, mirex, CCl_4, and gardona have been shown to be efficient dynamic quenchers of carbozole fluorescence. Dynamic quenching provides a measure of the collisional frequency between the quencher and the fluorophore. Having synthesized phospholipids containing carbozole, we have determined the diffusion and partitioning coefficients of the chlorinated hydrocarbons in membranes containing these probes. Lindane partitions strongly into lipid bilayers: P = 9000 at 37°C for dimyristoyl phosphotidylcholine vesicles; at 25°C P = 13000 for dioleoyl phosphotidylcholine and P=4000 for dipalmitoyl phosphotidylcholine vesicles. The diffusion coefficient for lindane in dimyristoyl phosphotidylcholine vesicles is $5.7 \cdot 10^{-7}$ cm^2/s at 37°C. These phospholipid-carbozole probes have also been used to measure the uptake rates of lindane, gardona, and DDE from particulates into membranes. Thus fluorescence quenching methods provide a useful means of studying the dynamic interactions of toxic molecules in cell membranes.

W-POS-J5 THE KINETIC MECHANISM BY WHICH TTFB TRANSPORTS PROTONS ACROSS LIPID BILAYERS. J. P. Dilger and S. McLaughlin, Dept. of Physiology and Biophysics, HSC, SUNY, Stony Brook, N.Y. 11794.

Substituted benzimidazoles transport protons across artificial bilayers and, in accordance with the chemiosmotic hypothesis, act as uncouplers of oxidative phosphorylation in mitochondria. In bilayers the charged permeant species is a HA_2^- complex formed between the neutral HA and anionic A^- species adsorbed to the interface (Cohen et al., 1977, J. Membrane Biol.). We have deduced the kinetic mechanism by which TTFB (tetrachloro-2-trifluoromethylbenzimidazole) transports protons across bilayers by measuring the relaxations of the current in response to voltage steps. In our model the current relaxations are described by six non-linear differential equations. Appropriate choices for the adsorption and permeability parameters gave good predictions for the dependence of the relaxations on voltage, pH and uncoupler concentrations. Independent measurements of the adsorption coefficients and membrane permeabilities confirm the adequacy of the model.

Supported by grant PCM76-04363 from the NSF

W-POS-J6 ^{13}C NMR STUDIES OF PROTEIN LIPID RECOMBINANTS. B. Sears, W. Curatolo, M.J. Janiak, A. Tall, J.D. Sakura*, G.G. Shipley, D.M. Small, L.J. Neuringer, Boston Univ., McLean Hospital and M.I.T., Boston, Mass.

To understand the effect of different proteins on membrane lipids, we have studied protein lipid recombinants of N-methyl ^{13}C dimyristoyl phosphatidylcholine (DMPC) with 2 protein systems normally associated with lipids: the proteolipid apoprotein (PLA) from myelin and apo-high density lipoprotein (apoHDL) from human serum. Without protein, the 68 MHz ^{13}C NMR spectrum of unsonicated DMPC dispersions gives a broad asymmetric resonance. Sonication causes a 0.8 ppm upfield shift and a large decrease in linewidth (65 → 12 Hz). PLA incorporated into unsonicated DMPC has an additional resonance whose chemical shift is similar to sonicated DMPC but whose linewidth (60 Hz) is like unsonicated dispersions. Recombinants of unsonicated DMPC and apoHDL also give an additional resonance having a chemical shift and linewidth (10 Hz) similar to that of sonicated DMPC. While in both recombinants the proteins alter the magnetic environment of the N-methyl carbons of the DMPC, the PLA has little effect on the rotational motions of DMPC wheras apoHDL causes large increases in the dynamic motions. This work is supported by USPHS grant HL 18263.

W-POS-J7 DIFFENTIAL SCANNING CALORIMETRY OF SPHINGOMYELIN-CHOLESTEROL MIXTURES. T.N. Estep, D.B. Mountcastle, Y. Barenholz*, R.L. Biltonen*, and T.E. Thompson, Dept. of Biochem., Univ. of Virginia, Charlottesville, VA 22901.

Synthetic sphingomyelins (SPH) containing saturated aliphatic chains with 16,18, or 24 carbons mixed with varying amounts of cholesterol(Chol) have been examined in aqueous dispersions via scanning calorimetry. For all three sphingomyelins increasing the mole ratio of Chol concomitantly reduces the enthalpy associated with the gel to liquid-cystalline phase transition. This enthalpy change approaches zero at approximately 25 mole % Chol. Both C-16 and C-18 SPH display a second, broader transition in the presence of Chol. For C-16 SPH the main transition temperature decreases from 41° to 36° over the range 0 to 19 mole % Chol. With C-24 SPH this transition occurs at 49° for samples containing less than 10 mole % Chol. Greater amounts of steroid cause a linear decrease to 45° at 25 mole %. Chol concentrations as low as 5.6 mole % cause the C-18 SPH transition to shift from 57° to 44°. Higher concentrations of Chol cause only a modest further decrement to 43°C.

Work supported by USPHS grants CA-18701 and GM 14628

W-POS-J8 ASYMMETRY OF THE GRAMICIDIN PORE IN ASYMMETRIC LIPID BILAYERS. O. Fröhlich, Dept. Pharm.& Physiol. Sci. U. Chicago, Chicago IL 60637 (intr. by W. Epstein).

In symmetrical artificial membranes gramicidin A induces a voltage-dependent conductance which depends on the absolute value of the potential but not its sign (E.Bamberg and P.Läuger, J.Membr.Biol. 11:177, 1973). In lipid bilayers (Montal-Mueller type) with asymmetric lipid distribution the single channel conductance and the voltage dependence of the macroscopic conductance caused by gramicidin become asymmetric. The asymmetry of the conductance relaxation after symmetric voltage steps around zero potential can be abolished by applying a d.c. potential across the membrane. Gramicidin appears to sense an internal electrical field (or its equivalent), and this virtual field depends on the ionic strength of the aqueous phase. The field, however, is not due to surface charges or the dipole potential since its polarity is opposite to that expected in asymmetric bilayers made from PE and PS or PE and GMO, and the asymmetry of the voltage dependence and of the single channel conductance even exists in asymmetric membranes consisting only of neutral lipids such as PC, PE or GMO. (supported by the Deutsche Forschungsgemeinschaft, SFB 138).

W-POS-J9 MEASUREMENT OF SURFACE PRESSURE IN AND REPULSION BETWEEN APPROACHING PHOSPHOLIPID MEMBRANES. M.McAlister, N.Fuller*, R.P.Rand, Brock University, Ontario, Canada and V.A.Parsegian, N.I.H. Bethesda, Md., U.S.A.

We have combined three complementary methods, osmotic, mechanical and vapour pressures, with X-ray diffraction, to measure both the structural consequences and the work of removing water from a multilayer stack of phospholipid membranes. The work can be divided into that which forces the membranes together (overcoming bilayer repulsion) and that which decreases molecular area on the bilayer surface (causing bilayer compression). Consequently over the whole range of shrinking we obtain interbilayer repulsive force and energy as they vary with bilayer separation; and bilayer surface pressure and energy as they vary with molecular area. For all lipids studied, a minimum of 84% (75% for PE) of the total work goes into overcoming bilayer repulsion. The dependence of these parameters on chain conformation and on head group is determined from measurements on egg and dipalmitoyl (melted and frozen) phosphatiylcholines and egg phosphatidylethanolamine (PE).

W-POS-J10 MEASUREMENT OF ELECTROSTATIC FORCES BETWEEN LECITHIN BILAYERS CHARGED BY DIVALENT CATIONS. L.J.Lis, and R.P.Rand, Brock University, St.Catharines, Ontario, and V.A.Parsegian, N.I.H., Bethesda, Maryland.

We confirm the findings of Inoko et al (BBA(1975)413: 24) that the effect of some divalent cations (Me^{2+}) is to swell the lattice spacing of the multilamellar system formed by dipalmitoyl lecithin (DPL) in aqueous solutions. Melted DPL shows similar swelling. Further, we have used a recently developed osmotic stress technique (LeNeveu et al,Biophys.J.(1977)18:601) to measure the repulsive forces between DPL bilayers swelled in divalent cation solutions (10mM $MgCl_2$ or 30mM $CaCl_2$) where the DPL acyl chains are frozen. For inter bilayer separations $30\text{Å} < d_w < 90\text{Å}$, the variation of force with bilayer separation is characteristic of electrostatic repulsion, indicating that Me^{2+} bind to DPL bilayers imparting a charge to them. Further, the change in force with separation suggests that, as the charged DPL bilayers approach, Me^{2+} desorb from the interface. The effect of screening the charged DPL bilayer with NaCl, $MgCl_2$ or $CaCl_2$ was also examined. For $d_w < 20\text{Å}$, the bilayer repulsion appears to be dominated by the hydration forces observed for neutral lecithin.

W-POS-J11 REQUIREMENTS FOR LECTIN BINDING IN PHOSPHOLIPID GLYCOLIPID VESICLES. W.Curatolo, A.O.Yau, D.M. Small, B.Sears. Biophysics Division, Boston University School of Medicine, Boston, Mass.

To investigate the role of glycolipids as membrane receptors we have studied the lectin-induced agglutination of phospholipid-glycolipid vesicles. The lectin from R. Communis (RCA) completely agglutinates sonicated vesicles of egg phosphatidylcholine (PC) and lactosyl ceramide (LC) but no agglutination is observed when galactosyl ceramide is substituted for lactosyl ceramide. Lactose or galactose reverses the agglutination. The agglutination depends strongly on the mole ratio of LC to PC and temperature. Agglutination is negligible below 5 mole% LC, but increases with increasing LC content. At 10 mole% LC the rate of agglutination shows a sharp maximum at 25°C which may be related to a broad acyl chain transition of LC occurring at ~20°C in sonicated vesicles. These results indicate 1) that RCA reacts with the terminal galactose of glycolipids providing the galactose is separated by at least 1 sugar from the ceramide backbone and 2) agglutination has a temperature maximum in the range of the LC chain transition.

This work is supported by USPHS grant HL 18263.

W-POS-J12 PARTITION OF CIS AND TRANS PARINARIC ACID AMONG AQUEOUS, CRYSTALLINE LIPID, AND LIQUID LIPID PHASES. L.A. Sklar, G.P. Miljanich, and E.A. Dratz, Division of Nat. Sci. II, University of California, Santa Cruz, Ca.95064

The distribution of the two geometrical isomers of parinaric acid (cis PnA and trans PnA) between crystalline lipid or liquid lipid phase and aqueous phase was studied at 25° by absorption spectroscopy. The crystalline lipid was dipalmitoylphosphatidylcholine (DPPC); the liquid lipid was 1-palmitoyl, 2-docosohexaenoylphosphatidylcholine (PDPC). The mole fraction partition coefficients for cis PnA are 5.3×10^5 (DPPC) and 9×10^5 (PDPC); for trans PnA, 5×10^6 (DPPC) and 1.7×10^6 (PDPC).

A phase diagram for the DPPC/PDPC system has been constructed from measurements of the temperature dependence of fluorescence quantum yield and polarization of four probes: cis and trans PnA and their methyl esters. The crystalline lipid/liquid lipid partition coefficients of the probes are calculated from the phase diagram by a simple mathematical analysis and found to be ~ 3 for the trans probes and ~ 0.6 for the cis probes, in good agreement with the absorption results. These probes should be useful in observing individual domains in complex lipid membranes. (Supported by USPHS-EY00175. L.A.S. is a Postdoctoral Fellow of the Helen Hay Whitney Foundation).

W-POS-J13 LATERAL DIFFUSION OF PEPTIDE ANTIBIOTICS, GRAMICIDIN S, IN PHOSPHOLIPID MULTIBILAYERS. E-S. Wu[a], F. Szoka[b], and K. Jacobson[b], [a]Department of Physics, University of Maryland Baltimore County, MD, 21228, and [b]Department of Experimental Pathology, Roswell Park Memorial Institute, Buffalo, NY, 14263

Lateral diffusion of NBD labeled gramicidin S (GS) in phospholipid multibilayers (MBL) has been studied by the method of fluorescence recovery after photobleaching. At 24°C the diffusion coefficient (D) in Egg phosphatidylcholine (EPC) MBL is 3.5×10^{-8} cm^2/s. In dimyristoylphosphatidylcholine (DMPC) MBL, the phase transition was observed as an over 100-fold change in D occurring at 23°C. Raising the GS concentration would lower the transition temperature (Tm) and broaden the transition range. Cholesterol reduced D above T_m, raised D below T_m, and also excluded NBD-GS from MBL. At 50% of cholesterol, almost all the NBD-GS was excluded and formed aggregates. The effect of GS in lipid mobility was also studied by measuring the diffusion coefficient of NBD-phosphatidylethanolamine in EPC-MBL with various GS contents.

This work was supported by NIH Grant CA-16743. K.J. is an established investigator of the AHA.

W-POS-J14 DIVALENT CATION BINDING TO PHOSPHOLIPIDS: EFFECT OF TEMPERATURE AND ANESTHETICS. J. Puskin and T. Martin*; Radiation Biology and Biophysics, University of Rochester, Rochester, NY 14642.

Mn^{2+} binding to phosphatidylserine (PS) and cardiolipin vesicles was monitored with EPR. The apparent affinity for Mn of the vesicles increased monitonically with temperature. This suggests that the association is stabilized, in part, by a reduction in fatty acid chain enthalpy. Normal alcohols, benzyl alcohol, chloroform, procaine and tetracaine all inhibited Mn binding. Inhibition by n-alkanols increased with chain length, paralleling the dependence of their lipid/water partitioning coefficients on the number of carbons. In comparing all the drugs, however, there was not a perfect correspondence between Mn displacement and either lipid partitioning or anesthetic potency. In conjunction with the binding study, vesicle fluidity was followed with a cholestane spin probe. It was found that the lower n-alkanols, benzyl alcohol and $CHCl_3$ fluidized the vesicles much more than the higher alcohols or amine anesthetics. These results indicate that neither changes in divalent cation binding or lipid fluidity provide a satisfactory explanation for anesthesia. (UR-3490-1283).

W-POS-J15 A Theoretical Model of Phase Transitions and Phase Diagrams for Lipid Bilayers. W. H. CHENG, and H. L. SCOTT+, Oklahoma State Univ.--A simple theoretical model for lipid bilayer phase transitions is presented. The scaled particle theory for mixtures of hard disks is used to describe the hard core interactions between molecules. Together with a kink model for rotational states and estimates of hydrophobic and van der Waals forces, we find an effective Hamiltonian to describe bilayer phase transitions. The results give surface pressure, area and enthalpy changes that are in good agreement with the experiment. The model is then generalized to binary mixtures of lipid, and the resulting phase diagrams are compared with experiment. We also present the first theoretical studies of the effects of cholesterol and protein on the lipid phase transition. The main motivation of this work is to present a reliable model using semiempirical potentials instead of the exact intermolecular interactions, so that the model may be used for the description of more complex phenomena.

+Supported in part by the National Science Foundation.

W-POS-J16 A.C. CALORIMETRY OF PHOSPHOLIPID DISPERSIONS. Ashok K. Jain and George S. Dixon, Oklahoma State U. The technique of a.c. calorimetry has been applied to the study of aqueous suspensions of synthetic phospholipids. The application of the method to liquid samples is discussed. Results are compared for heating and cooling runs. For commercial preparations of dipalmitoylphosphatidylcholine the half-width of the specific heat anomaly at the chain-melting transition is 0.8°C. The transition temperature is found to differ by less than 0.1°C between successive heating and cooling runs. The amplitude of the 9 Hz a.c. temperature signal was typically 20 mdeg. The effect of a spin-label on the specific heat is also discussed.

W-POS-J17 FLUORESCENCE STUDY OF NPN IN EGG PC VESICLES. A.M. Kleinfeld and A.K. Solomon. Biophysical Laboratory, Harvard Medical School, Boston, MA 02115.

The lipophilic fluorescent probe NPN (N-phenyl-1-naphthylamine was used to characterize sonicated PC (phosphatidyl choline) lipid bilayers. Lifetimes (τ) and polarizations (p) as a function of lipid:probe ratio (L:P) were measured by phase modulation nanosecond spectrofluorometry over the range of 0° to 40° C. For L:P greater than the critical value 50:1, τ and p were 7 ns and 0.23 at 20° C. As L:P decreased below 50:1, τ and p decreased monotonically to 5 ns and 0.07 for L:P $\sim$ 2:1. An Arrhenius plot of rotational correlation time exhibited a small but statistically significant break from linearity at $\sim$ 25° C, with enthalpy (ΔH) values of - 2.4 kcal/mole for T < 25° and - 1.7 kcal/mole for T > 25° C. We also determined the vesicle association constant (K) and number of lipids per NPN binding sites (n). A newly constructed fluorescence titration device permits reduction of probe concentration to maintain L:P > 100:1 throughout the titration range. Preliminary findings indicate that ln K versus 1/T is linear for T between 0° and 50° C with $\Delta H \sim 3$ kcal/mole and $n \sim 45$. [Supported by NIH grants HL05074-02 and HL14820-06.]

W-POS-J18 AN ACOUSTICAL STUDY OF THE ELASTICITY OF BLM. B.W. Brennan, U. of Vermont, Burlington, Vt. 05401

The use of ultrasound for tissue characterization has stimulated increasing interest in the interaction of acoustic energy with biological systems. Although much has been done on the propagation of compressional waves, very little attention has been devoted to transverse wave propagation along cell boundaries. In approaching this problem a study was begun on a model membrane system, the Bimolecular Lipid Membrane (BLM). A new technique was developed for forming and visualizing these BLM and the transverse waves propagating along them. This involves injection of BLM solution into a septum within a closed chamber and then partial withdrawal of the excess solution until spontaneous thinning occurs. The membrane is then vibrated by a needle attached to a ceramic bimorph. These membrane vibrations are visualized by interference of electro-optically strobed He-Ne laser light transmitted through the cell and then either onto a screen or into a Smartt interferometer. Preliminary wavelength measurements for capillary waves in the Kilohertz range on films of BLM-forming solution will be presented. Calculation of elastic parameters based on existing capillary wave theory will be discussed. Supported by NIH grant #GM08209.

TRANSPORT THEORY

W-POS-K1 NETWORK THERMODYNAMIC ANALYSIS AND SIMULATION OF TRANSIENT AND STATIONARY STATES IN A VARIETY OF PHYSIOLOGICAL SYSTEMS. D.C. MIKULECKY and S.R. THOMAS*.

Linear and nonlinear modeling and computer simulation of flows in organized membranes are done with networks [Mikulecky, *et al.*, J. theor. Biol.:68 (1977); Mikulecky *ibid*; Thomas and Mikulecky (1978); Microvasc. Res. (all in press) and Thomas (1977), Ph.D. Dissertation, Med. Coll. Va.]. Systems modeled/simulated include salt and water flow in kidney proximal tubule and other epithelia, short circuit current in frog skin, a graviosmotic series membrane system with application to plant physiology, compartmental analysis in frog skin, and volume flow rectification in RBC. The nonlinear two-port elements representing coupled flows have a piecewise linearization. Electrochemical two-ports have distinct advantages over equivalent circuits in series/parallel systems. Computer simulation of network behavior is achieved using ASTEC 2, which allows the specification of nonlinear constitutive relations by Fortran for n-ports. Computer simulation is done from a circuit graph, not from equations. Transients are treated using capacitors. (Supported in part by NATO grant No. 1239.)

W-POS-K2 TRANSIENT DIFFUSION IN A MEDIUM WITH PERMEABLE BARRIERS. J.E. Tanner, Naval Weapons Support Center, Crane, Indiana 47522.

An exact algebraic expression has been obtained for the distribution of particles diffusing from an instantaneous planar source through a medium containing regularly spaced planar barriers of equal but arbitrary permeability. Based on this, a transient, time-dependent diffusion coefficient is defined, (a) from the mean square displacement using the Einstein relation, and (b) from the loss of phase coherence of a set of nuclear spins diffusing in a magnetic field gradient. Numerical results for the diffusional distribution functions and for the diffusion coefficients, (both definitions), are presented over a wide range of system parameters; and the application of the results to evaluation of NMR spin-echo data from measurements on colloidal systems, such as biological cells , is discussed.
This work was supported by the Office of Naval Research, Contract N0001477WR70035.

W-POS-K3 THE DEVELOPMENT OF OSMOTIC FLOW THROUGH AN UNSTIRRED LAYER. J. Fischbarg and T.J. Pedley, Columbia Univ., N.Y., and Univ. of Cambridge, U.K.

Time-dependent and steady-state solutions for the convection-diffusion equation $\partial C/\partial t + Jv\partial C/\partial x = D\partial^2 C/\partial x^2$ were found both analytically and numerically. A membrane was assumed to be permeable to water (osm. permeab. LpRT) and impermeable to solute, with an unstirred layer (thickness δ) at the edge of which a concentration Cb was suddenly imposed. On the opposite side C was zero; Jv is the solvent flow and D the solute diffusion coefficient. The behavior of such system is determined by the parameter $\beta = LpRT \cdot Cb\delta/D$. In the steady state, the concentration of solute at the membrane (Cm) is given by $Cm = Cb \exp(-\beta Cm/Cb)$. For $\beta \leq 0.02$, $Cm = Cb(1-\beta+3\beta^2/2)$, and the time τ at which Cm is 0.95 of its steady-state value is $\tau = (3\delta^2/D)[(\pi^2/4)+3\beta]^{-1}$. With the present treatment, the extent to which unstirred layers may affect experimental measurements of Lp for membranes can be computed. For a hypothetical range extending from cell membranes ($\beta \simeq 0.001$) to extreme conditions in leaky epithelia ($\beta \simeq 2.8$), the corrections determined in this fashion go from negligible (0.1%) to a factor of 2.

Supported by USPHS and Sci. Res. Council.

W-POS-K4 REQUISITE PHYSICO-CHEMICAL INTERACTIONS IN CHANNEL AGGREGATION MECHANISMS.
J.D. Bond, and G. Baumann. Department of Physiology, Duke University Medical Center, Durham, N.C. 27710

Aggregation has been proposed as a possible mechanism for ion-channel formation in synthetic lipid bilayers. We have modified and extended the original aggregation model to explicitly incorporate the polar nature of certain channel-forming molecules; e.g., alamethicin has a dipole moment of sixty-seven debye. The insertion of the channel-forming moieties is analyzed in terms of the change in the state of membrane polarization subsequent to a depolarizing potential. It appears that both insertion and aggregation per se are consistent with the large dipole moments seemingly characteristic of certain channel-forming molecules. The interactions of the channel constituents with the lipid environment as well as the interaction between the monomeric channel subunits is investigated for the surface and the inserted states.
(Supported by NIH grants HL 12157 and 1 T 32 GM 07403).

W-POS-K5 POSSIBLE MOLECULAR REALIZATIONS OF AN AGGREGATION SCHEME AS A BASIS OF ELECTRICAL EXCITABILITY.
G. Baumann, and J.D. Bond. Department of Physiology, Duke University Medical Center, Durham, N.C. 27710

Aggregation is a chemical process in which a number of molecules, called monomers, combine one by one to form a product, called the aggregate. The concept of aggregation is applied to electrical gating of ionic channels in membranes assuming dipole and special hydrophobic/hydrophilic properties for channel-forming monomers to allow for interaction with the bilayer and the electric field across it. Several possible molecular realizations of such a scheme as a basis for voltage-dependent conductance in membranes are presented. Steady-state and kinetic consequences of each mechanism at the macroscopic and microscopic level are discussed. Predicted behavior for such features as single-channel fluctuations derived from a Monte Carlo algorithm, and the time development of gating and ionic currents are compared to experimental data from the literature.
(Supported by NIH grants HL 12157 and 1 T 32 GM 07403).

W-POS-K6 EQUILIBRIUM POTENTIALS FOR COUPLED ION TRANSPORT ACROSS MEMBRANES. S. G. Spangler and M. C. Goodall. Department of Physiology and Biophysics, University of Alabama in Birmingham, Birmingham, Alabama 35294

Consider a membrane containing only a passive 3 Na^+-2 K^+ exchange mechanism (countertransport). It will be shown that the equilibrium potential E_{BA} (in mv) is given by $E_{BA} = 120 \log_{10}[K^+]_B/[K^+]_A + 180 \log_{10}[Na^+]_A/[Na^+]_B$. (If $E_{BA} > 0$, side B is positive to side A.) This is anomalous in the sense that 1) direction of change in potential following a change in K^+ concentration on either side is opposite to what would occur if membrane were merely permeable to K^+ and 2) the magnitude of the slope of a plot of E_{BA} vs $\log_{10}$ of the concentration of an ion on one side of membrane is very large (2 or 3 x 60 mv). Similar anomalies result from cotransport of ions of unlike charge (1 Na^+-2 Cl^- cotransport offers possible mechanism of Cl^- transport by renal Na^+-K^+ ATPase). Maximum slopes occur when there is net transport of one charge. A tenfold increase in glucose concentration on side A of a membrane containing only a 2 glucose-1 Na^+ cotransport mechanism increases positivity of side B by 120 mv. A general analysis of coupled transport mechanisms will be presented. NIH and NSF support.

W-POS-K7 INFLUENCE ON CELL VOLUME AND MEMBRANE POTENTIAL OF MEMBRANE TRANSPORT. E. Jakobsson. Department of Physiology and Biophysics and Program in Bioengineering, University of Illinois, Urbana, Illinois 61801.

A set of five coupled equations has been written to describe the influence on cell volume and membrane potential of transport of ions and water across the surface membrane of a "typical" animal cell. Three of the equations relate the time rate of change of internal amounts of the major permeable ions (K^+, Na^+, Cl^-) to the properties of specific conductance channels and active transport systems for those ions. A fourth equation imposes the boundary condition of isotonicity of the intracellular and extracellular media. A fifth equation imposes the condition of bulk electroneutrality in the intracellular space. The steady-state solutions develop unphysical singularities in two cases: i) if the intracellular potential is assumed positive; and ii) unless at least some of the internal impermeant anions are present in fixed amounts, rather than regulated by concentration. Numerical computations of cell volume and membrane potential as a function of various membrane parameters will be presented.

W-POS-K8 LINEAR BEHAVIOR OF ENZYMES OUTSIDE THE RANGE OF EQUILIBRIUM. K. J. Rothschild, S. Ellias, A. Essig and H. E. Stanley, Boston University School of Medicine 02118

The linear phenomenological equations of nonequilibrium thermodynamics are limited theoretically to near equilibrium although a number of biological systems have been shown to exhibit a "linear" relationship between steady-state flows and conjugate thermodynamic forces outside the range of equilibrium. A multi-dimensional inflection point has been found around which enzyme catalyzed reactions can exhibit "linear" behavior between the logarithm of reactant concentrations and enzyme catalyzed flows. A set of sufficient conditions has been derived which can be applied to any enzyme mechanism in order to determine whether a multi-dimensional inflection point exists. The conditions do not appear overly restrictive and may be satisfied by a large variety of coupled enzyme reactions. It is thus possible that the linearity observed in some biological systems may be explained in terms of enzymes operating near this inflection point.

W-POS-K9 THERMODYNAMICS OF MICELLE FORMATION
D. Mountcastle, S. Ferber*, and R. Biltonen*, Dept. of Biochem., U. of Virginia, Charlottesville, VA. 22901

Mixing a concentration gradient of solution with its solvent in a flow calorimeter yields heat of dilution data as a continuous function of concentration (C). An exponential concentration gradient with time is selected because it is experimentally accurate and precise,[1] the independent variable is log(C), and the dilution ratio is a constant on the log scale. The ratio of the calorimetric signal to the concentration is directly proportional to $d\Phi/d\log(C)$, where Φ is the excess heat content of the solute. Thus a single experiment yields this derivative as a continuous function of concentration. Heats of dilution of detergents, including ionic species at different ionic strengths, have been measured as continuous functions of concentration through the critical micelle concentration (cmc) range. The data is analyzed in terms of a general polydisperse mechanism of aggregation which in principle yields all of the distribution functions of interest, without assuming any molecular model for the aggregation. The method is general for any self aggregating system measured by any suitable parameter.

1. D. Mountcastle, et al., Biopolymers 15, 355 (1976).

W-POS-K10 ELECTROGRAMS FROM CULTURED MYOCARDIAL CELL STRANDS.
R. Jones*, J. Jones, J. Wallace*, E. Lepeschkin* and S. Rush*. Depts. of Physiology, Case Western Reserve Univ., Cleveland, Ohio 44106 and Medicine, Univ. of Vermont, Burlington, Vermont 05401

Simultaneous measurement of extracellular electrograms, action potentials and propagation velocity in a system with simple geometry (myocardial cell strands) is useful for confirming electrocardiographic models. However, electrograms are difficult to register due to the small tissue mass and short-circuiting by the culture medium. Electrograms of the predicted form recorded with a glass capillary electrode, located near the cell mass, exhibited a poor signal-to-noise ratio and distortion by mechanical artifacts. A better method utilized a 1" square chamber divided by a 2mm septum which crossed the strand at right angles. Electrograms recorded from electrodes located at the ends of the chamber had a monophasic QRS complex of about 75 μV, an inverted T-wave, a high signal-to-noise ratio and absence of artifacts. Changing the pacemaker site by warming one sub-chamber temporarily inverted the signal. These results demonstrate a simple technique for recording stable electrograms similar to those predicted by electrocardiographic models. Supported by HL01486.

W-POS-K11 MORPHOLOGICAL RING MODEL OF CURRENT FLOW IN FROG ATRIAL TRABECULAE.
R. McKown, Dept. Physiology & Biophysics, University of Illinois, Urbana, Il. 61801

Following the statistical approach used by Mathias, Eisenberg, and Valdiosera (Biophys. J., v. 17, 1977) to model current flow in skeletal muscle fibers, the multicellular trabeculae of frog atria can be divided radially into cylindrical shells by constructing more-or-less concentric surfaces inbetween the parallel cells. Simple longitudinal segmentation then defines the (m,n) rings of tissue as the intersection of the m'th segment and the n'th shell. Conserving extra/intracellular currents from the (m,n) ring to the four adjacent rings while recognizing membrane current as a source/sink of extra/intracellular current leads to coupled finite-difference, anisotropic "Poisson" equations for the extra/intracellular potentials. By incorporating measurable morphological parameters i.e. % extra-cellular space, cell surface-to-volume ratio, nexal density and cell spacing; the model should allow the extraction of the specific membrane and nexal electrical parameters from tissue frequency response obtained with the double sucrose gap.

A P P E N D I X

A-TUAM-F15 Piezoelectric Theory of Electromechanical Effects in Nerve.* DAVID J. GROSS and WENDELL S. WILLIAMS, U. of Illinois at Urbana-Champaign.--It has been shown recently that the piezoelectric effect in bone can be modelled by the classical theory of piezoelectricity if the d_{ijk} tensor varies spatially.[1] We postulate that an electromechanical depolarization of nerve, the generator potential, can be modelled similarly. Early experiments on the generator potential showed that stress applied to sensory receptors produced membrane depolarization.[2] We show that a piezoelectric treatment of the situation where inner and outer membrane surfaces of the nerve are negatively charged can reproduce both the generator potential depolarization and also the change in axon diameter during the action potential as reported by Hill, et al. recently.[3] Preliminary experimental evidence with a poled polymer "membrane" confirms our hypothesis.
*Work supported by NIH Bioengineering Traineeship Program, University of Illinois.
[1]M. Johnson, Ph.D. Thesis, University of Illinois, 1977.
[2]J.A.B. Gray and M. Sato, J. Physiol. 122, 610-636 (1953).
[3]B. Hill, et al., Science 196, 426-428 (1977).

A-TUAM-F16 Piezoelectricity in Biological Tissues. W.S. WILLIAMS, M. JOHNSON AND D. GROSS, U. of Illinois at Urbana-Champaign.--The apparent "piezoelectric" response of bone has been know for 20 years, but bending measurements have not been reconcilable with predictions made by combining elastic beam theory, the linear theory of piezoelectricity and the piezoelectric coefficients measured in uniaxial compression, assuming the specimen to be homogenous. Previous work called attention to the importance of the stress-gradient; we now show that if this stress gradient is coupled with a corresponding spatial variation of the piezoelectric coefficients, associated with microstructural features, the observations can be interpreted. Two special cases are treated: 1) a divergence of the spontaneous polarization of collagen fibers, the piezoelectrically-active component; and 2) a cylindrical geometry with a radial component of the polarization. We suggest that the piezoelectric response of inhomogenous biological tissues is of general importance.

A-WPM-D16 A P^{31} NMR AND ULTRASTRUCTURAL STUDY OF "CALCIUM PARADOX" IN RAT HEART. D.P. Hollis, R.L. Nunnally* & B.H. Bulkley*. The Johns Hopkins Med. Insts., Baltimore, Md.

Necrosis occurs when myocardium is exposed to calcium (Ca++) after a brief period of Ca++ free perfusion but the pathophysiology of "calcium paradox" is unclear. Using P^{31} NMR the energy status and pH of the working perfused rat hearts were studied sequentially during normal perfusion, 12 minutes of perfusion with Ca++ free medium and during 3-12 minute intervals during reflow with normal perfusate. Ultrastructural studies were performed on biopsies taken at the end of the Ca++ free period, and the end of reflow. The results show preservation of pH and high energy phosphates during Ca++ free perfusion, with structural abnormalities largely limited to cell junctions. With re-exposure to Ca++ there was a sudden massive loss of high energy phosphates correlating extensive cell injury including mitochondrial swelling and disruption and contraction band formation. The results show that Ca++ deprivation injury is largely to cell junctions, and that metabolic integrity is well maintained until Ca++ reflow, findings consistent with the notion that activation of Ca++ ATPases and loss of high energy phosphates are instrumental in the necrosis of calcium paradox.

A-WPM-D17 FLUORESCENCE STOPPED FLOW STUDY OF THE ENZYMATIC ACTIVITY OF MYOSIN SUBFRAGMENT-1. F. Garland and H. C. Cheung, Biophysics Section, Department of Biomathematics, University of Alabama in Birmingham, Birmingham, AL 35294

The interaction of myosin subfragment-1 (S-1) with the fluorescent substrate ε-ATP ($1,N^6$-ethenoadenosine 5'-triphosphate) and corresponding diphosphate ε-ADP was studied by means of stopped flow measurements. Comparative experiments, in which intrinsic protein fluorescence was monitored, show that the S-1/ε-ATP binding process is qualitatively similar to that previously observed for S-1/ATP. When the reaction S-1 + ε-ATP was followed by using the tryptophan→ε-nucleotide energy-transfer pair, a biphasic trace was obtained: an initial rapid binding phase followed by a slow (k_{obs} = 0.13 sec^{-1}) first order process. Comparative experiments involving ε-ADP along with computer simulation calculations show that this slow phase must be due to a step (or steps) which preceeds product dissociation but follows the actual hydrolysis step. Experiments have also been done to determine what mechanistic differences might exist between S-1 having intact DTNB light chain and S-1 from which the DTNB light chain has been removed.